

**CORRELATION OF INELASTIC ANALYSIS
AND DESTRUCTIVE TESTS
ON A REINFORCED CONCRETE BUILDING**

by
COMPUTECH ENGINEERING SERVICES, INC.
2855 Telgraph Ave., Suite 410
Berkeley, Ca 94705

funded by
NATIONAL SCIENCE FOUNDATION

Any opinions, findings, conclusions
or recommendations expressed in this
publication are those of the author(s)
and do not necessarily reflect the views
of the National Science Foundation.

January, 1982

i b

REPORT DOCUMENTATION PAGE	1. REPORT NO. NSF/CEE-82036	2.	3. Recipient's Accession No. PB83 145938
4. Title and Subtitle Correlation of Inelastic Analysis and Destructive Tests on a Reinforced Concrete Building			5. Report Date January 1982
7. Author(s) M.R. Button, R. Donikian, E. Crespo			6.
9. Performing Organization Name and Address Computech Engineering Services, Inc. 2855 Telegraph Avenue Suite 410 Berkeley, CA 94705			8. Performing Organization Rept. No.
12. Sponsoring Organization Name and Address Directorate for Engineering (ENG) National Science Foundation 1800 G Street, N.W. Washington, DC 20550			10. Project/Task/Work Unit No.
15. Supplementary Notes Submitted by: Communications Program (OPRM) National Science Foundation Washington, DC 20550			11. Contract(C) or Grant(G) No. (C) (G) PFR7900181
16. Abstract (Limit: 200 words) Results are presented of a study of the dynamic response of a non-seismically designed, eleven-story reinforced concrete building. The analytical response was determined with the use of a linear elastic computer analysis program, and was correlated with its measured response from small amplitude, non-destructive, mechanically induced shaking. The influence of the stairwell, infill panels and foundation flexibility on the dynamic characteristics of the structure was included in the analysis. The predicted analytical inelastic response of the structure was correlated with the inelastic response measured from mechanically induced, large amplitude shaking tests which induced maximum roof displacements and caused severe structural damage. In addition, the best fit nonlinear model of the structure was used to predict the response of the structure when subjected to earthquake-induced ground motions. It was concluded that in areas of high seismic risk, the structure would represent a significant safety problem. In areas of low seismic risk, the structure would retain its structural integrity and remain functional after an earthquake.			13. Type of Report & Period Covered
17. Document Analysis a. Descriptors Earthquakes Hazards Dynamic structural analysis Buildings b. Identifiers/Open-Ended Terms Ground motion c. COSATI Field/Group			14.
18. Availability Statement NTIS			19. Security Class (This Report)
			20. Security Class (This Page)
			21. No. of Pages
			22. Price

SEISMIC RETROFIT SCHEME

FOR THE BUILDING

We are currently performing an in-house study to evaluate the seismic performance of the test structure in California using a base isolation/energy dissipation retrofit concept. The retrofit scheme utilizes energy dissipators that were developed in New Zealand. They consist of an elastomeric bearing with a lead plug insert and are placed at the base of each column. They have been used on a five-story building in New Zealand and about fifteen bridges.

The results to date look very encouraging, and it appears that this retrofit scheme will enable the test structure to resist with minimum damage a maximum credible earthquake for California.

The basic mechanism of the retrofit scheme significantly reduces the seismic forces in the structural members and provides a significant reduction in the accelerations at each floor level. The latter reduction will significantly reduce or eliminate any non-structural damage, and the former should prevent any significant damage occurring in the non-seismically designed joints.

Computech Engineering Services, Inc.

ABSTRACT

This report presents the results of an analytical study on the dynamic response of a non-seismically designed eleven-story reinforced concrete building. The study was conducted in three phases. In the first phase the analytical response of the structure was correlated with its measured response from small amplitude, non-destructive, mechanically induced shaking. The analytical response was determined with the use of a linear elastic computer analysis program. The influence of the stairwell, infill panels and foundation flexibility on the dynamic characteristics of the structure was included in the analysis.

In the second phase, the predicted analytical inelastic response of the structure was correlated with the inelastic response measured from mechanically induced, large amplitude shaking tests. These tests induced maximum roof displacements of the order of 18 inches and caused severe structural damage to the building. Several new features were developed for the nonlinear computer program used in the correlation study to model the nonlinear behavior observed in the tests.

The final phase of the study used the "best fit" nonlinear model of the structure to predict the response of the structure when subjected to earthquake induced ground motions characteristic of different seismic risk zones in the United States. It was concluded that in areas of high seismic risk, the structure would represent a significant safety problem. In areas of low seismic risk, the structure would retain its structural integrity and would be functional after an earthquake.

Recommendations for future research are presented to better evaluate the seismic safety of existing structures similar to the test building.

ACKNOWLEDGEMENTS

The research reported herein was funded by a grant from the National Science Foundation, Grant No. PFR-7900181. This support is gratefully acknowledged.

T.E. Kelly performed the small amplitude analyses. Dr. M.R. Button, R. Donikian and E. Crespo performed the large amplitude and earthquake analyses. The principal investigator was Dr. R.L. Mayes. A. Putnam edited and typed the manuscript and tables.

TABLE OF CONTENTS

ABSTRACT	(i)
ACKNOWLEDGEMENTS	(ii)
TABLE OF CONTENTS	(iii)
1 INTRODUCTION	1
1.1 SCOPE OF THE REPORT	2
2 TEST STRUCTURE AND EXPERIMENTAL PROGRAM	3
2.1 DESCRIPTION OF TEST STRUCTURE	3
2.2 DESCRIPTION OF TESTS PERFORMED	6
2.2.1 Small Amplitude Tests	6
2.2.2 Large Amplitude Tests	7
2.3 DISCUSSION OF DAMAGE	9
2.3.1 Status Before Large Amplitude Tests	9
2.3.2 Damage After Moderate East-West Shaking	9
2.3.3 Damage After Completion of East-West Tests	9
2.3.4 Damage During North-South Tests	10
3 CORRELATION OF SMALL AMPLITUDE TEST RESULTS	30
3.1 INTRODUCTION	30
3.2 ANALYTICAL TECHNIQUES	30
3.2.1 SAP IV Computer Program	31
3.3 ANALYTICAL MODEL	31
3.3.1 Modelling Assumptions	32
3.3.2 Modelling of Frame	33
3.3.3 Diaphragm Properties	33
3.3.4 Stairs	33
3.3.5 Infill Walls	34
3.3.6 Mass distribution	36
3.3.7 Column Base Fixity	36

3.4	REDUCTION OF EXPERIMENTAL DATA	37
3.4.1	Forced Vibration Test Procedures	37
3.4.2	Equation of Harmonic Motion	37
3.4.3	Extraction of Mode Shapes	41
3.4.4	Results of Mode Shape Extraction	42
3.5	CORRELATION STUDIES PERFORMED	43
3.6	RESULTS OF CORRELATION	43
3.7	DISCUSSION OF RESULTS	44
3.7.1	Effect of Stairs	45
3.7.2	Effect of Infill Panels	45
3.7.3	Effect of Soil Properties	45
3.7.4	Effect of Solution Parameters	46
3.8	CONCLUSIONS FROM SMALL AMPLITUDE CORRELATIONS	46
4	PROCEDURES FOR LARGE AMPLITUDE CORRELATION	70
4.1	NORTH-SOUTH TESTS	70
4.1.1	Summary of the N-S Large Amplitude Tests	70
4.1.2	Summary of Damage During N-S Tests	71
4.2	SCOPE OF THE CORRELATION STUDIES	72
4.2.1	Response Quantities for Correlation	72
4.2.2	Structural Models	73
4.3	COMPUTER PROGRAMS	73
4.3.1	New Features Developed for DRAIN-TABS	73
4.3.1.1	Forced Vibration Response	74
4.3.1.2	Instantaneous Eigensolver	75
4.3.2	Program Verification	75
4.4	BEAM AND JOINT MODELS	75
4.4.1	"Crimped Hysteresis" Beam Element	76
4.4.2	Degrading Stiffness Joint Element	77
4.4.3	Evaluation of Element Parameters	79
4.5	MODEL PRIOR TO NORTH-SOUTH TESTS	80
4.6	MODEL FOR DEGRADING STRUCTURE	81
4.6.1	Initial Modelling	81
4.6.2	Adjustment of Model Parameters	82
4.6.3	Load Level	83
5	RESULTS OF LARGE AMPLITUDE CORRELATION	89
5.1	MODE SHAPES AND FREQUENCIES	89
5.2	TIME HISTORY	90
5.3	FINAL CORRELATION	91
6	EARTHQUAKE RESISTANCE OF TEST STRUCTURE	104
6.1	TEST BASE-SHEAR FORCES	104
6.2	ANALYTICAL MODEL	104
6.3	SELECTION OF GROUND MOTIONS	105

6.4	ANALYSES PERFORMED	106
6.5	RESULTS	107
6.6	DISCUSSION OF RESULTS	108
6.6.1	Time History Response	108
6.6.2	Structural Damage	109
7	CONCLUSIONS	134
7.1	SMALL AMPLITUDE CORRELATION	134
7.2	LARGE AMPLITUDE CORRELATION	134
7.3	SEISMIC PERFORMANCE	134
7.4	RESEARCH RECOMMENDATIONS	135
8	REFERENCES	137



1 INTRODUCTION

The structural engineering profession was presented a unique opportunity in the early 1970's when 33 relatively modern and undamaged 11-story buildings were considered to be uninhabitable for social reasons and were marked for demolition. A full-scale structural laboratory thus presented itself. The realities of politics and finance intervened, however, and eventually only one 11-story tower was available for full-scale testing. The test structure, located in St. Louis, was non-seismically designed in 1953.

The development of a suitable experimental test program took place over a two-year time period and is described in detail in reference 3. The three distinct phases of the test program resulted in the following three reports:

- | | |
|-------------|---|
| Reference 1 | "Material and Dimensional Properties of an Eleven Story Reinforced Concrete Building" |
| Reference 2 | "Moderate Level Vibration Tests of an Eleven Story Reinforced Concrete Building" |
| Reference 3 | "Dynamic Tests of a Reinforced Concrete Building" |

The test program was designed to provide a significant contribution to understanding the dynamic response of a full size non-seismically designed eleven-story reinforced concrete building. The first phase of the test program consisted of a survey of the structure to determine its dimensional and material properties. The second phase consisted of a series of small amplitude tests to determine the dynamic characteristics of the buildings. The third phase consisted of a series of large amplitude forced vibration tests to determine the degree and nature of their damaging effect.

A substantial amount of valuable data resulted from the experimental program. For the first time, detailed response data (accelerations and displacements) were produced on a full-scale building that was cyclically tested well into the inelastic range. This data provided a real test for the ability of state-of-the-art non-linear computer programs to predict the overall structural behavior observed in the tests.

The results of the large amplitude tests [3] also indicated that the non-seismically designed building was capable of resisting the 1976 Uniform Building Code design base shear forces for Seismic Zone 4 when subjected to the sinusoidal motion induced by the moving mass shaker. However, it was concluded from these results that until further analyses were performed, it could not be inferred that the structure was capable of resisting an earthquake ground motion which induced a base shear force of the same magnitude. Utilization of the test results in analytical correlation studies was the next logical step after the test program and is the subject of this report. The objectives of the correlation studies reported herein are as follows:

1. Utilizing existing linear dynamic analysis computer programs, evaluate the correlation between the dynamic characteristics obtained from the analysis and small amplitude tests. As part of this study, evaluate the effect of the stairwell and external cladding on the dynamic characteristics of the structure.
2. Determine the degree of correlation between the results obtained from the large amplitude tests and those determined using non-linear dynamic analysis computer programs.
3. Utilizing the "best fit" analytical model from the correlation with the large amplitude tests, evaluate the seismic resistance of the test structure subjected to earthquake ground motions characteristic of different seismic risk zones in the United States.

1.1 SCOPE OF THE REPORT

A summary of the test structure and experimental forced vibration test program is given in Chapter 2. The analytical correlation with the small amplitude forced vibration tests is given in Chapter 3. This includes an assessment of the effects of the stairways, infill panels and foundation on the dynamic characteristics of the test structure. The procedures and results of the analytical correlation with the large amplitude forced vibration tests are given in Chapters 4 and 5, respectively. The response of the "best fit" non-linear analytical model to seismic ground motions typical of various regions in the United States is given in Chapter 6. Conclusions and recommendations on future analytical and experimental developments are given in Chapter 7.

2 TEST STRUCTURE AND EXPERIMENTAL PROGRAM

An extensive description of the test structure and experimental program is given in reference 3 and is summarized in the following subsections.

2.1 DESCRIPTION OF TEST STRUCTURE

The test structure was part of a building originally designated as Building C3 (Figure 2.1). Building C3, like every other apartment building in the Pruitt-Igoe Housing Complex, was eleven stories tall above the ground level and its long dimension was in the E-W direction. The building had an overall length of 360 ft (109.7), with a narrower 29 ft (8.8m) wide and 270 ft (82.3m) long center portion flanked at the East and West ends by a 45 ft x 41 ft (13.7 x 12.5m) "end tower" (see Figure 2.1). Building C3 was constructed in the period March 1, 1954 through March 29, 1955.

The sequence of demolition of the group of buildings near C3 is shown in Figure 2.2. The original cluster of structures, i.e. A2, C3, A4, is shown in Figure 2.2(a). During 1972 the narrower center portion of C3 was removed to the ground level by blasting (Figure 2.2(b)), leaving the two end-towers standing by themselves. The portions of C3 which were to remain were separated from the rest of the structure by cutting the connecting beams and slabs with jack-hammer and torch. During the latter part of 1976, the rest of the cluster (apart from the test structure) was demolished by conventional means (Figure 2.2(c)). The test building was the completely isolated W-tower of Building C3. Clearly, the test structure was not new. It had sustained (a) a nearby blast strong enough to demolish a separated part of the building, and (b) several accidental impacts with a heavy lead sphere which led to superficial damage to the outside walls only. Essentially, however, the building remained structurally undamaged. The record of elastic dynamic performance, as well as careful visual inspection, indicated that overall there was no noticeable degree of damage prior to the sequence of tests performed as part of the testing project.

The plan of the test structure was identical on every floor above ground level. A plan showing the column and beam locations is given in Figure 2.3 (square symbols are the columns and the solid lines are the beams). The cross section is rectangular, with nine peripheral columns and four interior ones. The columns are mainly square in cross-section, although some are rectangular. The upper columns are tied and the lower columns are spirally reinforced. The spiral reinforcement terminated above and below a joint, leaving each beam-column joint without confining reinforcement. Details of column and beam dimensions and reinforcement, as well as joint details are given in references 1 and 3.

The set of identifying numbers given in Figure 2.3 for the columns corresponds to the identification in the original plans. The centerline dimensions of the structure are given in Figure 2.4.

The building elevation in Figure 2.5 shows eleven floors of 8.5 ft (2.59m) height each above ground level, a crawl-space (basement), the piers (i.e.,

the columns below the crawl-space floor) and the footings. The pier lengths, and thus the footing elevations, are variable, ranging from 1 ft to 7 ft (0.3 to 2.1m). The footings are individual spread footings for each column, except that columns 45 and 46, and 47 and 48 have a shared pedestal (Figure 2.6). Each footing is a two-level pedestal of reinforced concrete.

In summary, the test-structure is a rectangular building, approximately 41 ft x 45 ft (12.5 x 13.7m) in plan and approximately 94 ft (29m) in height above the ground. The height-to-width ratio is thus about 2:1. The structure has eleven stories of equal height above the ground, and a low crawl-space below the ground. The structure consists of columns, beams, slabs, piers and footings. In addition, the crawl-space periphery consists of a 12 in. (0.30m) thick reinforced wall which is monolithic with the columns. The slabs, designed as one-way, are 5 in. (0.127m) thick except in the West end of the floor (Figure 2.7) where there is a 4 in. (0.102m) slab. The structure was designed according to the 1953 ACI Code for a concrete strength of 3000 psi (20.5 MPa).

Several features of the structure are of relevance to the observed behavior under shaking:

1. A substantial portion of the mass of the concrete was below ground level. The volume of the concrete above the ground level is about 13,700 cu. ft (389cu.m.) out of a total of 19,100 cu. ft (540 cu.m.). Thus, about 30% of the mass was below the ground, concentrated mainly in the massive footings and the basement walls. This explains the lack of any significant response to the dynamic excitation in the bottom of the crawl-space and in the ground near the building. In addition, the sensitive seismographs at St. Louis University, about 1.6 miles (2km) from the test site, did not pick up any vibrations from the test. It must then be concluded that for all practical purposes the dynamic forces did not penetrate into the soil around the test-structure and that the test frame was essentially fixed at the ground level.
2. The beam-to-column joints were without any confining reinforcement, and this permitted the occurrence of the characteristic joint failure observed, especially in the N-S shaking where the concrete eventually spalled out of the corner columns completely, leaving only the exposed main reinforcement.
3. The bottom reinforcing bars at the beam ends were generally not anchored into the joint, thus permitting an easy pull-out of the bottom bar under positive joint moment. This resulted in the characteristic hinging observed.

The nominal design strength of the concrete used was 3000 psi (29.7 MPa).

The cylinder strengths of the concrete, taken during construction, ranged from 2830 psi (19.5 MPa) to 5130 psi (35.4 MPa) with an average of 3800 psi (26.2 MPa). Core samples taken as part of the testing project gave an average of 5,600 psi (38.6 MPa), and results of a Schmidt hammer investigation showed an average of 8020 psi (55.3 MPa). The core samples taken were non-standard in dimension, and when the results were adjusted for this factor, the cores gave results in close agreement with the Schmidt hammer results. The steel reinforcing had a nominal yield stress of 50 ksi (345 MPa). The actual yield stress of the insitu reinforcing bars was determined by laboratory samples taken from demolished adjacent buildings, giving a range of yield stress values of 55 to 62.5 ksi (379 to 431 MPa).

The slabs were designed as one-way slabs, but were reinforced enough transversely so that they acted essentially as two-way slabs. Portions of the slab in the SE corner were inadvertently loaded to approximately 700 psf (34 kPa) during the erection of the large amplitude shaker on the tenth floor. Although this was an order of magnitude larger than the design live load of 70 psf (3.35 kPa), no undue distress was observed. The dimensions of the beams and columns were essentially the design values. Although the concrete strength was considerably higher than the design value, the structure was thus for all practical purposes built according to the plans. The footings sat on silty brown clay which extended some 10 to 20 ft (3 to 6m) below the footings to broken limestone. The original structural design considered only gravity loads. Beams were designed with moment coefficients and columns were designed for axial load only.

Prior to testing the whole building was clad in walls from the second story up, leaving the space between the ground and the first floor (level 1) free of any walls. Above level 1 the whole building was encased in a wall extending around the entire periphery. In the NE portion of the E wall, where the test-building joined the previously demolished central portion of C3, the wall consisted of one thickness of 8 in. (0.203m) thick concrete block (Figure 2.8). This wall was interrupted by a door between the two central columns. The remaining portion of the E wall (SE corner) was in excellent condition and was not interrupted by windows. This wall, as well as the remaining walls on the S, W and N periphery, consisted of one thickness of 8 in. (0.203m) concrete block between the columns and one thickness of 4 in. (0.102m) brick extending beyond the column faces. The brick was supported by a steel angle at every second floor level, and every second brick in every sixth course was turned at right angles to dovetail into the block wall behind it. The quality of workmanship of the wall construction was of a high grade. The N and S walls were interrupted in each floor by three windows, one extending almost from column-to-column (Figure 2.8). There were four smaller windows in the W wall. There were almost no window panes left but the window frames were in place.

The stairwell (landings and stairs) was enclosed by concrete block walls which were interrupted by one door on the N and the S wall (Figure 2.8). The walls were 8 in. (0.203m) blocks on the N and S side, and 12 in. (0.305m) blocks on the W side.

The stair-system (Figures 2.5 and 2.8) consisted of reinforced concrete

stairs between the landings. These stairs provided the only access to the tenth floor where the test equipment was located.

2.2 DESCRIPTION OF TESTS PERFORMED

The dynamic testing of the building consisted of both small and large amplitude tests. The small amplitude tests had the following objectives:

1. To determine the dynamic characteristics of the structure by methods that have been extensively used over the past decade.
2. To compare the results obtained in 1 above with those obtained from the large amplitude forced vibration tests.
3. To use the information obtained in 1 to plan the large amplitude forced vibration tests.

The large amplitude tests had two main objectives:

1. To determine changes in mode shapes, frequencies, and damping values as the force level of excitation increased.
2. To determine the resistance capability of the non-seismically designed building as the force level of excitation increased.

2.2.1 Small Amplitude Tests

The eccentric mass vibrators used in these tests were located in the SW corner of the 10th floor. All tests were performed with the cladding in place. Two different types of tests were performed: The first, a frequency sweep test, was performed to determine resonant frequencies and damping values. The second, a response shape test was performed to determine the response of the building at various resonant frequencies.

For a given test with the shaker set to a fixed eccentricity, identification of resonant periods and damping values took place in two phases over the period range of interest. Phase one consisted of a slow frequency sweep and the frequency content of the response was observed using a spectrum analyzer. The principal purpose of this slow sweep was to determine the period ranges over which detailed data would be taken.

Phase two of a given test consisted of an extremely slow frequency sweep to establish an upper bound during which bursts of data were taken at small enough incremental periods to allow sufficient resolution of resonant peaks and to adequately define modal damping ratios and phase relationships. Response of the building in each of the first eight

modes was mapped. Table 2.1 presents a summary of all frequency sweep tests and their results. As shown in Table 2.1, frequency sweeps were performed at four different force levels in the lowest two translational modes. It should be noted that these force levels were considerably lower than those used in the large amplitude tests. Response shape tests were performed for eight of the nine resonant periods given in Table 2.1. A response shape was not determined for the third torsional mode. Details of the frequency sweep test results and of the response shapes are presented in reference 2.

2.2.2 Large Amplitude Tests

The large amplitude tests were performed with the moving mass vibrator mounted on the 10th floor, and were conducted in the E-W direction with the external cladding (infill walls) in place and in the N-S direction with external cladding removed. A summary of the tests performed in both directions is given in Tables 2.2 and 2.3.

Two types of tests were performed. Damping tests were performed to determine resonant periods and damping values of modes of interest at various input force levels. Mode shape tests were performed to determine the mode shapes at various resonant periods.

1. Damping Tests

Damping tests were performed such that the force level during a given test varied approximately as a function of the frequency squared.

The approximate resonant period at a required force level was determined by a slow continuous sweep beginning at approximately 1.0 second below the estimated resonant period and sweeping up above the actual resonant period.

During this sweep, two recordings were made. First, the signal of the reference accelerometer on the 10th floor was analyzed by a spectrum analyzer and the peak of the resulting curve was used to identify the resonant period. Second, the force signal from the moving mass vibrator was plotted against the signal from the reference accelerometer on a two channel oscilloscope. Theoretically, for an elastic system at resonance, the two signals are 90 degrees out of phase and the resulting plot traces a circle on the oscilloscope. Both methods were used to identify the resonant period during the sweep.

In addition to identifying the resonant period, the continuous sweep enabled the structure in most cases to achieve a stable structural condition at a particular force level. This was helpful because as the input force level increased in 5,000 pound increments, the structural system changed. An example of this was hinging that occurred in the beams and

stairwell of the lower levels. At higher force levels in the first modes, the continuous sweep was not performed because the structural changes were more significant and consequently, data was required as these changes occurred.

Once the resonant period was identified, a stepwise sweep was performed at appropriate period intervals to determine the damping and resonant period at the particular input force level.

At various stages throughout the large amplitude test program, standard damping tests were performed. The test consisted of a damping test described above at a nominal input force level of 5,000 lbs. The objective of the standard damping test was twofold. First, it provided the means of comparing changes that occurred in the damping and resonant periods of the building during various stages of the test sequence. Second, it provided the means of determining whether or not changes that occurred in the damping and resonant periods at large input force levels remained the same at lower force levels.

2. Mode Shape Tests

Mode shape tests were performed at various phases of the test program to determine in detail the response of the building in resonance. Prior to each mode shape test a continuous frequency sweep, described above, was performed to determine the resonant period. The building was then vibrated at the resonant period and the data was recorded. The response of the structure was measured at 11th, 9th, 7th, 5th, 3rd, 1st and basement levels. At each level the response at 25 grid points was recorded. At each point a triaxial accelerometer was used enabling the three-dimensional response to be obtained. The sequence of tests performed in the E-W direction with the cladding in place is listed in Table 2.2. Standard damping tests were performed throughout the test sequence to provide a method of comparing changes that occurred in the building and to determine whether or not the changes that occurred at large input force levels remained the same at lower force levels. The damping tests in both the N-S and E-W directions were planned so that the nominal force level at resonance increased in 5,000 lbf increments. Mode shape tests were performed in both the E-W and N-S directions both before and after the large amplitude tests.

The sequence of tests performed in the N-S direction with the cladding removed is listed in Table 2.3. Also listed in the Table are the resonant periods and damping values obtained from the frequency response curves.

2.3 DISCUSSION OF DAMAGE

The novel feature of the testing project was that repetitive damage-producing cycles of lateral load were administered to a full scale, structurally sound reinforced concrete frame building, which was designed and built according to the current state of the art in the 1950's. The significant data from the tests were the accelerations and displacements measured in various parts of the structure and the dynamic properties which were computed from them. This section of the report presents a qualitative description of the observed damage during the progress of the test program.

Damage observation was made continuously during the whole testing period. The following discussion is based on observed damage after the completion of major phases of the testing.

2.3.1 Status Before Large Amplitude Tests

Prior to the commencement of the large amplitude shaking, the building was essentially undamaged from a structural point of view. There were a few hairline cracks in the beams and the columns of the top floor (at level 11) which were induced by the small amplitude shaking and there were some diagonal cracks in the E-W filler walls around the stairwell on the 4th, 5th and 11th stories. The stairs were completely intact, and the outside brick facade was essentially intact except for a small part of the SW corner which was inadvertently hit by a headache ball when the adjacent building was demolished. The only modification to the structure was the removal of a portion of the roof slab to facilitate the placement of the test equipment.

2.3.2 Damage After Moderate East-West Shaking

Damage to the slab and structural frame was slight after the fully clad structure was subjected to a series of test runs (Test 12E-D) with 5 and 10 Kip force levels. It consisted mainly of hairline cracks at the column tops (notably in column 48, 1st story) and at the ends of some E-W beams (notably in beams B4 at levels 1 and 2 - see Figure 2.9 for beam designations). Cracks developed all across the joints between the stairs and the stairway landing at the 1st story and the ground level landings.

2.3.3 Damage After Completion of East-West Tests

All of the damage to the structure above level 8 was restricted to hairline cracks at some column tops and beam ends, and no new cracks were discovered between levels 5 and 8. No substantial structural damage was discernible above level 5. Major structural damage occurred at level 1, with damage diminishing with height. All of the E-W beams on levels 1 and 2 had cracks at their ends, as did most of the beams on levels 3 and 4. Typically, the most severe cracking and spalling

took place on level 1.

Typical interior joint X-cracks are seen in Figure 2.10, which shows the joint of column 45 at the top of story 1. The top of column 1 (SW corner) in story 2 is shown in Figure 2.11. This same column, at one level below, exhibits a crack through the beam and into part of the column. Typical level 1 beams had end cracks which opened and closed during the motion of the building. The most severe column damage occurred at the top of column 44 in the 2nd story. The most severe beam cracking occurred at the E end of beams B4 in level 1, and Figures 2.12 and 2.13 illustrate the progression of damage, including the fracture of the reinforcing steel. During the final severe E-W cycling, it appeared from the observed motion of the structure that the E-W beams connected to the exterior columns on levels 1 and 2 acted essentially as hinges when the bottom beam steel was in tension (Figure 2.14). The slab on levels 1 and 2 cracked through from N to S across the building.

The stairway up to the fourth level was severely cracked at each joint between the stairs and the landing. This joint heaved up and down during each cycle of loading. The lowest joint (between the ground and level 1) is shown after the E-W tests in Figure 2.15. Top and bottom stairway joints are shown in Figures 2.16 and 2.17.

The N-S beams and the N wall were essentially undamaged. Damage to columns, beams, stairs and walls diminished progressively from the 3rd to the 5th story, with the structure-stair-wall system intact and acting as a unit above level 5. Below that level the walls and the stairway system were broken up and the beams were hinging. As testing continued, damage seemed to be confined to the lower three to four floors, the top riding along as the softening and damaged lower floors swayed back and forth. Little damage was observed on the 10th floor where the heavy moving machinery subjected the frame and the slab to continued severe impacts. It appears that once softening started on level 1, the damage became isolated on the lower part of the building.

2.3.4 Damage During North-South Tests

The cladding was removed from all but the upper two floors of the building and the shaking apparatus on the 10th floor was rotated 90 degrees to produce forces in the N-S direction. The removal of all of the brick and block cladding did not result in any additional damage to the structure.

Tests performed up to 16N-D produced damage that consisted of the development of flexural cracks between the column faces and the N-S beam ends. The motion of the building during the first mode N-S tests consisted of N-S translation of the whole building and of torsion centered toward the E of the building. This torsional motion at the first translational mode tended to wrack the W face considerably more than the E face, and damage was mainly confined to the beams and

columns on the W face.

For the larger input-force level tests (Tests 17N-D to 41N-D), severe damage was inflicted on the W portion of the structure. This damage occurred in essentially two ways:

1. With continued shaking, more and more joints in the NW (column 41) and SW (column 1) column failed, and
2. Columns 43 and 44 crushed in compression.

There was also damage in the joints of the center columns on the W face (column 42). A typical damaged joint of this center column tier (column 42, level 4) is shown in figure 2.18, where the damage prior to Test 25N-D consisted of spalling, and after Test 31N-D part of the lower beam reinforcing bar was exposed. The extent of damage to this joint did not increase with later tests. The other joints of this column experienced similar damage, with all joints losing some concrete from level 1 through level 8. The corner columns (columns 1 and 41) were damaged rather more severely, all joints from level 1 through level 8 losing almost all the concrete from the joints, leaving fully exposed the beam flexural reinforcing.

The photo in Figure 2.19 shows a portion of the NW corner (column 41), and illustrates the severe joint damage at the end of the tests. All columns appeared to be hinged at both ends between stories, with the reinforcing holding them in place. Figure 2.20 shows the inside of the joint in corner column 41 at level 3 at the conclusion of the tests. Figure 2.21 shows the outside of this same joint. The following damage was evident after the last test (Test 41N-D): All the joints below the 9th level in the two W corner columns (columns 1 and 41) had lost almost all of the concrete from the joints, and the column in the NW corner of the 6th story was visibly pushed out. The joints in the center column line of the W face (column 42) were also damaged up to level 8, but not as severely as the corner columns. Interior columns 43 and 44 were severely crushed in the 2nd, 3rd and 4th stories, with column 44 completely crushed in the 4th story. The other columns showed little additional damage, except that during the last run X cracks began to develop in the joints of level 5 in the two E central columns (columns 47 and 48), theoretical response.

**Table 2.1 Summary of Results of Frequency Sweep Tests
(Small Amplitude Shaking)**

Force (lb_F)	Peak Acc. cm/sec²	Resonant Frequency Hz	Dominant Response	Damping Ratio (%)
4,258	62.22	1.43	E-W First Mode	0.88
2,575	37.59	1.44	E-W First Mode	1.52
2,676	40.92	1.47	E-W First Mode	1.34
1,053	9.42	1.53	E-W First Mode	1.45
5,115	70.37	1.56	N-S First Mode	0.98
3,136	59.77	1.58	N-S First Mode	1.40
3,206	47.01	1.61	N-S First Mode	1.28
1,221	13.94	1.64	N-S First Mode	1.52
2,226	40.92	2.22	First Torsional	1.70
1,278	23.55	2.28	First Torsional	1.26
5,397	60.75	4.68	E-W Second Mode	1.87
6,021	55.84	4.94	N-S Second Mode	1.77
2,638	21.30	7.15	Second Torsional	1.74
1,372	13.44	7.35	Second Torsional	2.04
8,326	25.52	12.70	E-W Third Mode	3.94
5,015	10.89	14.05	N-S Third Mode	
8,231	-	17.4-18.5	Third Torsional	

TABLE 2.2 Tests Performed in the East-West Direction With External Cladding

TEST NO.	TYPE OF TEST	NOMINAL FORCE LEVEL (LBF)	FORCE LEVEL AT RESONANCE (LBF)	RESONANCE PERIOD (SECS)	DAMPING** (%)
1E-SD	Standard Damping	*5,000	4,760	0.73	1.4(2.2)
2E-SD	Standard Damping	5,000	5,050	0.43	---
3E-SD	Standard Damping	5,000	4,310	0.22	2.6(3.3)
4E-S	Sweep	10,000	---	0.87	---
5E-SD	Standard Damping	5,000	5,190	0.81	3.6
6E-SD	Standard Damping	5,000	4,620	0.22	3.3
7E-SD	Standard Damping	5,000	2,770	0.78	3.0
8E-SD	Standard Damping	5,000	6,400	0.22	2.9
9E-D	Damping	10,000	8,940	0.23	2.5(2.3)
10E-D	Damping	10,000	7,800	0.84	3.4(1.8)
11E-M	Mode Shape	10,000	8,900	0.23	---
12E-D	Damping	10,000	10,430	0.43	---
13E-M	Mode Shape	10,000	10,500	0.43	---
14E-M	Mode Shape	10,000	10,500	0.88	---
15E-SD	Standard Damping	5,000	3,960	0.89	---
16E-SD	Standard Damping	5,000	4,920	0.23	---
17E-D	Damping	15,000	15,880	0.25	3.7(2.5)
18E-D	Damping	20,000	18,090	0.28	5.2(2.5)
19E-D	Damping	25,000	29,920	0.31	8.2(3.9)
20E-D	Standard Damping	5,000	4,590	0.93	4.0(1.8)
21E-SD	Standard Damping	5,000	4,860	0.29	6.3(5.2)
22E-D	Damping	15,000	10,740	1.18	4.5(1.9)
23E-D	Damping	20,000	18,800	1.67	(2.2-3.1)
24E-D	Damping	25,000	---	1.92	(3.0-3.9)
25E-SD	Standard Damping	5,000	4,990	0.39	5.6(3.4)
26E-D	Damping	10,000	11,250	1.92	3.6
27E-M	Mode Shape	10,000	9,200	0.41	---
28E-M	Mode Shape	10,000	10,800	1.85	---

* The direction of sweep for this sweep was up, i.e., from a lower to higher frequency.

** The first damping value was obtained from the frequency response curve. The values in parentheses were determined by the time domain method.

TABLE 2.3 Tests Performed In the N-S Direction With External Cladding Removed

TEST NO.	TYPE OF TEST	NOMINAL FORCE LEVEL (LBF)	FORCE LEVEL AT RESONANCE (LBF)	RESONANCE PERIOD (SECS)	DAMPING (%)
1N-SD	Standard Damping	5,000	5,170	1.04	3.1
2N-SD	Standard Damping	4,000	3,610	1.23	3.5
3N-SD	Standard Damping	5,000	4,500	3.52	2.6
4N-SD	Standard Damping	4,000	3,530	0.31	3.7
5N-M	Mode Shape	5,000	3,800	1.22	---
6N-M	Mode Shape	5,000	4,600	1.06	---
7N-M	Mode Shape	5,000	4,300	0.32	---
8N-M	Mode Shape	5,000	4,100	0.29	---
9N-SD	Standard Damping	5,000	4,680	1.08	2.5
10N-SD	Standard Damping	4,000	2,920	1.25	3.5
11N-SD	Standard Damping	5,000	5,000	0.28	2.1
12N-SD	Standard Damping	4,000	3,670	0.32	2.8
13N-D	Damping	10,000	9,910	0.19	2.5
14N-D	Damping	7,500	7,640	0.34	3.0
15N-D	Damping	15,000	15,140	0.30	3.2
16N-D	Damping	10,000	10,570	0.35	3.4
17N-D	Damping	20,000	20,160	3.25	2.8
18N-D	Damping	13,000	12,930	2.72	3.7
19N-D	Damping	*13,000	13,180	2.70	2.0
20N-D	Damping	*20,000	19,410	0.31	1.6
21N-D	Damping	25,000	26,960	0.32	2.8
22N-D	Damping	15,000	15,260	0.40	3.2
23N-D	Damping	20,000	22,840	0.42	5.6
24N-SD	Standard Damping	5,000	5,190	0.30	2.5
25N-SD	Standard Damping	4,000	3,290	0.37	3.4
26N-SD	Standard Damping	5,000	5,320	1.09	3.0
27N-SD	Standard Damping	4,000	3,430	1.32	3.0
28N-D	Damping	10,000	8,480	1.23	3.1
29N-D	Damping	10,000	9,610	1.89	---
30N-D	Damping	15,000	---	1.47	---
31N-D	Damping	15,000	---	2.44	---
32N-M	Mode Shape	5,000	5,100	2.50	---
33N-M	Mode Shape	5,000	5,800	1.33	---
34N-M	Mode Shape	5,000	5,600	0.34	---
35N-M	Mode Shape	5,000	5,800	0.52	---
36N-SD	Standard Damping	5,000	5,470	0.34	2.8
37N-SD	Standard Damping	5,000	5,050	0.53	3.9
38N-SD	Standard Damping	5,000	4,720	1.39	3.1
39N-SD	Standard Damping	5,000	5,900	2.50	6.8
40N-D	Damping	10,000	8,130	1.45	2.3
41N-D	Damping	25,000	---	---	---

* The direction of the stepwise sweep was up, i.e., from a lower to higher frequency. For all other tests the direction of the sweep was down, i.e., from a higher to lower frequency.

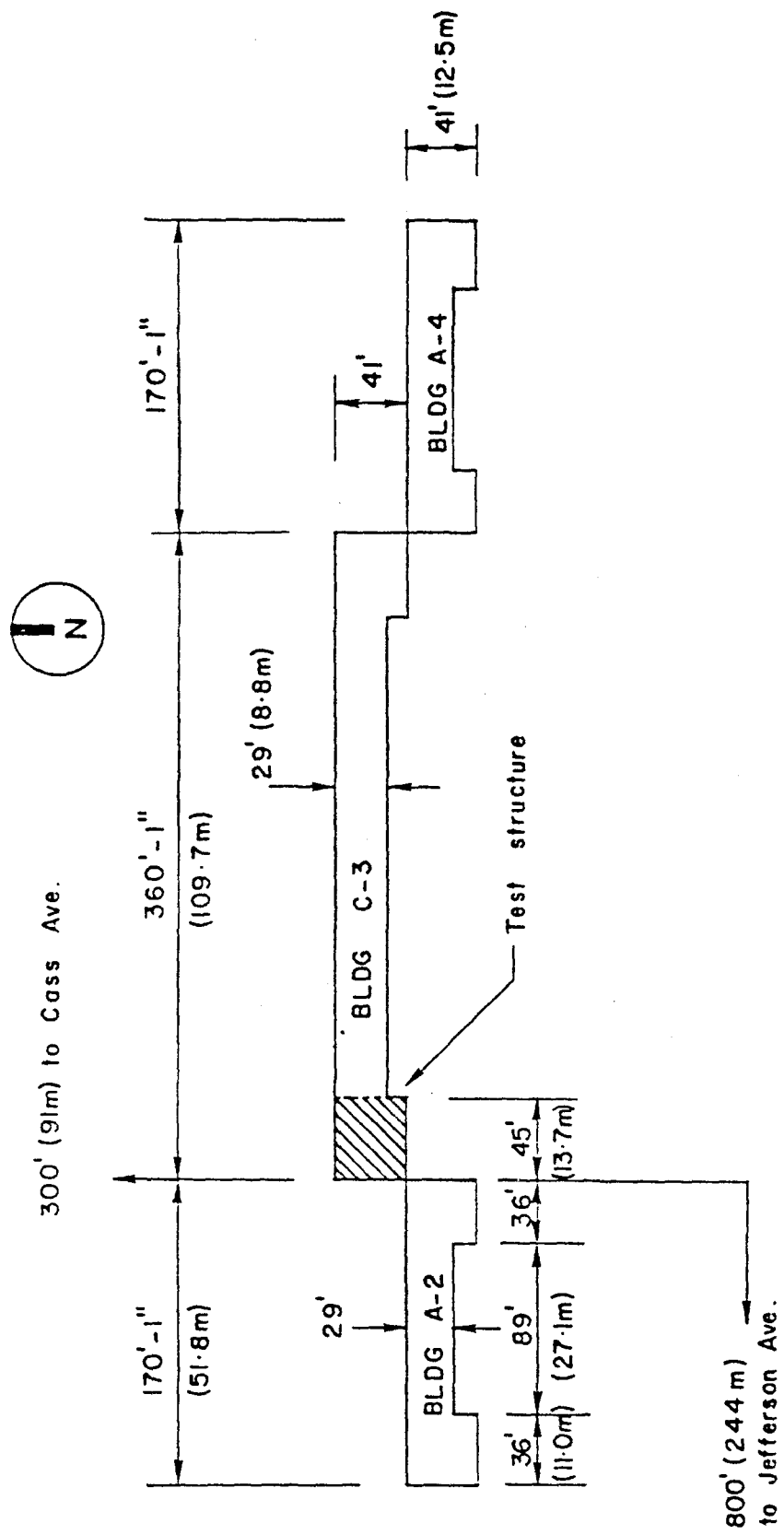


Figure 2.1 Overall Plan Dimensions

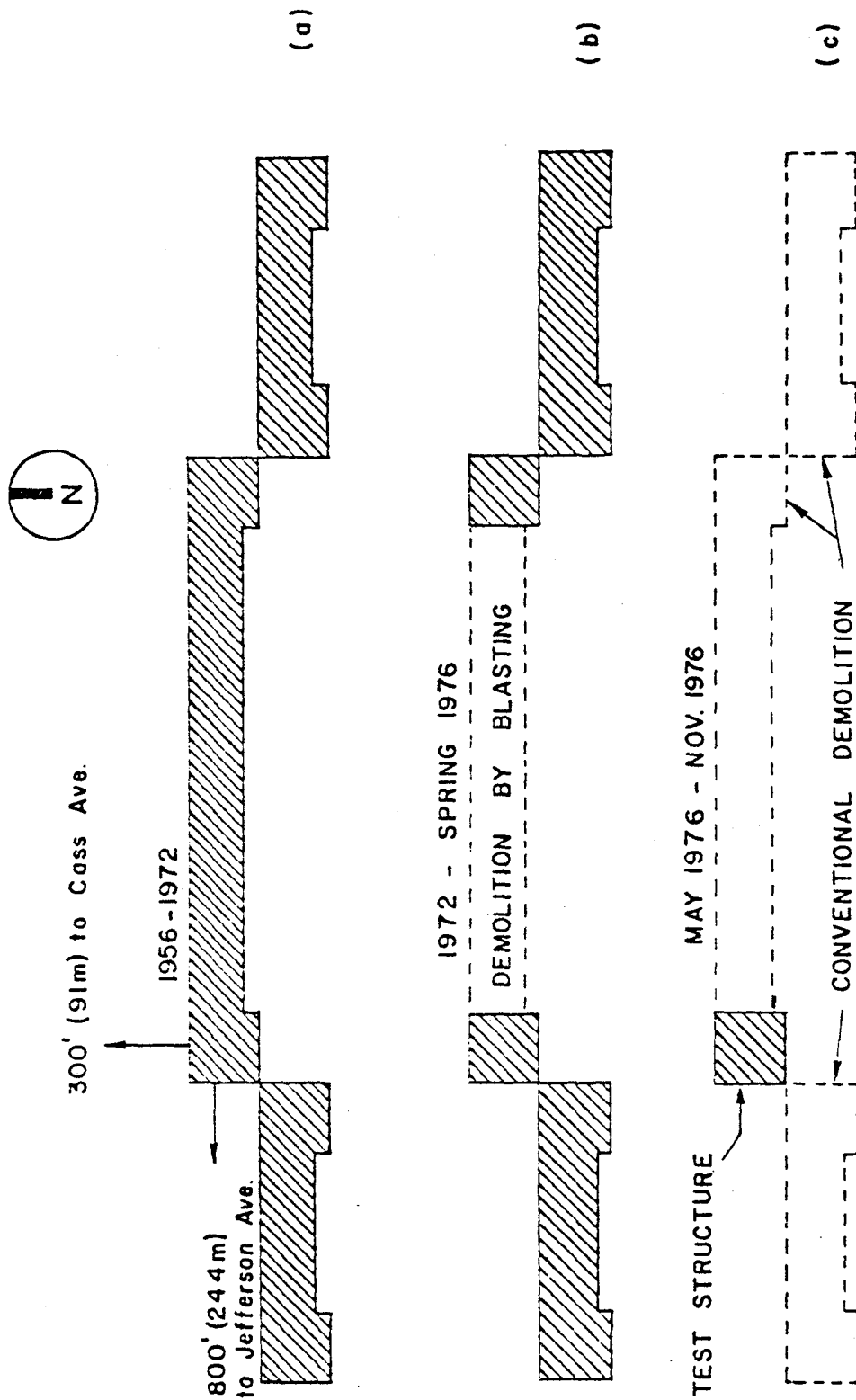


Figure 2.2 Demolition Scheme

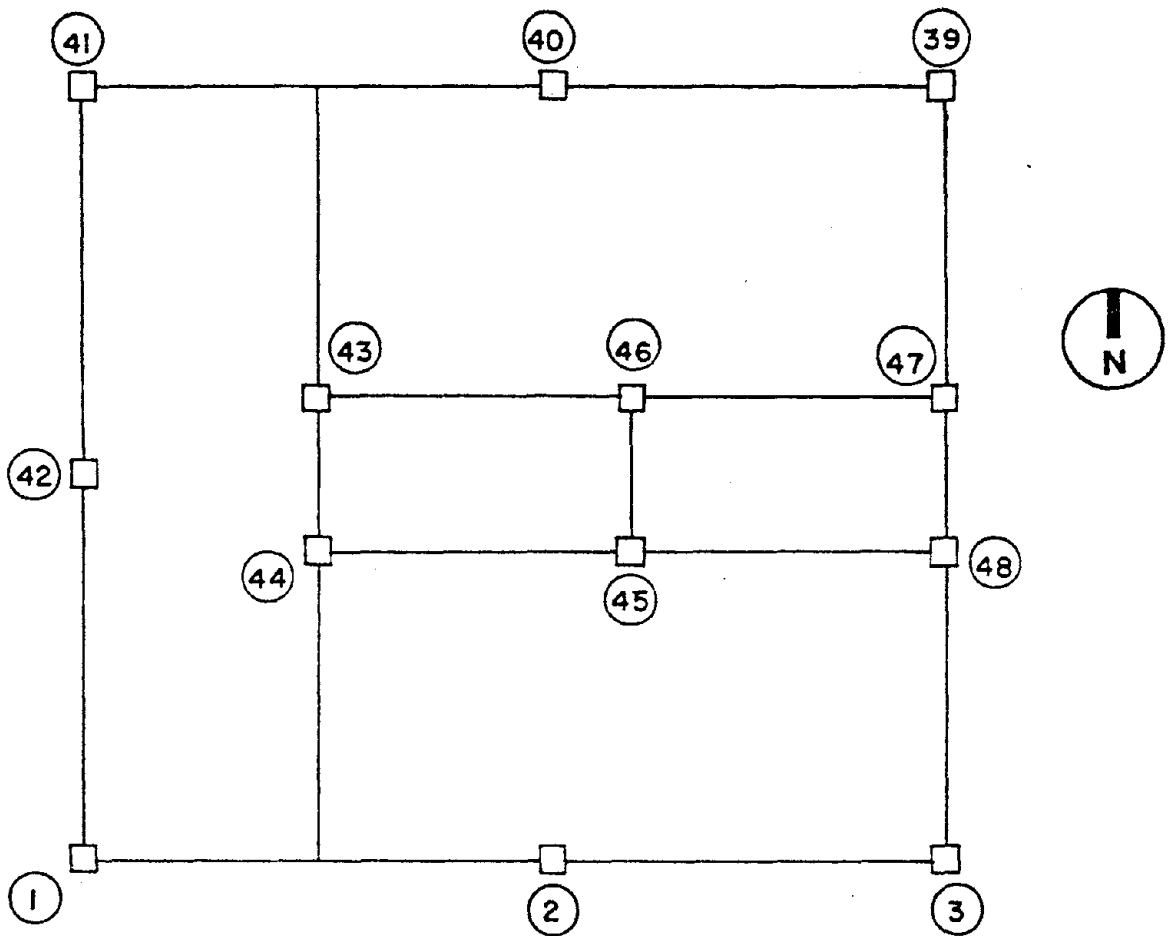


Figure 2.3 Column Designations

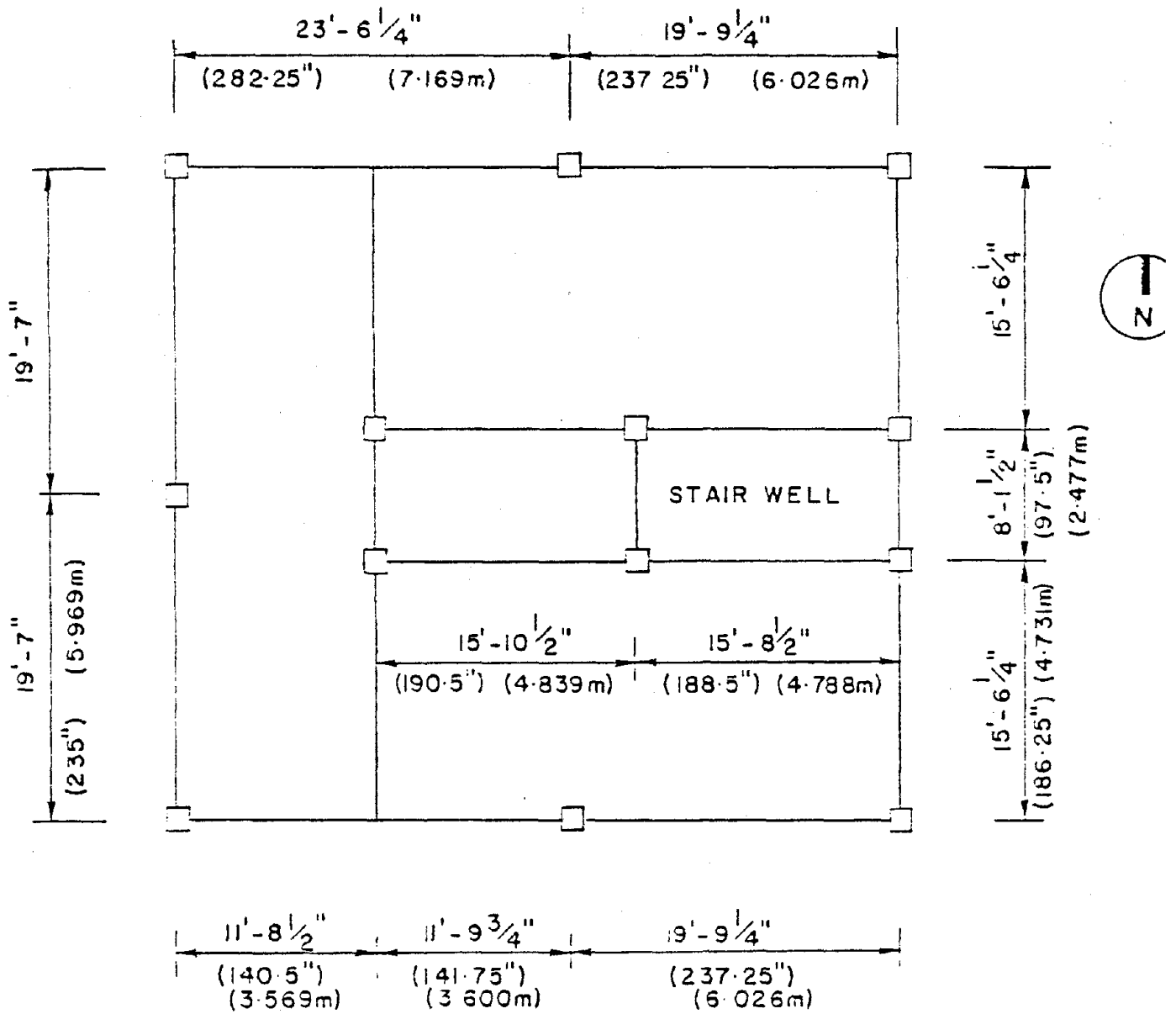


Figure 2.4 Theoretical Floor Plan Dimensions Between Column Centers

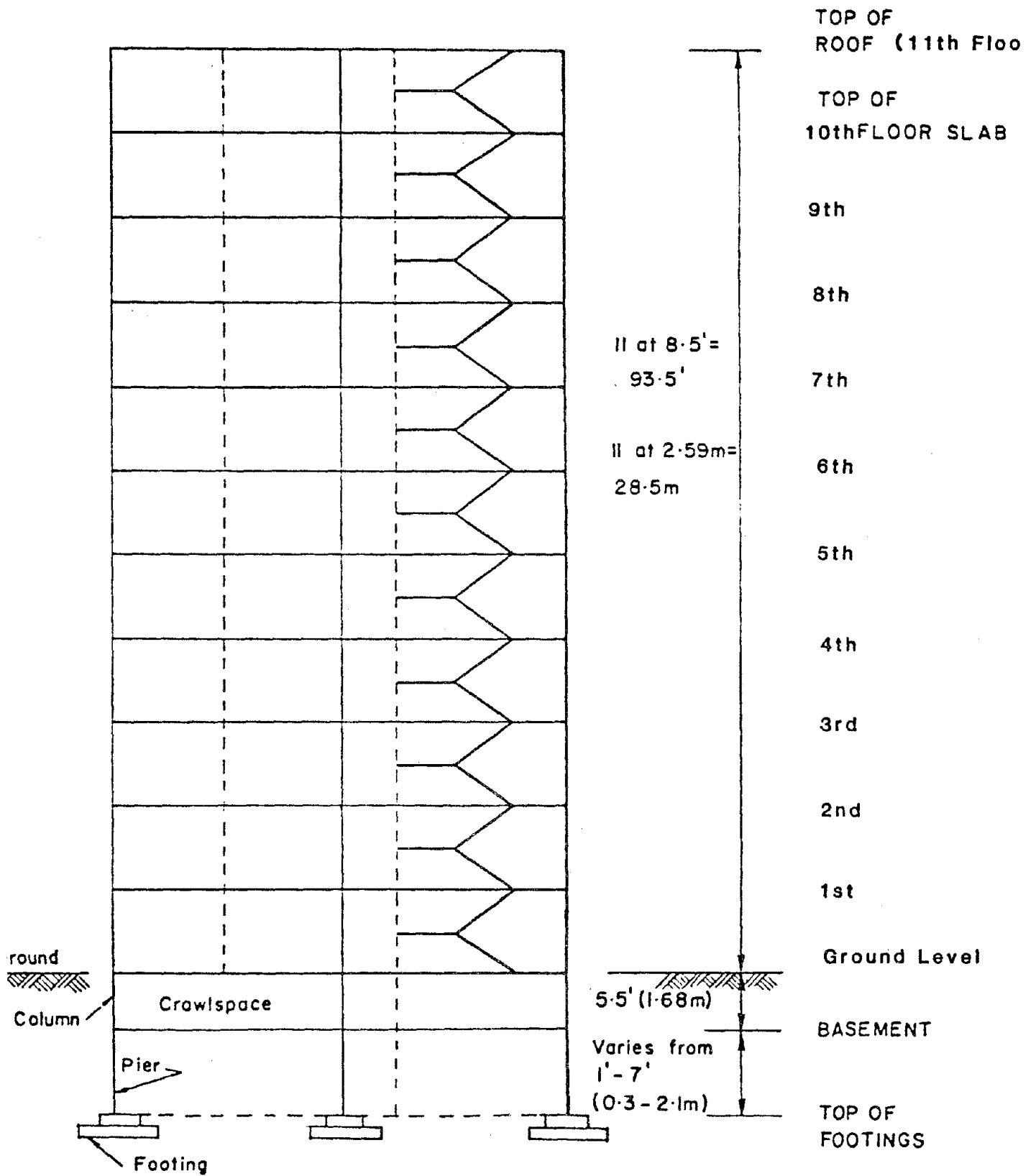


Figure 2.5 Building Elevation

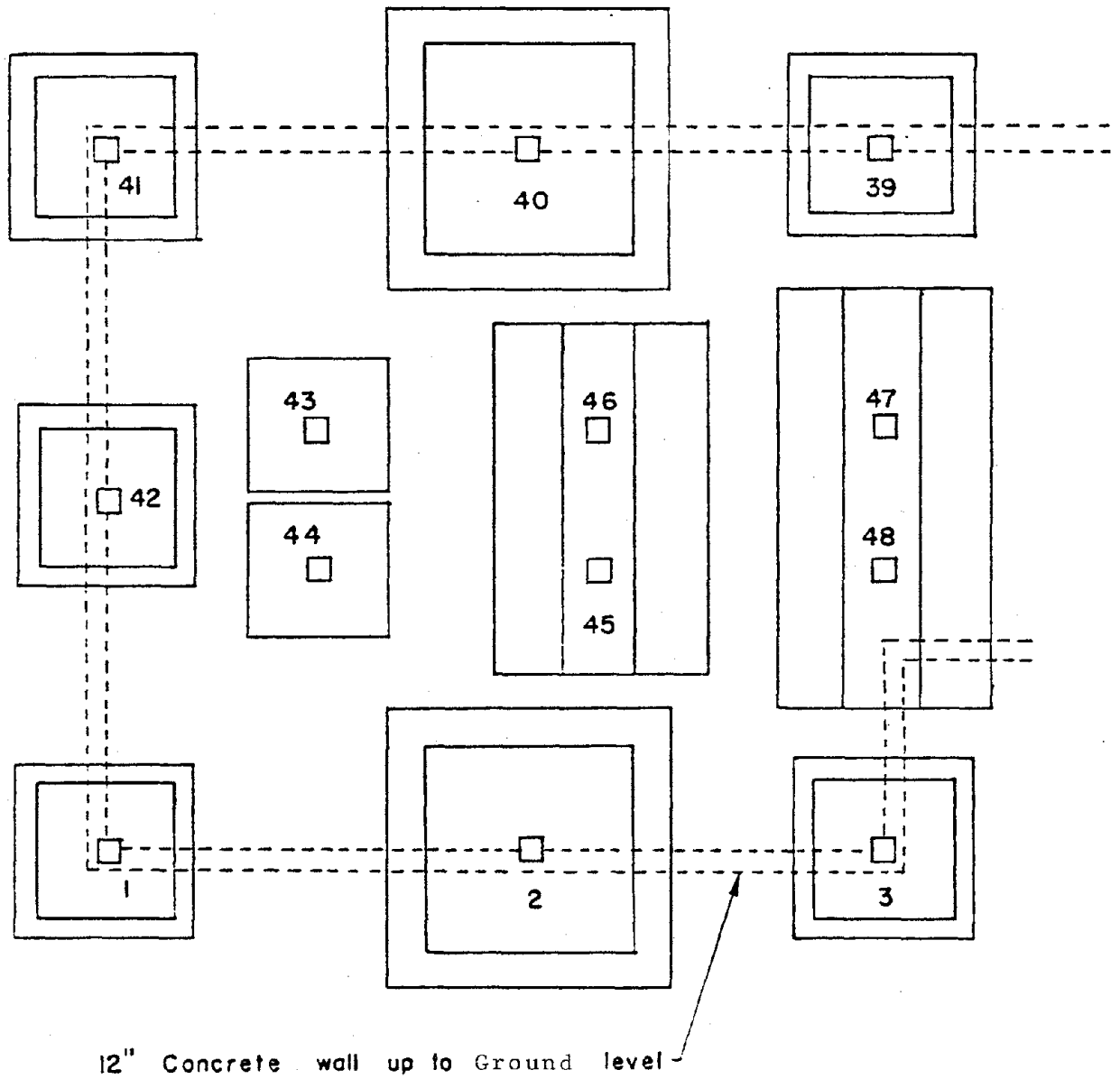


Figure 2.6 Footing Plan

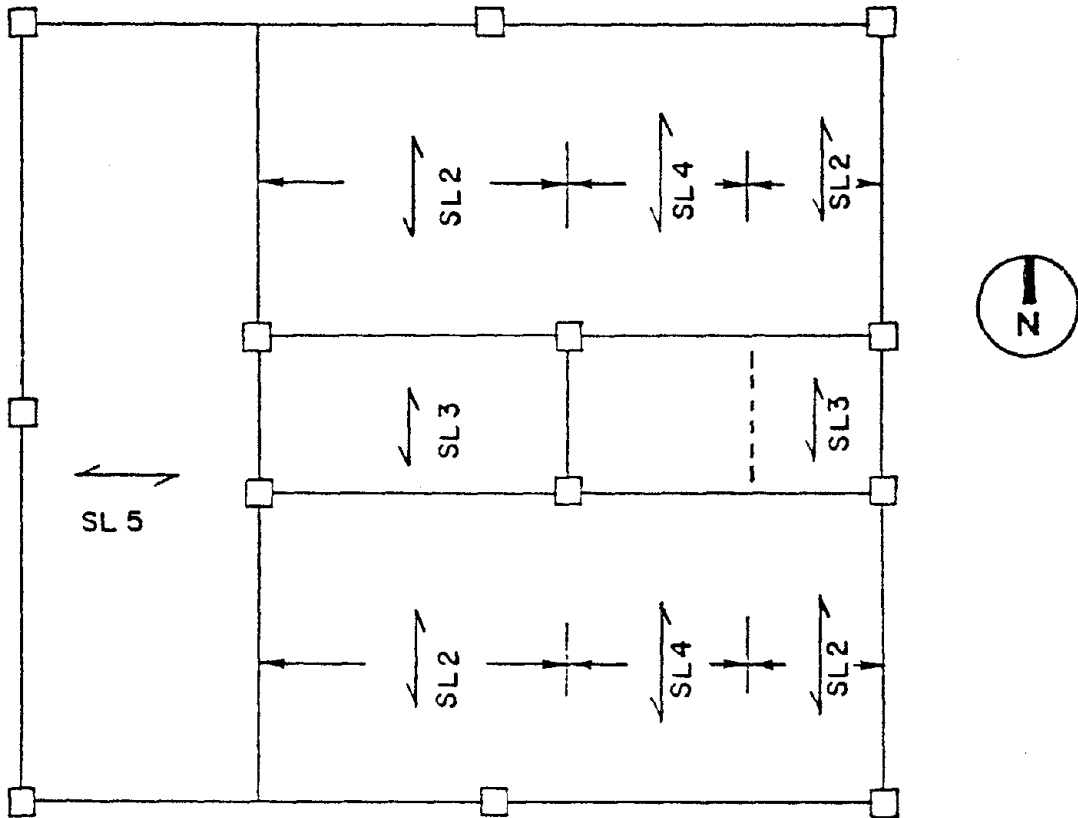
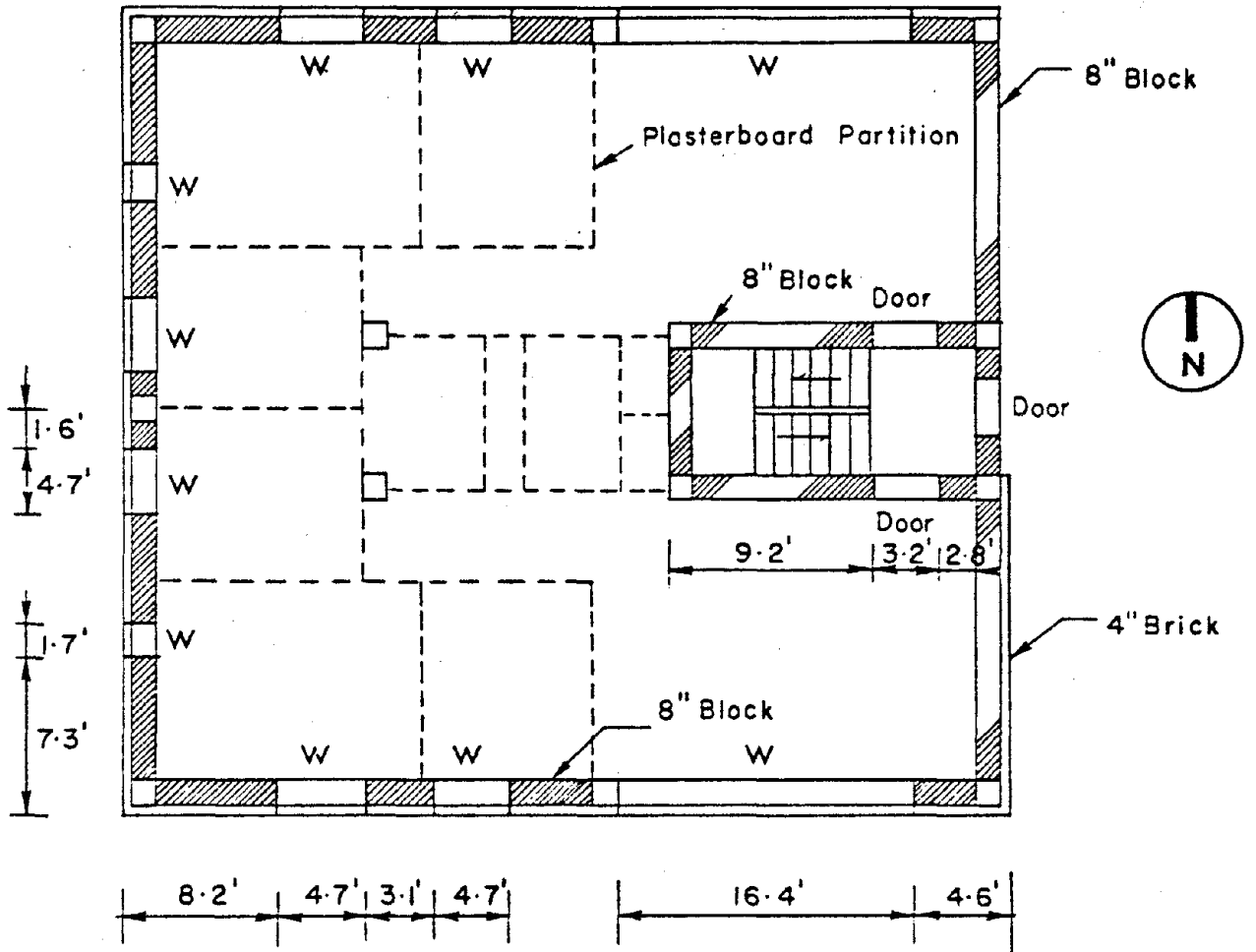


Figure 2.7 Slab Designations



Window height : $4' - 2\frac{5}{8}"$

Figure 2.8 Cladding

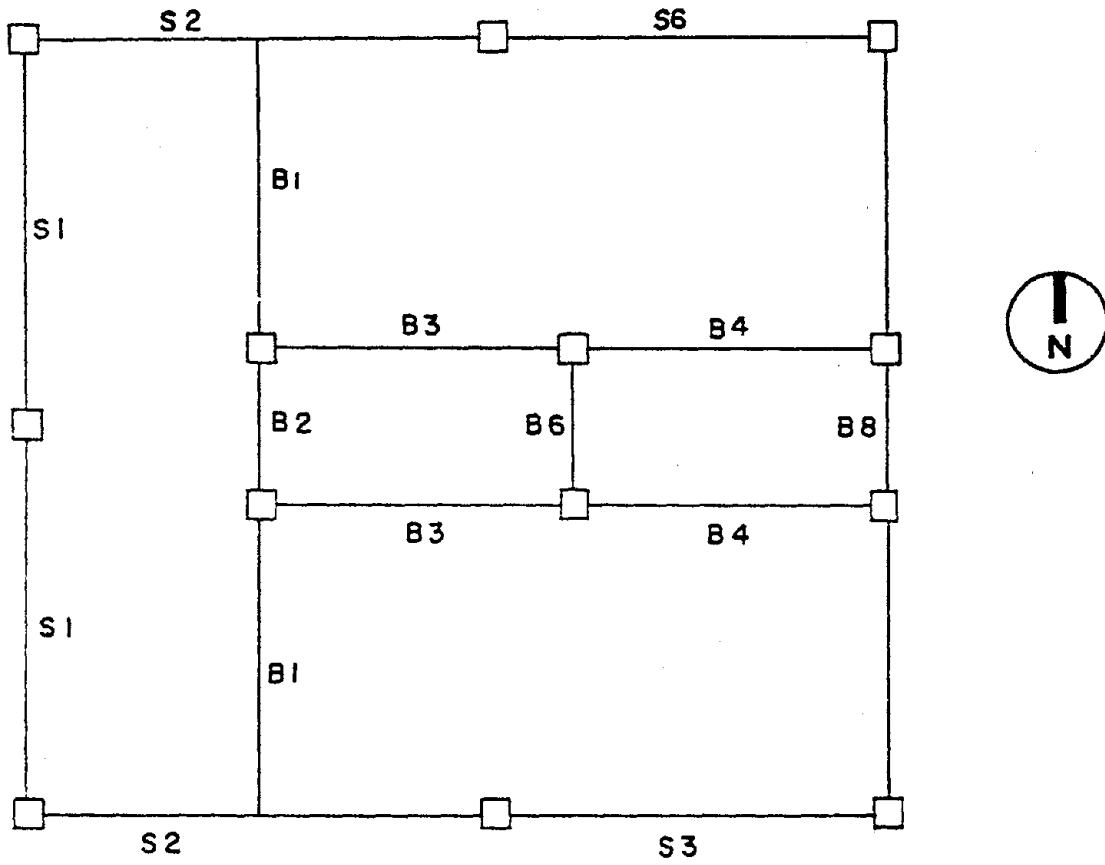


Figure 2.9 Beam Designations

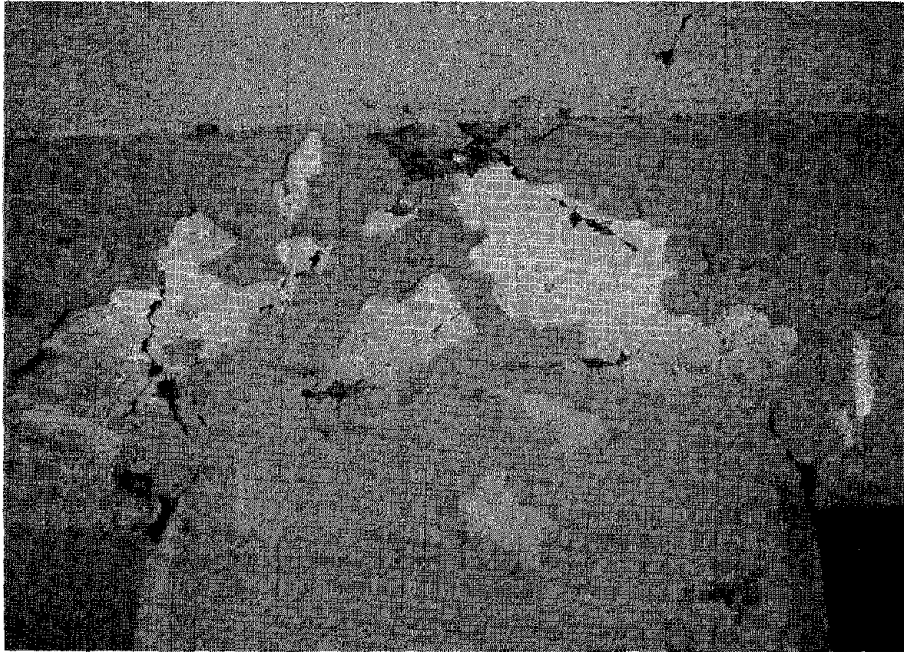


Figure 2.10 Cracked Joint, Column 45, Level 1. During E.W. Tests

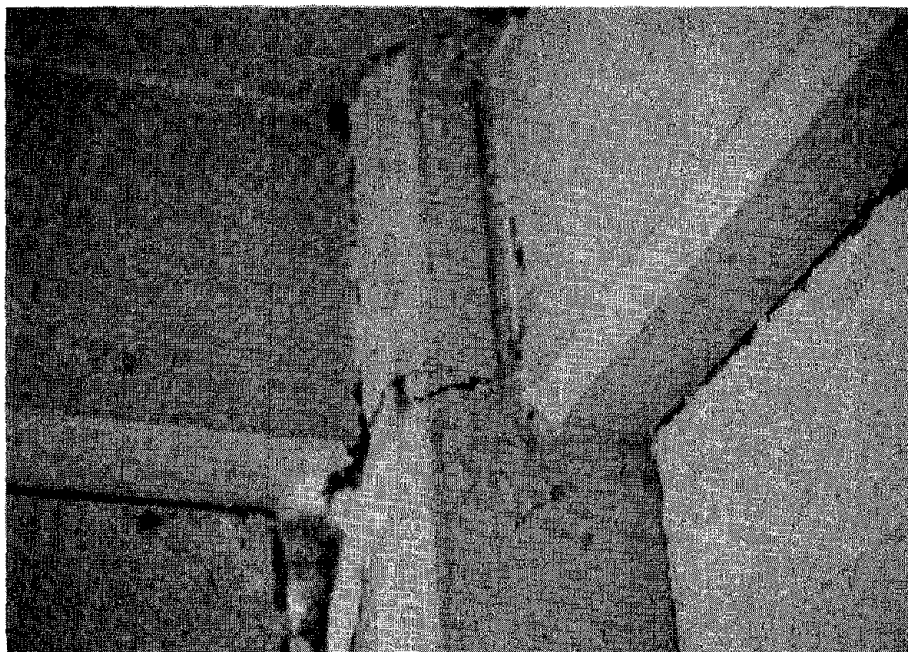


Figure 2.11 Joint, Column 1, Level 2. During E.W. Tests

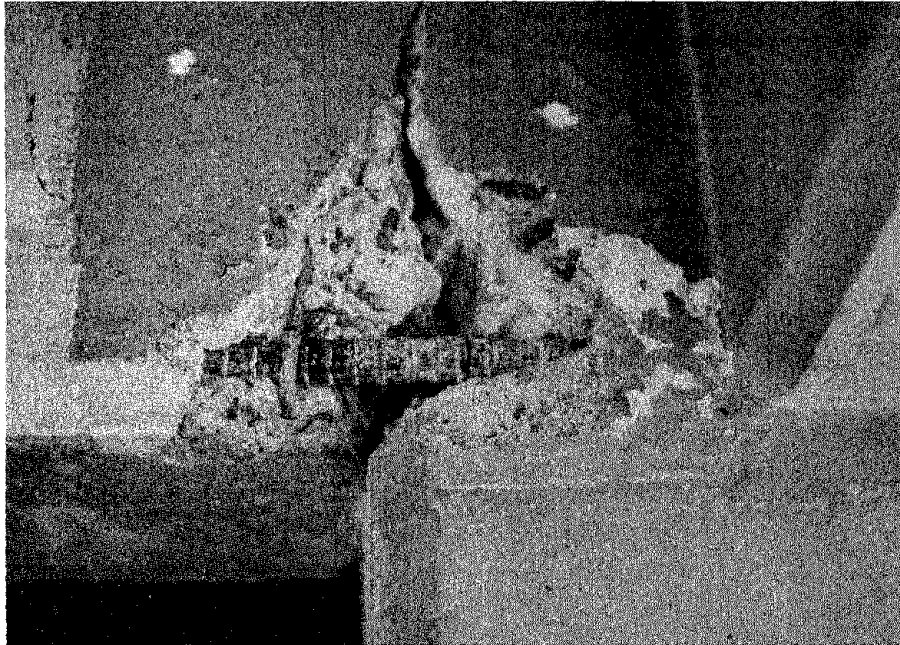


Figure 2.12 East End of Beam B-4 Level 1. After E.W. Tests

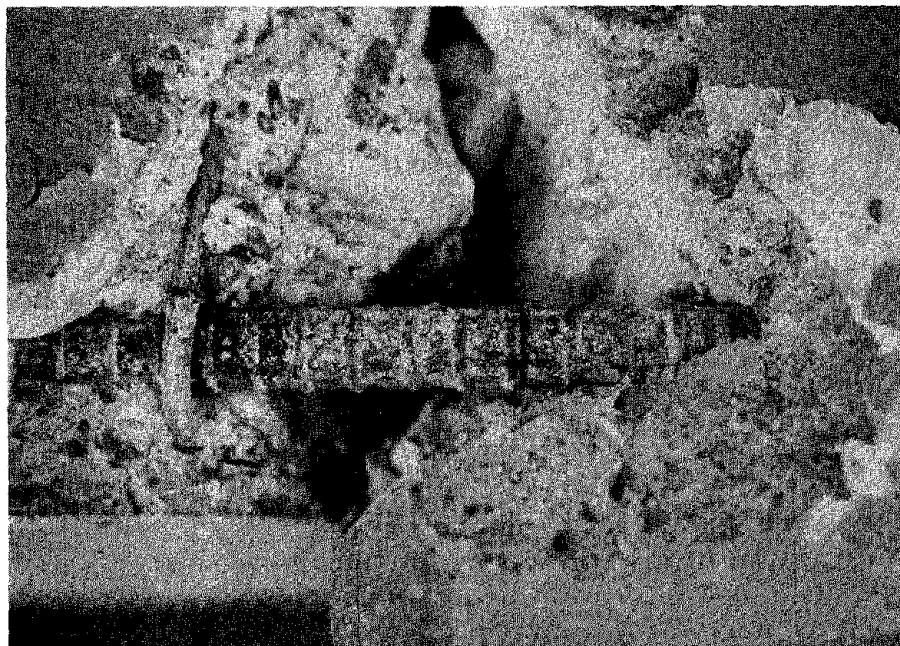


Figure 2.13 Fractured Reinforcing Bar, East End of Beam B-4, Level 1

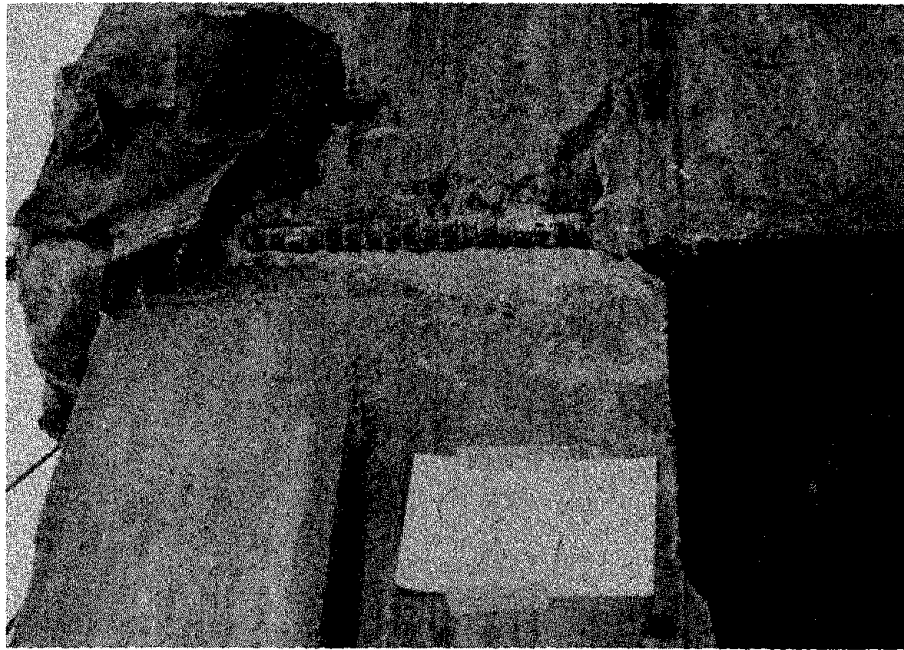


Figure 2.14 Exposed Reinforcing Bar, After E.W. Tests

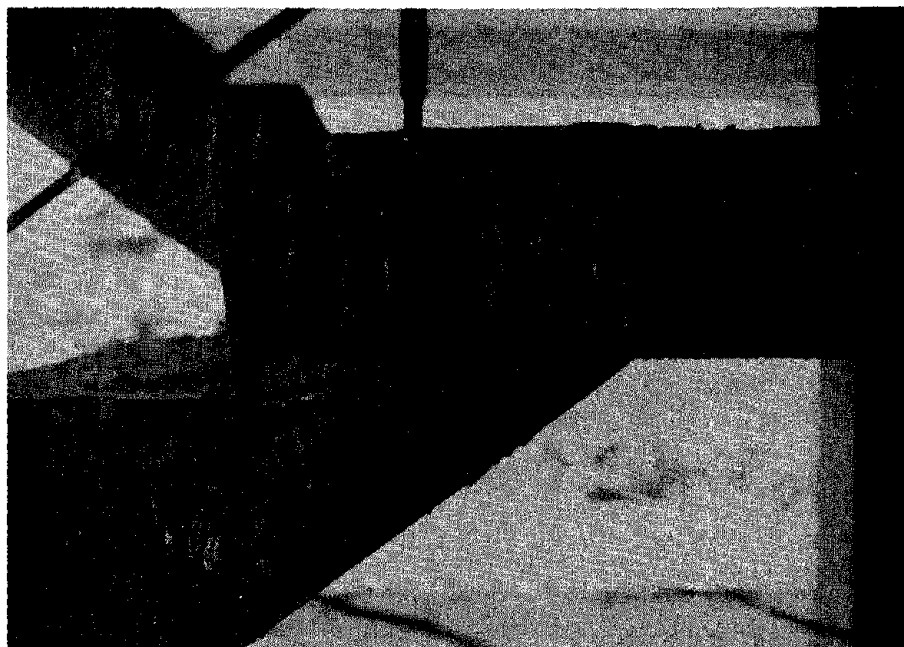


Figure 2.15 Stairway Joint Damage, After E.W. Tests



Figure 2.16 Top of Stairway Joint. After E.W. Tests

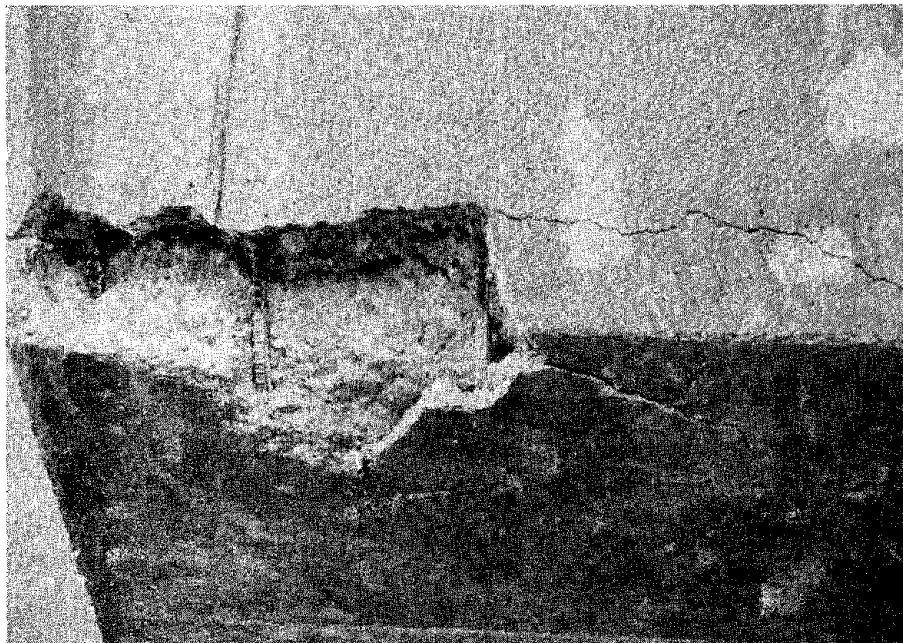


Figure 2.17 Bottom of Stairway Joint. After E.W. Tests

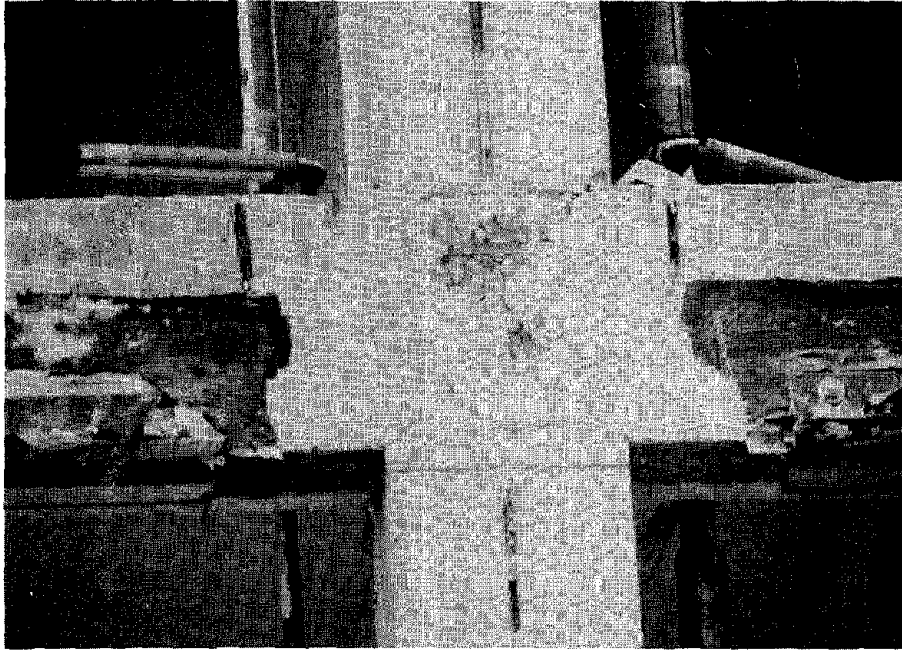


Figure 2.18 Damage in Joint, Center Column 42. West Face

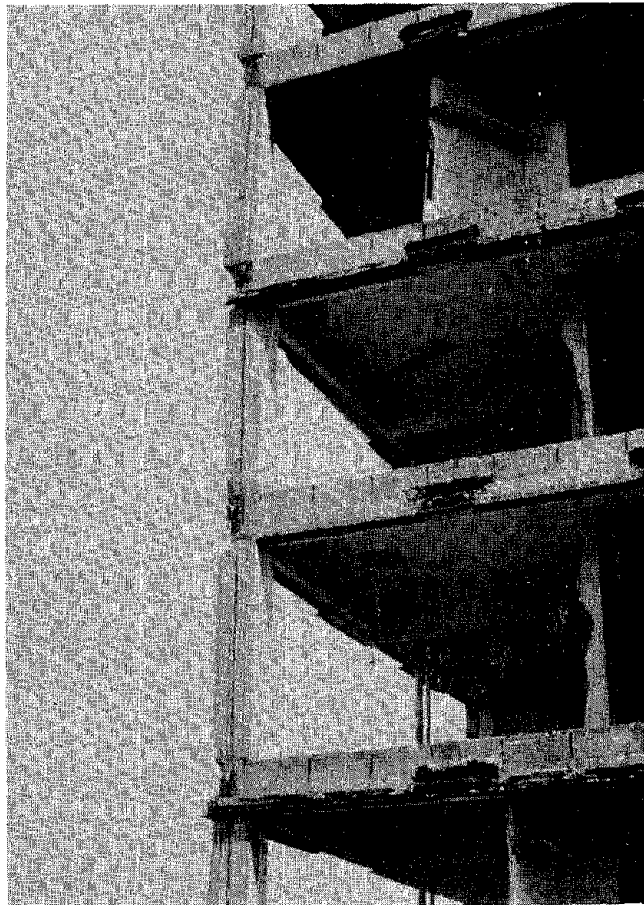


Figure 2.19 Column 41, Level 3. Interior Joint

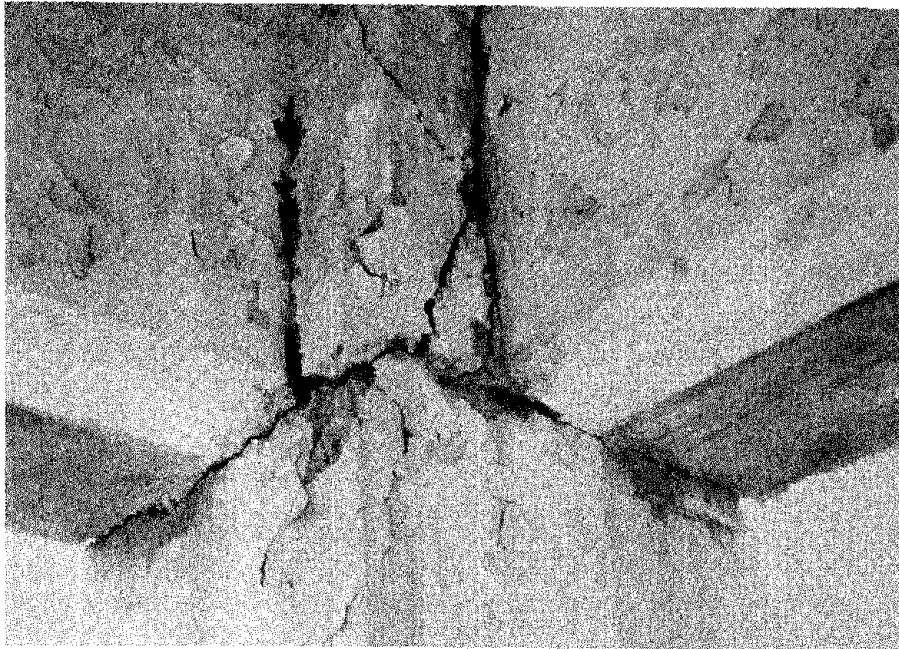


Figure 2.20 Column 41, Level 3

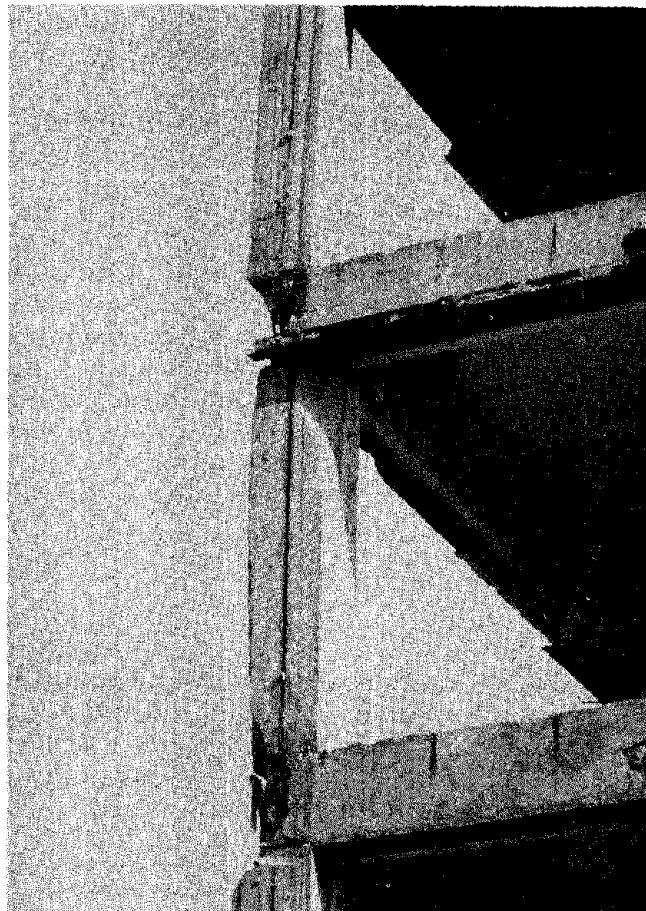


Figure 2.21 North West Corner (Column 41) After Testing

3 CORRELATION OF SMALL AMPLITUDE TEST RESULTS

3.1 INTRODUCTION

The first stage of the experimental test program involved a series of small amplitude tests performed by Applied Nucleonics Company (ANCO) to determine frequencies, response shapes and damping values. The results are reported in detail in reference 2 and a summary is given in Chapter 2 of this report.

The analytical studies reported in this chapter involved a series of correlation studies with the small amplitude tests. The structure was modelled using the general purpose computer program SAPIV [4]. Structural properties were derived from the plans, and material properties were obtained from the material and dimensional survey of the building performed before the shaking tests began [1].

The analytical model was used to obtain natural frequencies and mode shapes. The effect of variations of a number of parameters on the dynamic characteristics of the model was studied and included:

- A. The stiffness of the infill walls
- B. The effective stiffness of the stairways
- C. The effective section properties of the frame sections.

Because of the omni-directional nature of the applied excitation and the closely spaced frequencies of the first two triplets of fundamental frequencies the response shapes obtained from the small scale tests could not be directly compared with the mode shapes obtained from the analysis. In order to make a comparison with the analytical mode shapes an attempt was made to reduce the tested response shapes to mode shapes. A computer program was written to solve the equation of harmonic motion using trial frequencies and eigenvectors and adjusting the eigenvectors iteratively in an attempt to obtain a match with the measured accelerations. The "best fit" mode shapes obtained from this procedure were then used in the correlation with the analytical results.

3.2 ANALYTICAL TECHNIQUES

A major objective of this research was to determine the extent to which currently available analytical techniques could predict the response of actual structures. Thus the analytical studies were performed with the use of public domain computer programs. Modelling of the structure was performed using assumptions consistent with normal structural analysis.

The computer program SAPIV (described in detail in Subsection 3.2.1) was used for this phase of the work. Special computer programs were written to accomplish the additional analytical work required to transform experimental response shapes into mode shapes. The theoretical basis and operation of these programs are described in Section 3.4.

3.2.1 SAP IV Computer Program

SAP IV is a general purpose finite element program for the linear elastic static and dynamic analysis of structural systems of arbitrary configuration. This version is an enhanced revision of the original SAP program developed by Professor E. L. Wilson and others at the University of California, Berkeley.

The program contains a library of finite elements which includes the following:

- o Three Dimensional Beam
- o Truss
- o Two-dimensional plane stress/plane strain
- o Three Dimensional Solid
- o Axisymmetric solid
- o Plate/shell
- o Spring (translational or rotational)

These element types may be used singly or in compatible combinations. Analysis options include static analysis, eigenanalysis, response spectrum analysis or time history analysis.

For the small scale test correlation study the eigenanalysis solution techniques were used to obtain the frequencies and mode shapes of the structure. Plot routines available within the SAP IV program were used to obtain the mode shapes graphically and a special purpose program was written to obtain graphic comparisons of the computed and measured mode shapes.

3.3 ANALYTICAL MODEL

The general dimensions of the model used in the SAP IV program were obtained from the structural drawings, and are as shown in Figure 3.1. The initial series of analyses took advantage of a number of features available in the SAP IV program to reduce computational time. In particular, "slave" nodes were used to reduce the number of degrees of freedom and the number of subspace iterations used in the eigensolution was limited. "Slaving" nodes which are interconnected by a rigid diaphragm reduces the total number of degrees of freedom and the size and cost of the analysis. However as implemented in the SAP IV program use of the slaving option imposes two main restrictions on the user:

- (a) Only beam elements may be incident on the "slave", or dependent, nodes
- (b) Lumped masses may be applied only at "master", or independent, nodes.

A comparative analysis was performed with all nodes independent to ascertain the effects of these limitations on the theoretical response. The results were compared with those obtained from the analysis using "slaved" nodes. The agreement was good and slaving was used in the remainder of the analyses.

For solution of the eigenproblem computation time is directly proportional to the number of iterations performed. Thus, a limitation on the number of iterations leads to savings in time at the expense of some accuracy in solution. The initial parametric studies used a convergence tolerance of 0.5 with a maximum of 4 iterations. The final run was then repeated with a tolerance of 0.00001 and a limit of 16 iterations to determine the effect of this approximation.

The actual measured values reported in reference 1 were used for the material properties and member dimensions. The measured concrete strength was used to derive a value of the modulus of elasticity for concrete using the ACI-318 equation of

$$E=57000\sqrt{f'c} \quad (3.1)$$

The stairs were modelled as equivalent diagonal struts spanning between floors, and the infill walls were also modelled as struts. The properties assigned to these struts were one of the parameters studied in the SAP IV analyses.

In the following sections detailed information on the methods used to derive properties for each section of the building are given.

3.3.1 Modelling Assumptions

A number of assumptions about the structure were made prior to the derivation of the detailed model, in particular:

- full column fixity occurs at the first floor level, i.e. at the top of the basement walls
- rigid floor diaphragms are assumed

These assumptions are based on field observations and experimental results which showed that very little motion occurred in the structure below the ground level, and also that no distortion occurred in the diaphragm.

It should be noted that these assumptions are consistent with those generally used for structural analysis. They are usually made for reasons of economy. The experimental study provided data on which to judge the validity of these assumptions for an actual structure.

3.3.2 Modelling of Frame

Reference 1 showed that the dimensions of the columns and girders did not vary significantly from the values shown on the structural drawings so the latter values were used in determining the properties for the model. Column areas and moments of inertia were calculated assuming a rectangular section. For the girders T-beam or L-beam sections were used as appropriate. For the columns the axial area was taken as the gross concrete area and the shear area in each column as 80% of this value. The moment of inertia about each axis was based on the gross concrete dimensions. Effective flange widths were calculated for the girders according to the provisions of ACI-318. The shear area was taken as the area of the web and the moment of inertia calculated based on the gross area of concrete.

Measurements of concrete strength reported in reference 1 showed that the average concrete ultimate compressive strength was $f'_c=8$ k.s.i. Using equation (3.1) the value of the modulus of elasticity, E , was calculated to be 5,100,000 p.s.i. This value was used for all beams and girders.

The master/slave option available in the SAP IV program was used because of the rigid floor diaphragm assumption. To enable proper mass distribution, four interior nodes on each floor were selected as master nodes, and the remaining floor nodes were connected to these.

3.3.3 Diaphragm Properties

At each level all beams and girders are interconnected by the floor slab with a minimum thickness of approximately 4". The experimental results showed that this slab effectively formed a rigid diaphragm and the floors retained their rectangular shape when displaced. Therefore the horizontal members joining the master nodes on each floor were modelled with a very large stiffness in their transverse direction. This effectively enforced rigid diaphragm action.

3.3.4 Stairs

Although the stairs have a relatively complex geometry their effect on the overall frame stiffness is similar to that of an inclined strut member. For the SAP IV model beam elements spanning between floors were used to approximate their effect.

The properties of these inclined beams were computed from the overall stair dimensions as:

$$\begin{aligned} A &= (B \times T) / 2.0 \\ I_x &= 0.5 (B \times T^3) / 12.0 \\ I_z &= 0.5 (T \times B^3) / 12.0 \end{aligned}$$

where

$$\begin{aligned} B &= \text{Width of stair tread} = 3'-9" \\ T &= \text{Average stair thickness} = 4.5". \end{aligned}$$

These values were originally selected as an initial approximation, but as the results show, the properties based on this gross stiffness provided satisfactory results. This could be expected as the tests showed that the stairs retained their integrity until cracking occurred under the large displacement loadings.

The stair geometry and the members used to model them are shown schematically in Figure 3.2.

3.3.5 Infill Walls

At the time of the small amplitude tests the structure was fully clad above the first floor level with unreinforced masonry blockwork between exterior columns around the building perimeter and also around the stairwell. A 4" brick veneer was used connected to the 8-inch blockwork forming the exterior walls. All of these masonry courses contributed to the building mass but as the brickwork was outside the column lines it could be assumed to have little effect on the building stiffness.

The concrete masonry infill panels restrict pure frame type deformations and therefore must be assumed to contribute to the overall stiffness. Very little data on the blockwork was available other than that it was 8" unreinforced concrete block. Observations reported from the small amplitude tests were that "during Tests 2 and 3 cracking of shear and filler walls was observed, particularly in the stairwell areas at the fourth, fifth and eleventh floors" [2]. This suggests that at least some walls were interacting with the frame. General observations during the later large amplitude tests [3] noted that while some walls did move with the frame, others had sufficient distance around their boundaries to be isolated from the frame deformations.

Therefore beyond the fact that it can be inferred that some walls interact with the frame no systematic data is available as to which walls could be considered separated from the frame and which walls were part of the lateral load resisting system. Because of the indeterminate nature of the walls' response the effect of these elements was one of the major parameters studied in this phase of the investigation.

To model the infill panels, a single diagonal strut spanning between

columns was used. Consideration was given to modelling these panels with plane stress finite elements, but this formulation was not compatible with the use of "slaved" nodes, and as later analyses confirmed, it was believed that the additional computational effort would not be warranted because of the highly variable nature of the wall interaction.

Preliminary strut properties were derived by equating deflections. Referring to Figure 3.3, the deflection of the wall is the sum of the shear and flexural deflections, D_v and D_f respectively. Each of these components may be computed as follows:

$$D_v = \frac{Vf}{G} \left[\frac{h_1}{BT} + \frac{h_3}{BT} + \frac{h_2}{\sum d_i T} \right] \quad (3.2)$$

For the rectangular walls the shear factor, f , was assumed to be 1.3.

$$D_f = \frac{Vh_2^3}{12 EI_t} \quad (3.3)$$

where $I_t = \frac{Td_i^3}{12}$

For a shear force V the total infill deflection equals $D_v + D_f$.

For the equivalent truss member the horizontal displacement for a force V is given by:

$$D_1 = \frac{VB \cos \beta}{EA} \quad (3.4)$$

From the "Reinforced Masonry Handbook" [8] typical values for masonry blocks were taken as:

$$E = 1,350,000 \text{ psi}$$

$$G = 540,000 \text{ psi} = 0.4 E$$

Using these relationships equivalent strut properties were computed for each infill panel and these are detailed on Figure 3.4.

The method by which these properties were derived assumes a homogeneous, linearly elastic material and as the field observations note the behavior of the walls was far more complex than this. However, the above procedure served as a starting point for the analysis. Modifications to these properties are discussed in later sections.

3.3.6 Mass distribution

The calculation of the structure mass is a relatively straightforward process given the dimensions and materials for each element. The following weight densities were assumed:

- (1) Reinforced concrete 150 pcf
- (2) Concrete Masonry 50 psf
(8" hollow core, ungrouted, normal weight aggregate)
- (3) Brickwork 40 psf
(4" brick)

The dimensional study of the building had shown relatively minor variations in column and girder sizes from those specified on the plans. The specified dimensions were used, therefore, to compute weights. As the slab forms a relatively high proportion of the total weight, the mean measured thickness was used to compute slab weight, i.e. 4.043" for nominal 4" slab and 5.331" for the 5" nominal slab.

Because of the lack of positive connection between the blockwork and the columns the full weight of the masonry walls was assumed to act on the floor on which the wall rested rather than being distributed to the floors above and below the wall.

In the analytical model the mass was lumped at the four master nodes at each floor level. The translational mass was computed for each node according to the tributary area. An additional lumped rotational inertia was added at each master node so that the correct second moment of mass for the floor was obtained.

3.3.7 Column Base Fixity

The dynamic testing of the structure indicated that the base of the structure was effectively fully fixed by the crawl space walls and the mass of concrete below the ground level. Therefore all column bases were considered fully fixed at the ground level. To check the effects

of this assumption two analyses were performed with an approximate model of the soil properties.

For these runs a modulus of subgrade reaction in the range of those encountered for stiff clays such as those underlying the test structure was assumed. Using this modulus and the area of spread footing under each column an effective vertical stiffness was computed and a boundary element with this axial stiffness inserted under each column. Only vertical movement was considered with no attempt made to model rotation of the footings.

3.4 REDUCTION OF EXPERIMENTAL DATA

As stated in the introduction to this section, the omnidirectional nature of the excitation force prevented a direct comparison of the test and analytical results. The test response shapes required reduction to obtain mode shapes. The procedures used for this reduction are described in the following subsections.

3.4.1 Forced Vibration Test Procedures

A complete description of the tests performed is given in reference 2 and a summary is provided in Chapter 2 of this report. To interpret the test results the experimental response curve is compared to theoretical response curves obtained from the analysis of an appropriate mathematical model of the structure. The dynamic properties of the mathematical model whose theoretical response fits the experimental results are considered to be the dynamic properties of the structure.

The response shapes measured during testing are the actual response of the structure to the applied forcing function, and thus are a combination of various normal modes of the structure. For structures with well separated modes the response shapes at particular frequencies will provide a good estimate of the actual mode shape. The response will include some coupling, however, for closely spaced modes. An attempt to separate the "pure" mode shapes from the coupled response shapes obtained from the tests is detailed in the following sections.

3.4.2 Equation of Harmonic Motion

The equations of motion for single and multi degree of freedom systems loaded with a harmonic forcing function may be obtained from standard textbooks on dynamics, e.g. reference 9. For a linearly elastic system the normal modes of vibration may be uncoupled and the total response obtained as the sum of the response of each mode. Similarly, for loading in more than one direction the response due to each load component may be combined to give the total response.

Consider a structure with rigid diaphragms, such as that shown in Figure 3.5, loaded with an omnidirectional shaker at the top floor. The loading functions are:

$$\begin{aligned} F_x &= mr\omega^2 \sin(\omega t) \\ F_y &= mr\omega^2 \sin(\omega t - \frac{\pi}{2}) \\ F_\theta &= mr\omega^2 R \sin(\omega t - \alpha) \end{aligned} \tag{3.5}$$

where $\alpha = \tan^{-1} \left(\frac{e_x}{e_y} \right)$

and $R = \sqrt{(e_x^2 + e_y^2)}$

The acceleration at mass i resulting from harmonic loading at mass ℓ is:

$$\begin{aligned} \ddot{x}_i &= \sum_{j=1}^N \frac{\phi_j^i \phi_j^\ell mr\omega^2 \left(\frac{\omega}{\omega_j}\right)^2 \sin(\omega t - \psi_j)}{\sqrt{[1 - \left(\frac{\omega}{\omega_j}\right)^2]^2 + (2\beta_j \frac{\omega}{\omega_j})^2}} \\ \psi_j &= \tan^{-1} \left(\frac{2\beta_j \frac{\omega}{\omega_j}}{1 - \left(\frac{\omega}{\omega_j}\right)^2} \right) \end{aligned} \tag{3.6}$$

ϕ_j is the j th normal mode.

For a particular forcing function, define

$$m\ddot{r} = P \quad (3.7)$$

$$A_j = \frac{\omega^2 \left(\frac{\omega}{\omega_j}\right)^2}{\sqrt{\left[1 - \left(\frac{\omega}{\omega_j}\right)^2\right]^2 + \left(2\beta_j \frac{\omega}{\omega_j}\right)^2}}$$

A_j is effectively an amplification factor for a particular mode j . The value of this factor is strongly dependent on the value of the ratio of the forcing frequency to the modal frequency, (ω/ω_j) , and will have its maximum value as the ratio approaches unity.

Equation 3.6 may be expressed as

$$\ddot{x}_i = \sum_{j=1}^n \phi_j^i \phi_j^l P A_j \sin(\omega t - \psi_j) \quad (3.8)$$

Consider the first triplet of two translational plus the torsional mode, with frequencies of ω_1, ω_2 , and ω_3 . Assume that each mode has three components, i.e. ϕ_j^x, ϕ_j^y and ϕ_j^θ where subscript j refers to the mode and the superscript refers to the floor level. (Note that because of the rigid floor diaphragm assumption the eigenvector at each floor level is described by three components.)

For an omnidirectional shaker, the force can be considered as the three components acting on the respective mode shape components, i.e.

F_x acting on ϕ_j^x
 F_y acting on ϕ_j^y
 F_θ acting on ϕ_j^θ

where the shaker is positioned at floor 11, the top level. The acceleration in a particular direction will be the sum of the modal accelerations in that direction from each mode and from each load, e.g. in the x direction at floor l :

(3.9)

$$\begin{aligned} \ddot{x}^{\ell} = & \sum_{i=1}^3 P \Phi_{ix}^{\ell} A_i [\Phi_{ix}^{\ell} \sin(\omega t - \psi_i) + \Phi_{iy}^{\ell} (\omega t - \frac{\pi}{2} - \psi_i) \\ & + \Phi_{i\theta}^{\ell} R \sin(\omega t - \alpha - \psi_i)] \end{aligned}$$

Similarly

(3.10)

$$\begin{aligned} \ddot{y}^{\ell} = & \sum_{i=1}^3 P \Phi_{iy}^{\ell} A_i [\Phi_{ix}^{\ell} \sin(\omega t - \psi_i) \\ & + \Phi_{iy}^{\ell} \sin(\omega t - \frac{\pi}{2} - \psi_i) \\ & + \Phi_{i\theta}^{\ell} R \sin(\omega t - \alpha - \psi_i)] \end{aligned}$$

and

$$\begin{aligned} \ddot{\theta}^{\ell} = & \sum_{i=1}^3 P \Phi_{i\theta}^{\ell} A_i [\Phi_{ix}^{\ell} \sin(\omega t - \psi_i) \\ & + \Phi_{iy}^{\ell} \sin(\omega t - \frac{\pi}{2} - \psi_i) \\ & + \Phi_{i\theta}^{\ell} R \sin(\omega t - \alpha - \psi_i)] \end{aligned}$$

At the nth floor

(3.11)

$$\begin{aligned} \ddot{x}^n = & \sum_{i=1}^3 P \Phi_{ix}^n A_i [\Phi_{ix}^{\ell} \sin(\omega t - \psi_i) \\ & + \Phi_{iy}^{\ell} \sin(\omega t - \frac{\pi}{2} - \psi_i) \\ & + \Phi_{i\theta}^{\ell} R \sin(\omega t - \alpha - \psi_i)] \end{aligned}$$

Similar expressions may be obtained for the Y and Θ directions

These equations define 9 unknowns for a total of 9 equations. However the equations contain both the squares of the eigenvector components and also the cross coupled terms of these components. This form does not guarantee a unique solution. More important, each set of equations is time dependent and the response measurements are taken at a value of ωt at which the response in a particular direction is a maximum. Therefore the equations are not determinant even if the frequencies and damping are assumed known.

The measured response shapes are accelerations at a number of levels and these accelerations are a combination of the modes as derived in the above equations. To obtain "pure" mode shapes from the response shapes an iterative procedure as described in the following section was attempted.

3.4.3 Extraction of Mode Shapes

An iterative attempt to solve the equations derived in the previous section was used. For a given set of frequencies and modal damping, eigenvector components at the loaded level were assumed. This defined the eigenvector components at all other levels. The accelerations at each level for each forcing frequency were then computed and compared with the measured accelerations. Based on this match the loaded floor eigenvectors were adjusted and the procedure repeated.

The procedure required that the measured response values be converted to three components per floor, two translational and one torsional. The actual measured quantities were the two translational components at the corners of each level. This transformation required an estimate of the center of rotation of each floor level, information that could not be extracted from the test results. Therefore the iteration was carried out for three positions of the center of rotation relative to the geometric center of the structure : 0", 40" and 90". The value of 40" was computed from the SAP IV results based on the rotation at the top floor and 90" was computed from the second floor rotated shape. The results did not prove sensitive to the assumed position of the center of rotation because the same eccentricity is used both to transform the measured accelerations to floor rotations and also to transform the eigenvector rotations back to equivalent translations. This has a cancelling effect.

The difference between the measured and analytical mode shapes would be expected to be most marked for closely spaced modes. Because each triplet is well separated from the next higher triplet negligible coupling was assumed between modes of different triplets. Therefore the mode shape extraction was performed over the first three modes and then the next three modes in separate analyses. The third triplet was ignored because of uncertainty in the measured data and also because the modes are fairly widely separated.

3.4.4 Results of Mode Shape Extraction

Table 3.1 lists the measured floor accelerations, converted to two translations plus one rotation per floor. These values have been normalized to a value of 1.000 at the top level for translations and to a value of 0.00100 for rotational response. Also listed in Table 3.1 are the eigenvectors obtained as those giving the best fit to the measured response shapes. These eigenvectors have been normalized in the same manner as the floor response values.

Table 3.2 illustrates the extent to which the derived mode shapes matched the experimental data for each of the first two triplets. The first box for each Table lists the response accelerations computed at the loaded floor level using the best-fit eigenvectors and solving for the actual applied loads. In the second box are the target values, the actual measured accelerations converted to two translations and a rotation. The third box gives the ratio of the two, i.e. the extent of correlation.

In Table 3.2 the X direction corresponds to N-S, the mode excited by load 3. Y is E-W, excited by load 1 and R is the rotation, excited by load 3.

A number of points may be noted from Tables 3.1 and 3.2, in particular:

1. The correlation was generally very good for the primary displaced direction, i.e. the direction corresponding to the load direction.
2. The coupled terms did not always agree well. For example, the Y acceleration due to a torsional load in the first triplet was only 21% of the measured value. Note however that the absolute values of these accelerations were generally small relative to the primary direction.
3. The response shapes and mode shapes listed in Table 3.1 generally had similar shapes, especially for the primary direction.
4. The coupled directions were generally of smaller magnitude relative to the primary terms for the mode shapes compared with the response shapes. This was especially marked for the closely spaced first two translational modes, e.g. the Y (E-W) component of the first N-S mode was approximately 30% smaller than for the response shape.
5. Very little difference between the response

shape and the mode shape was found for the second triplet. This is probably because the coupled terms were relatively small in the measured response shapes.

In general the exercise did not make a great difference to the shapes used for comparison with the SAP IV results. The only significant difference was in the E-W component of the first N-S mode, where the mode shape had a value about 30% smaller. The mode shapes as obtained from the analysis described in this section were used for the subsequent comparisons reported in the following sections.

3.5 CORRELATION STUDIES PERFORMED

The basic SAP IV model was assembled with the assumptions listed in Section 3.3 and the material properties derived as specified in that same section. The correlation with the experimental data (frequencies and mode shapes) was then successively improved by adjustment of the following parameters:

- o Stair properties
- o Soil properties
- o Infill panel properties

When the "best fit" with the experimental results had been obtained the analysis was re-run using a tighter convergence tolerance and also with all nodes free rather than some slaved to master nodes at each floor level.

A total of 15 SAP IV runs were performed. For the first five runs only the translational modes were obtained and for the later runs the first three modes in each of the translational directions and in the torsional direction were extracted.

Runs 1 to 5 studied the gross effects of the infill panels, the stairs and the method of modelling the diaphragm. Runs 7,8,11 and 12 were used to study the effects of varying stiffness properties for the concrete and infill panels. Runs 9 and 10 included soil springs. The final two runs were used to determine the effects on the results of the solution strategies and of the slaved nodes.

3.6 RESULTS OF CORRELATION

An overall summary of the frequencies obtained from the SAP IV analyses is given in Table 3.3. The respective measured frequencies for each mode are also listed in Table 3.3

An example of the mode shapes obtained from the SAP IV program is given in figures 3.6 to 3.14. In these figures the mode shape is drawn over the undeflected shape of the structure. Note that the full model is not shown

in these plots, only the perimeter girders and the corner columns. The particular mode shapes of figures 3.6 to 3.14 are for run 7, which included the concrete frame, the stairs and infill panels on the east and west walls only. The concrete stiffness was based on its full value and the masonry was one half of the elastic modulus.

In run 7 the frequencies in the first two triplets gave reasonable agreement in the translational modes with the measured values. The E-W mode shapes also agreed reasonably well with the measured response shapes but the N-S mode shapes had a greater variation.

By run 13 the agreement with the measured frequencies was good for all six modes of the first two triplets. The E-W and torsional mode shapes also agreed well with the extracted best fit modes for both triplets. However, again the N-S first and second modes showed a considerable variation. The agreement of frequencies, E-W mode shapes and torsional mode shapes suggested that the model had the correct mass and stiffness properties and so the experimental data was examined to see whether an explanation for the N-S discrepancy could be found.

One anomaly in the measured data was that the N-S response shapes showed higher accelerations in the east frame than in the west frame. The east side of the building contains an additional column plus the stairs and stairwell walls, making it stiffer than the west side. As the center of stiffness would be to the east side of the geometric center it would be expected that the west frame motions under floor rotations would be greater because of the greater lever arm. This was confirmed by observations in the later large scale testing.

Because of this it was suspected that the nodal numbering sequence in the report of the test results had inadvertently been reversed. Based on this assumption the best fit eigenvectors were recalculated to match accelerations assuming reversed node numbering. The resultant vectors were plotted against the mode shapes obtained from run 13, and these are reproduced as figures 3.15 to 3.20. This showed similar results in the E-W and torsional directions but a greatly improved correlation in the N-S direction. Therefore, although not conclusive it appears that the numbering sequence was in fact reversed from east to west.

3.7 DISCUSSION OF RESULTS

The results showed that quite good agreement with the measured frequencies of the first two triplets could be obtained but that the measured frequencies of the third triplet were considerably higher than those obtained from the analysis.

The mode shapes generally correlated well with the best fit mode shapes extracted from the experimental data in the E-W and torsional directions but the N-S shapes did not agree well unless a sign change in the measured response N-S values was admitted.

In the following sections the influence of various parameters on the results is discussed.

3.7.1 Effect of Stairs

The stairs were modelled as strut members based on their gross section properties. Because of their geometry they could be expected to have negligible effect on the north south response but a marked influence on the east west response.

Runs 2 and 3 show the influence of the stairs on the translational frequencies. The first E-W mode with stairs agrees well with the measured value. When the stairs are removed the frequency differs greatly from the measured value. There is little effect on the N-S frequencies. Therefore it appears that the method adopted to model the stairs is appropriate. Furthermore, the stairwell has a significant influence on the E-W frequency.

3.7.2 Effect of Infill Panels

The influence of the infill panels was the most indeterminate parameter in the analysis of this building. Only limited field observations were available to judge the influence and degree of participation of each infill wall in the response.

It was apparent between run 2, with no infills, and runs 4 to 15 that the walls did influence the behavior, especially in the north south direction. Walls in only the east and west sides of the models gave reasonable agreement in the north south frequencies. However, as shown in run 7 the torsional stiffness was too low and the frequencies in the torsional modes were lower than the measured values.

Infills modelled in all walls improved the torsional match as shown in run 8 but tended to raise the stiffness in the east west direction, even if only 75% of the concrete and wall modulus was used. Run 12 had an arbitrarily assigned wall stiffness and thus could not be suggested to give appropriate values to use for design purposes.

3.7.3 Effect of Soil Properties

From the building layout and the experimental results it was expected that the building base could be assumed fixed. To check the influence of this assumption on the analysis, run 8 was repeated with soil springs of two different stiffnesses inserted under the column bearing pads, and the results were obtained as runs 9 and 10 respectively. In general

the frequencies were similar and the correlation was no better with the soil springs. Therefore it was concluded that the fixed base assumption was appropriate.

3.7.4 Effect of Solution Parameters

Two solution strategies adopted to save computer time were a limitation in the number of iterations and the slaving of floor nodes. The effect of the former is demonstrated in the results from runs 12 and 13. Run twelve had only two iterations whereas run 13 used 7 iterations. The effect on frequencies was slight. Note however that the eigenvectors converge more slowly than the eigenvalues so that a greater number of iterations improves the accuracy of the eigenvectors more than the eigenvalues.

The model with all nodes independent, run 15, produced generally similar results to run 13 with slaved nodes although some frequencies differed to some extent. It is obvious that the structure with slaved nodes gives a reasonable model, and in fact the slaving provides a better representation of the diaphragm rigidity while reducing the size of the problem.

3.8 CONCLUSIONS FROM SMALL AMPLITUDE CORRELATIONS

The SAP IV model using properties based on the building plans gave reasonable agreement with the measured response, although it was apparent that the indeterminate nature of the interaction of the infill walls would prevent efforts to obtain an exact match.

It was further apparent that to obtain any correlation a model would have to include an approximation for the effects of both the stairs and the infill walls.

A simple truss model for the stairs based on their gross concrete properties appeared to provide satisfactory results and such a model should be adequate for design purposes.

It was clear that some allowance must be made for the infill panel stiffness. For unreinforced walls with no special construction procedures such as in the St Louis building, a complex model does not seem warranted. From the results obtained it seems that the walls should be modelled by simple strut members with properties based on the shear stiffness of the walls. A reduction of the modulus of elasticity to about one-half the published masonry values would appear necessary to allow for the incomplete interaction.

MODE	FLOOR	RESPONSE SHAPE			MODE SHAPE		
		X	Y	R	X	Y	R
(E-W) ₁ 1.51 hz	11	-0.103	1.000	0.00041	-0.008	1.000	0.00053
	9	-0.083	0.883	0.00041	0.015	0.894	0.00053
	7	-0.055	0.759	0.00035	0.038	0.750	0.00038
	5	-0.028	0.552	0.00035	0.045	0.553	0.00038
	3	-0.041	0.393	0.00014	0.015	0.394	0.00015
(N-S) ₁ 1.61 hz	11	1.000	-0.682	0.00118	1.000	-0.439	0.00163
	9	0.818	-0.581	0.00100	0.827	-0.367	0.00133
	7	0.782	-0.591	0.00091	0.806	-0.408	0.00122
	5	0.564	-0.427	0.00045	0.571	-0.296	0.00082
	3	0.427	-0.300	0.00027	0.429	-0.204	0.00041
(T) ₁ 2.20 hz	11	0.128	0.004	0.00100	0.077	0.000	0.00100
	9	0.117	0.011	0.00099	0.068	0.005	0.00100
	7	0.105	0.007	0.00097	0.057	0.007	0.00097
	5	0.095	0.009	0.00087	0.054	0.018	0.00087
	3	0.093	0.007	0.00071	0.059	0.014	0.00071
(E-W) ₂ 4.70 hz	11	0.170	1.000	-0.00033	0.122	1.000	-0.00019
	9	0.029	0.242	-0.00045	0.019	0.245	-0.00047
	7	-0.126	-0.500	0.00004	-0.084	-0.500	0.00000
	5	-0.536	-0.848	0.00022	-0.462	-0.849	0.00009
	3	-0.198	-1.017	0.00020	-0.150	-1.019	0.00000
(N-S) ₂ 4.95 hz	11	1.000	-0.100	-0.00140	1.000	-0.114	0.00143
	9	0.169	-0.057	-0.00007	0.171	-0.057	0.00009
	7	-0.737	0.069	0.00096	-0.742	0.076	0.00095
	5	-1.338	0.090	0.00126	-1.342	0.105	0.00124
	3	-0.972	0.107	0.0015	-0.971	0.124	0.00152
(T) ₂ 7.25 hz	11	0.078	0.001	0.00100	0.077	0.000	0.00100
	9	0.021	-0.012	0.00030	0.020	0.011	0.00030
	7	-0.016	-0.013	-0.00038	-0.016	0.014	-0.00037
	5	-0.061	0.006	-0.00084	-0.058	0.007	-0.00084
	3	-0.087	0.004	-0.00092	-0.086	0.005	-0.00091

TABLE 3.1 : NORMALIZED RESPONSE SHAPES AND MODE SHAPES

COMPUTED ACCELERATIONS			
LOAD	X	Y	R
1	0.7	-5.6	0.0023
2	-4.2	2.9	0.0052
3	5.6	-0.7	0.0422

COMPUTED ACCELERATIONS			
LOAD	X	Y	R
1	-0.9	-5.8	0.0020
2	-4.4	0.5	0.0064
3	-6.9	-0.1	-0.0591

MEASURED ACCELERATIONS			
LOAD	X	Y	R
1	0.6	-5.6	0.0023
2	-4.2	2.9	0.0052
3	5.5	-0.2	0.0424

MEASURED ACCELERATIONS			
LOAD	X	Y	R
1	-0.9	-5.8	0.0020
2	-4.4	0.5	0.0064
3	-7.0	-0.1	-0.0590

MEASURED/COMPUTED			
LOAD	X	Y	R
1	0.82	1.00	1.00
2	1.00	1.00	1.00
3	0.98	0.21	1.01

MEASURED/COMPUTED			
LOAD	X	Y	R
1	0.99	1.00	1.00
2	1.00	1.00	1.00
3	1.00	1.04	1.00

(a) First Triplet

(b) Second Triplet

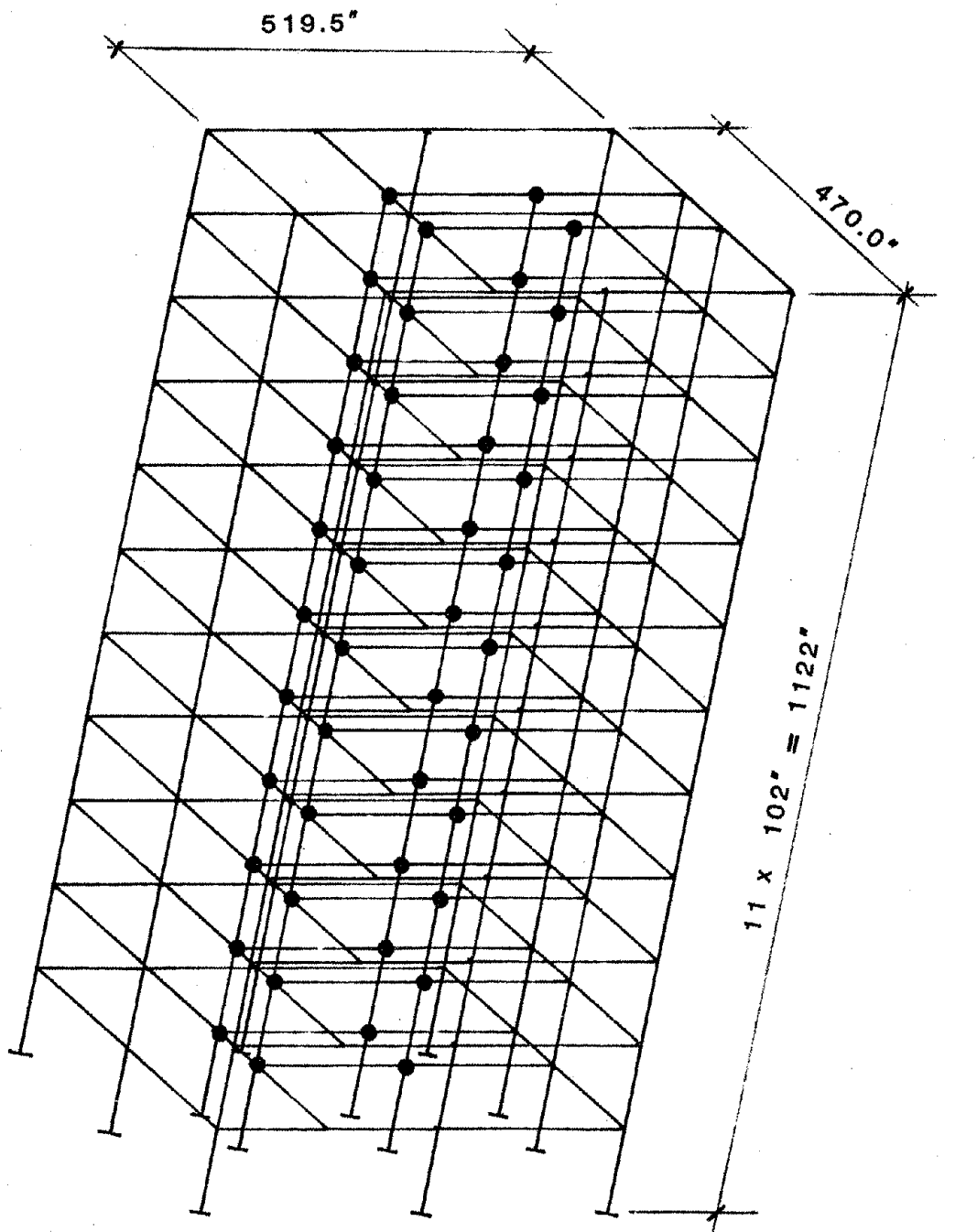
TABLE 3.2 : COMPARISON OF MEASURED ACCELERATIONS AND ACCELERATIONS FROM COMPUTED MODE SHAPES.

	FIRST TRIPLET			SECOND TRIPLET			THIRD TRIPLET		
	N-S	E-W	T	N-S	E-W	T	N-S	E-W	T
MEASURED	1.61	1.51	2.20	4.95	4.70	7.25	15.05	12.70	18.0
RUN 2	0.98	1.54		2.81					
RUN 3	0.97	1.11		2.78	3.11				
RUN 4	1.67	1.55		4.78					
RUN 7	1.56	1.55	2.04	4.51	4.78	5.81	8.35	8.85	10.38
RUN 8	1.60	1.72	2.27	4.58	5.21	6.51	8.92	9.93	10.50
RUN 9	1.34	1.43	2.45	5.01	5.80	6.43	10.54		7.17
RUN 10	1.53	1.62	2.51	5.12	5.88	7.30	9.33	7.70	10.29
RUN 12	1.56	1.65	2.20	4.47	5.00	6.28	8.43	9.50	8.95
RUN 13	1.56	1.62	2.17	4.46	4.92	6.20	8.38	8.75	9.27
RUN 15	1.53	1.56	1.89	4.38	4.72	5.44	8.28	8.70	9.78

RUN DESCRIPTION

2. Frame and stairs only. 1.0 Ec.
3. As for 2 but stairs deleted.
4. East infills added. 1.0 Em.
7. East and West infills. 0.5 Em.
8. All infills, 0.75 Ec and 0.75 Em.
9. Base springs. K= 100 lb/cu.in.
10. Base springs. K= 200 lb/cu.in.
12. Infill walls above level 2 only. 0.75 Ec with 0.4 Em for all except stairwell, 0.5 Em and Ease wall, 1.0 Em.
13. As for 12 but tighter tolerance.
15. As for 13 but all nodes independent.

TABLE 3.3 : COMPUTED vs MEASURED FREQUENCIES



NOTE: Frame members only shown

● MASTER NODES

FIGURE 3.1 : "SAP IV" MODEL

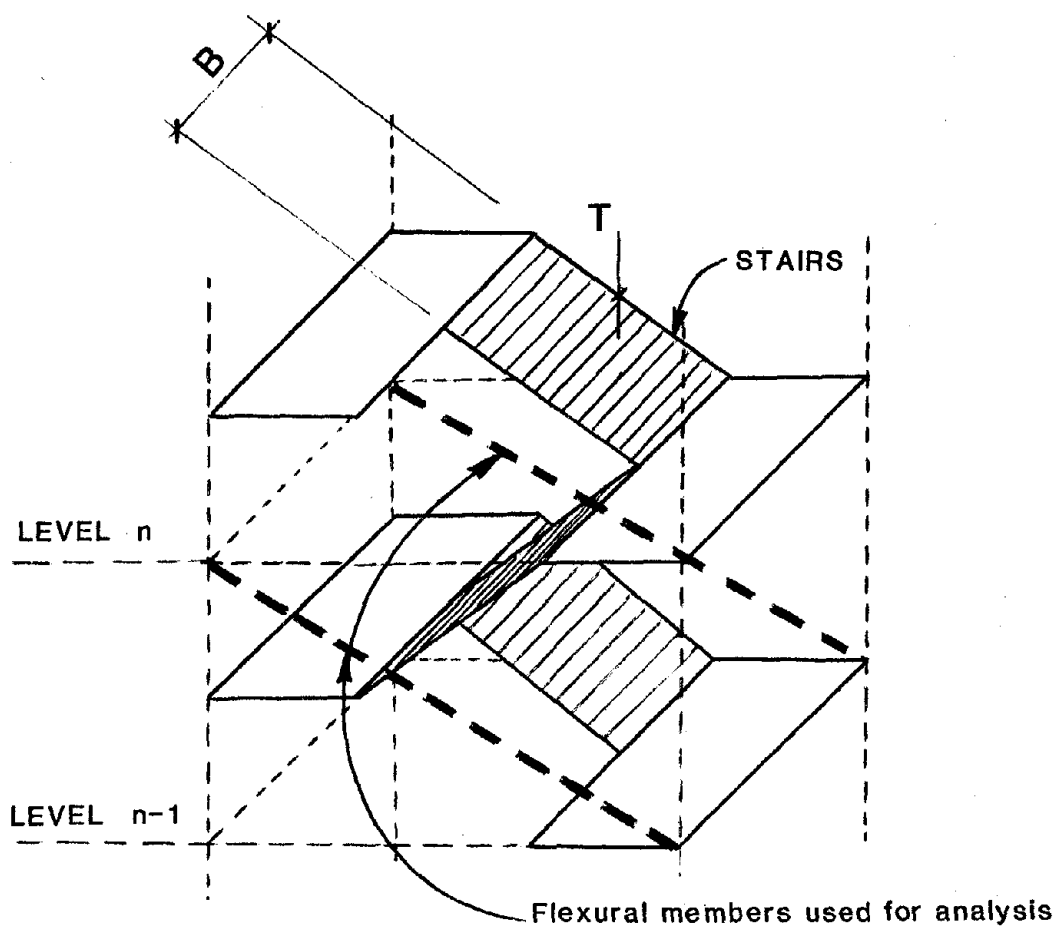


FIGURE 3.2 : DIAGRAMMATIC REPRESENTATION OF STAIR MODEL

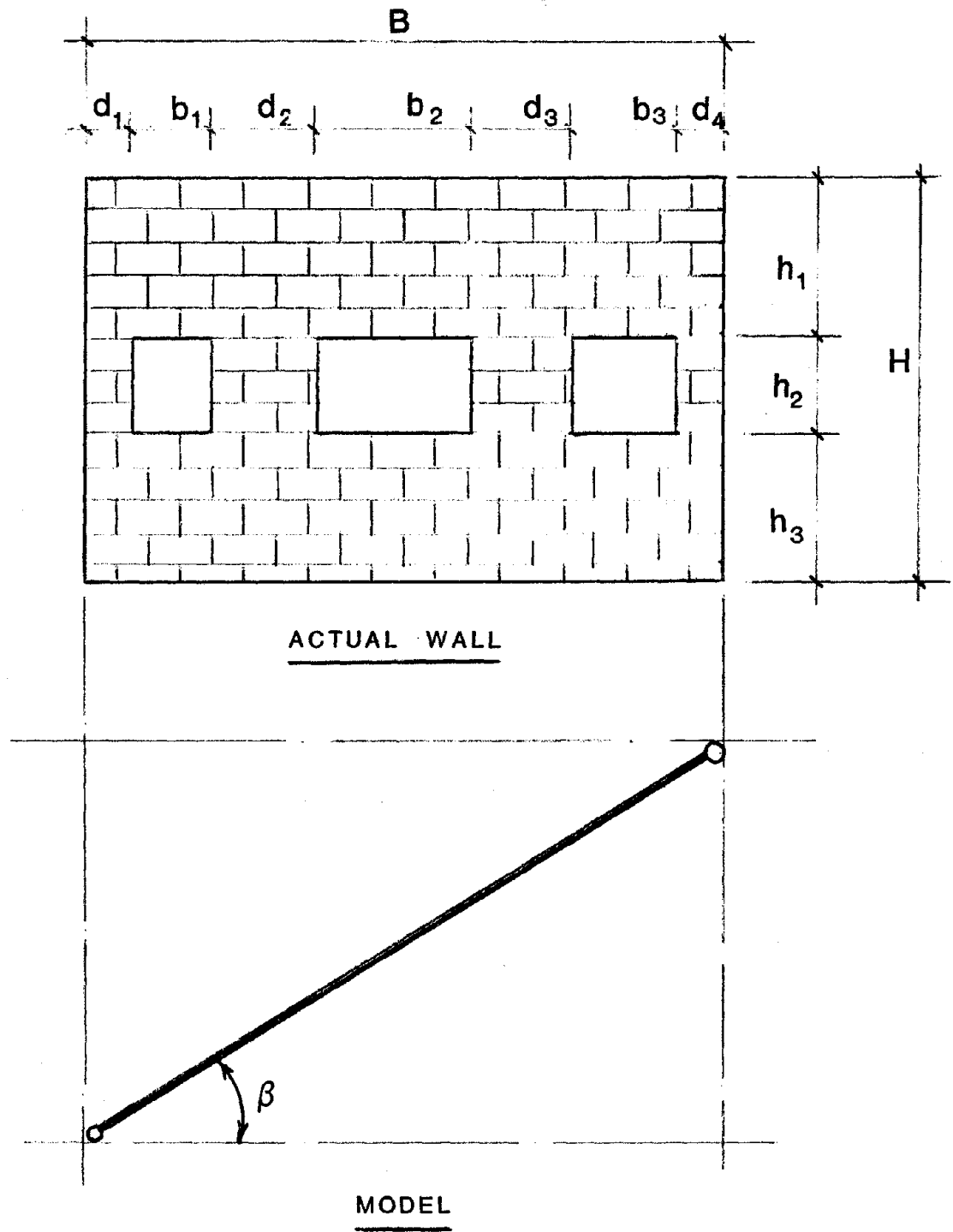
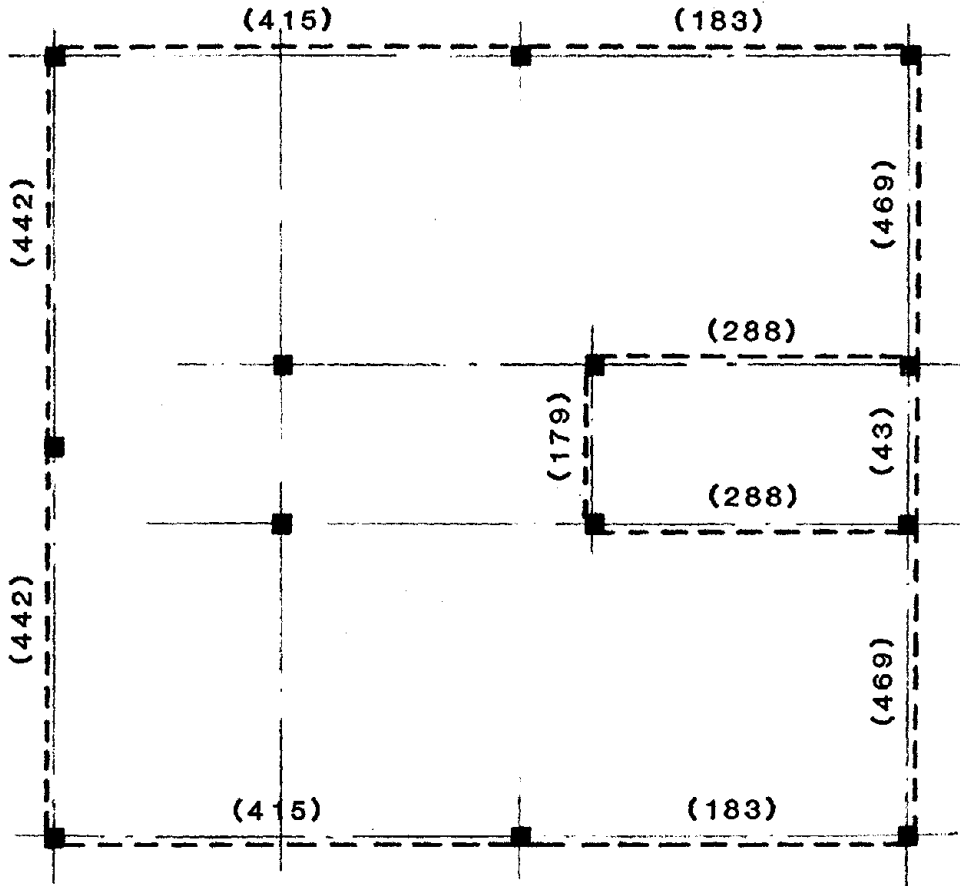
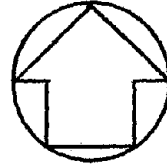


FIGURE 3.3 : DIAGRAMMATIC REPRESENTATION OF INFILL WALL MODEL

NORTH



----- Position of strut
() Area of strut (sq. in.)

FIGURE 3.4 : AREA OF EQUIVALENT STRUTS

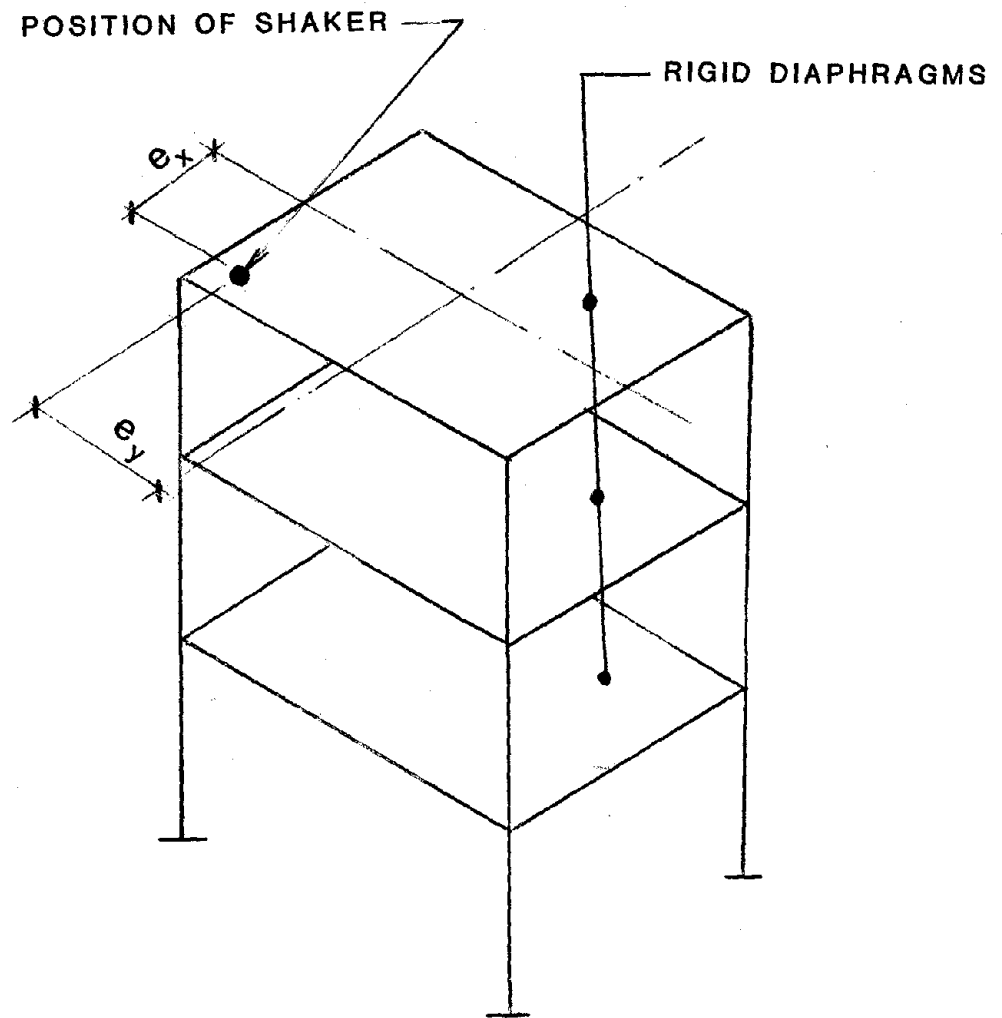


FIGURE 3.5 : SIMPLE MODEL OF OMNI-DIRECTIONAL LOADING

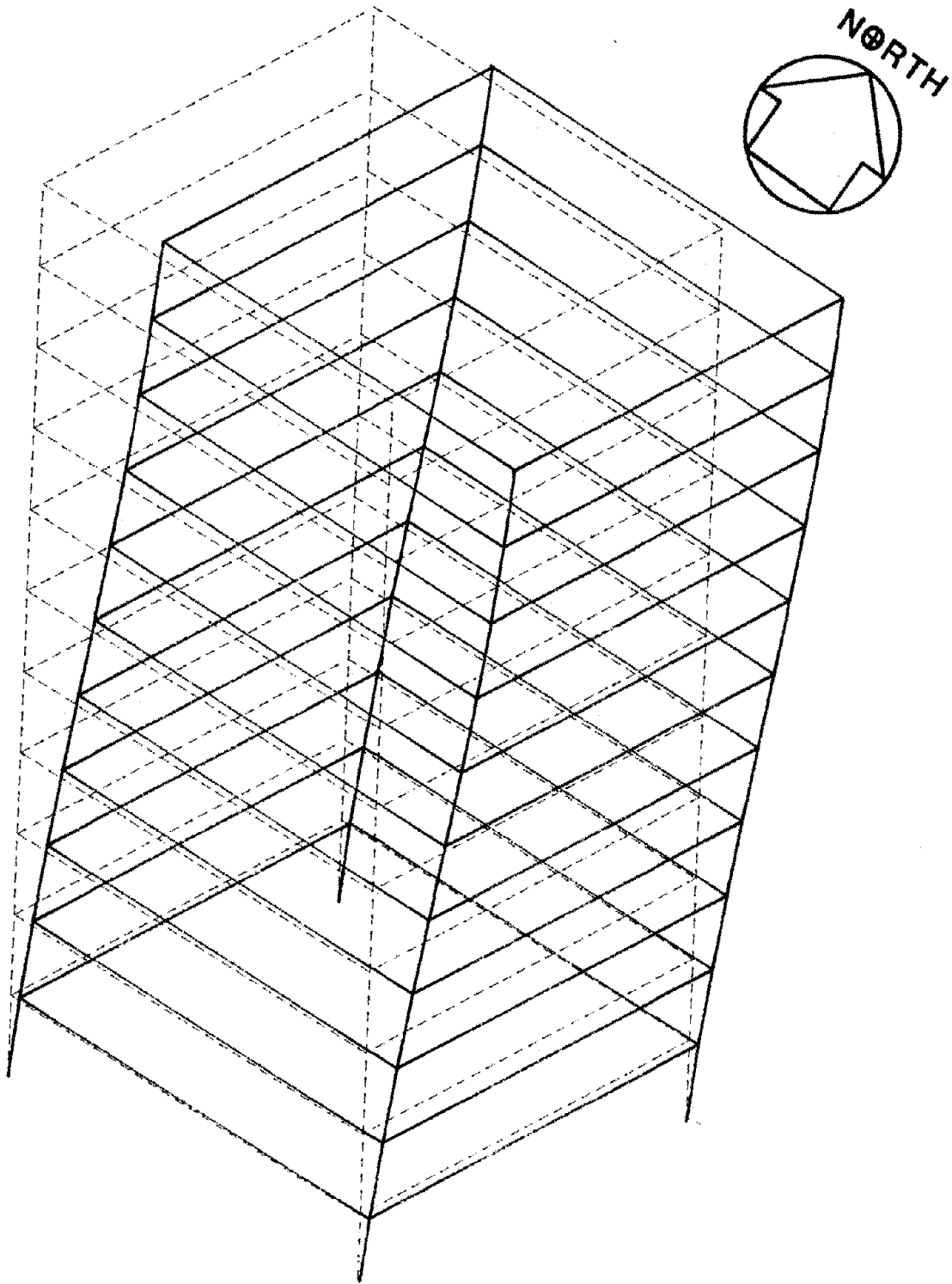


FIGURE 3.6 : COMPUTED MODE SHAPE - MODE 1 FREQUENCY = 1.55 hz

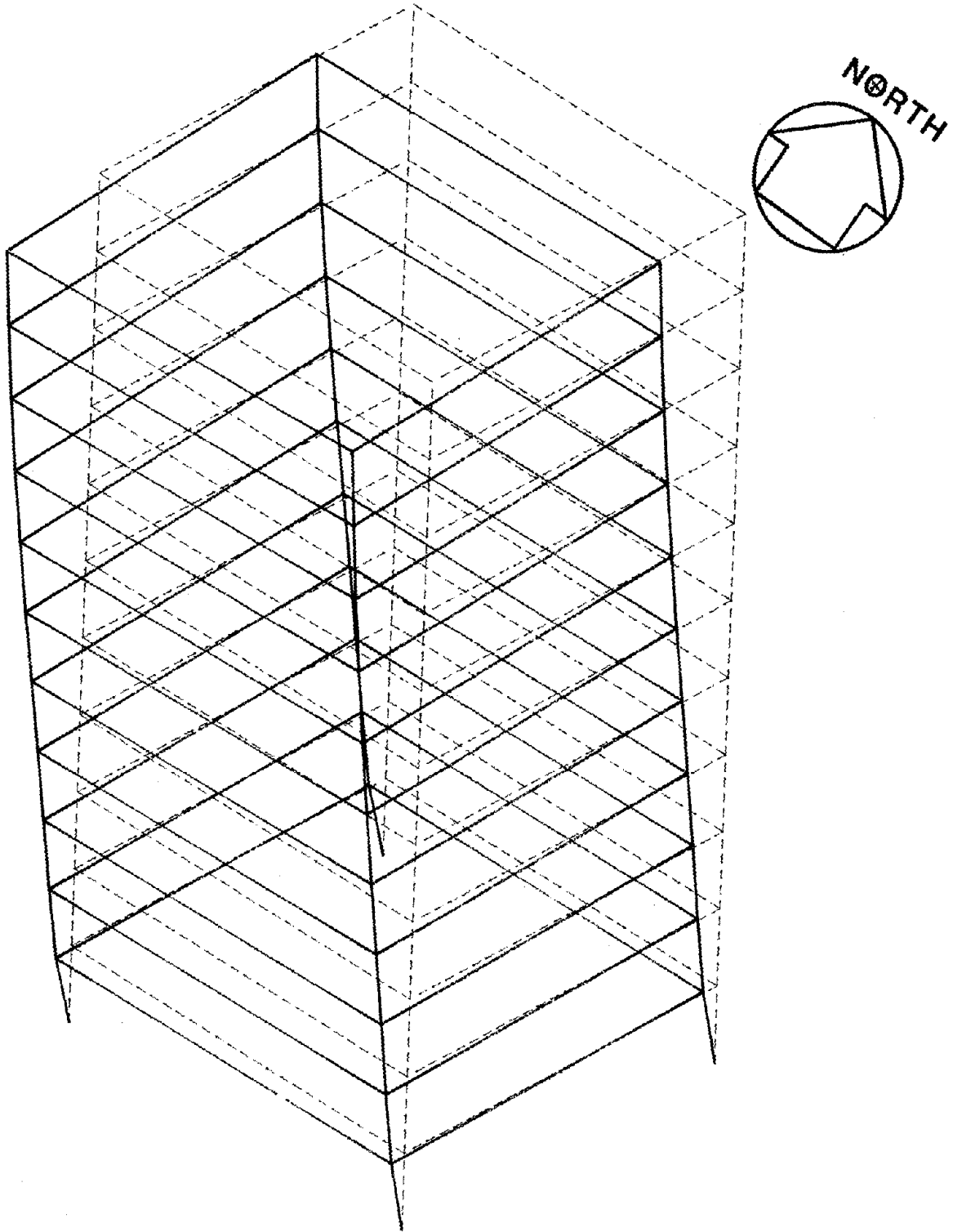


FIGURE 3.7 : COMPUTED MODE SHAPE - MODE 2 FREQUENCY = 1.56 hz

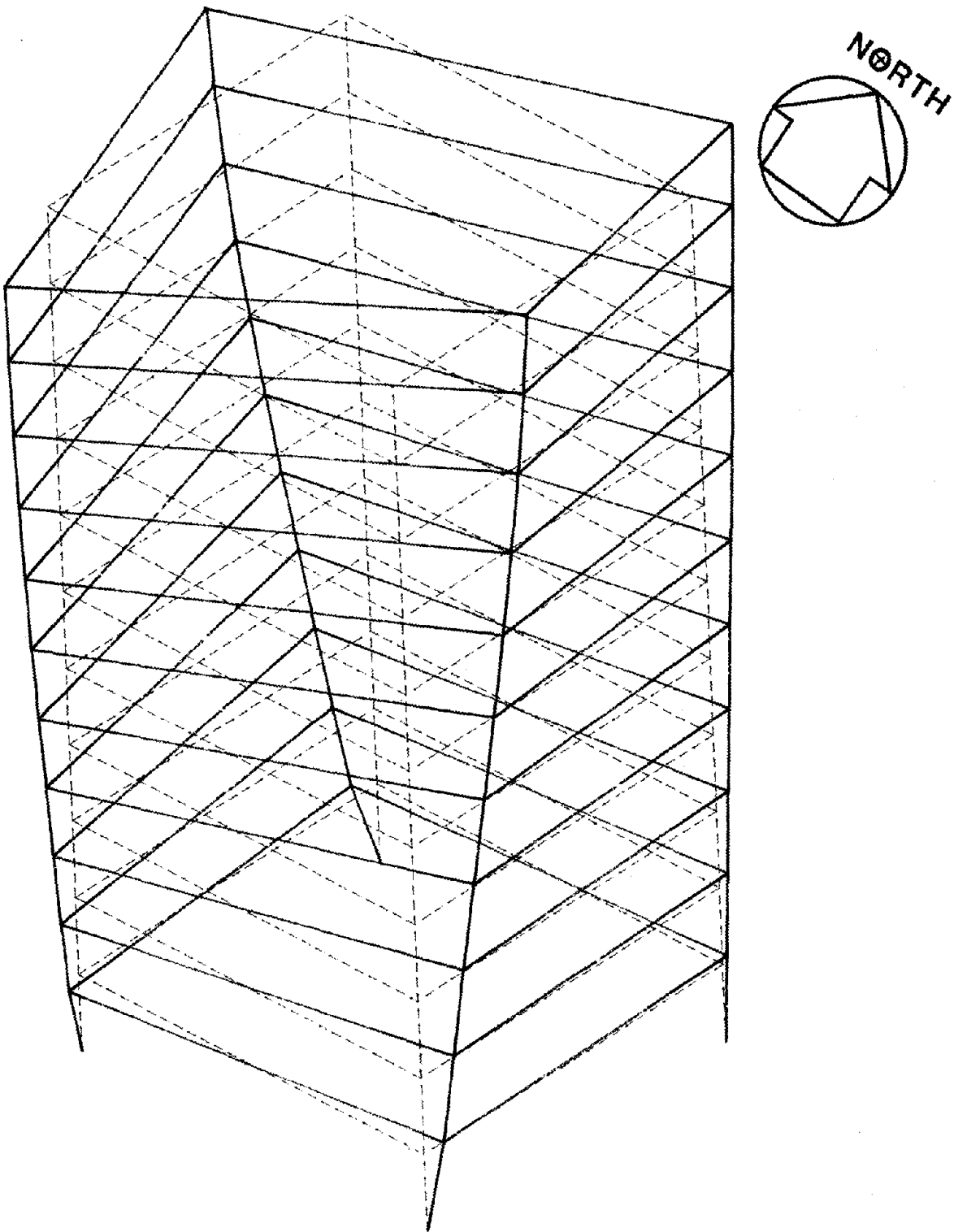


FIGURE 3.8 : COMPUTED MODE SHAPE - MODE 3 FREQUENCY = 2.04 hz

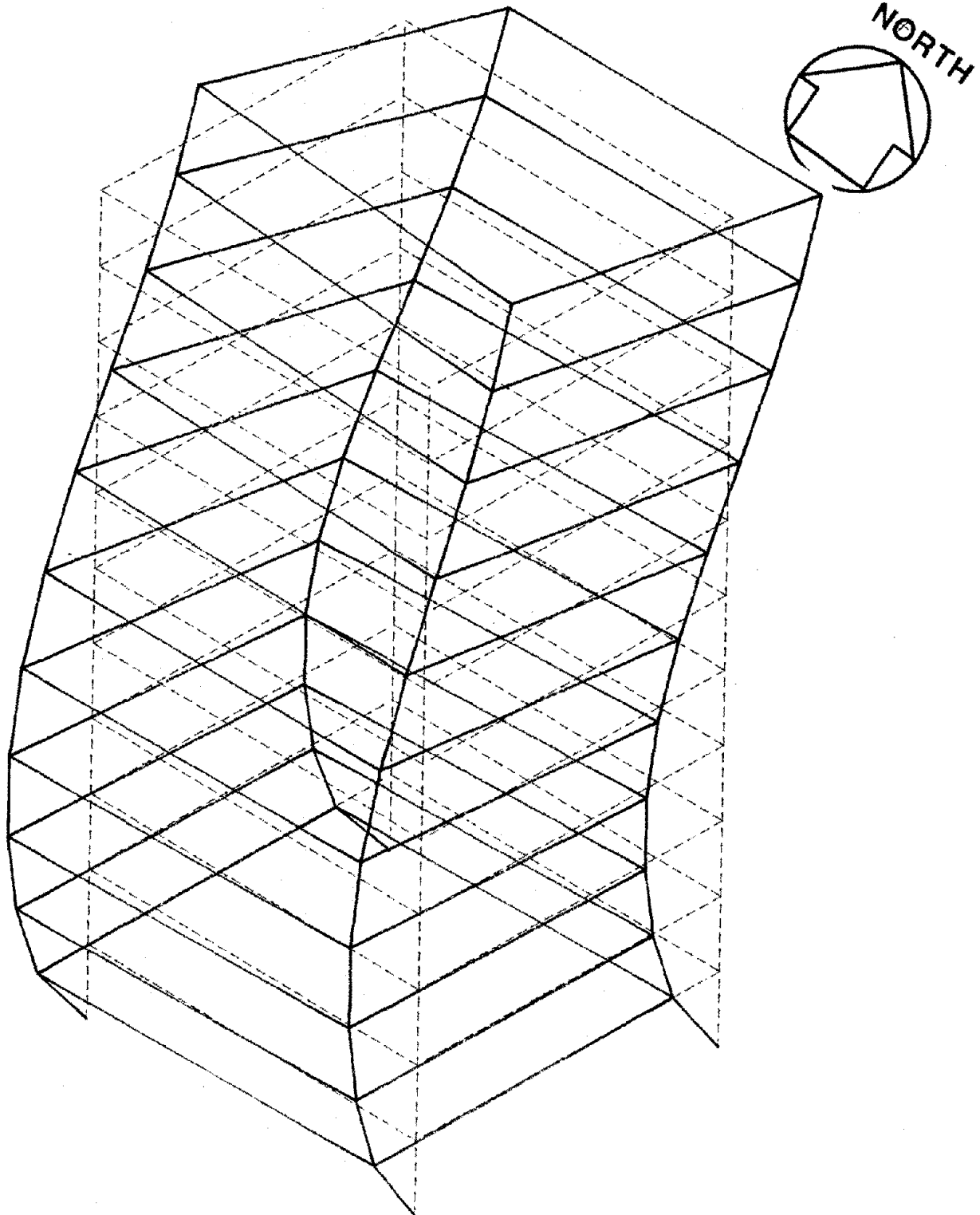


FIGURE 3.9 : COMPUTED MODE SHAPE - MODE 4 FREQUENCY = 4.51 hz

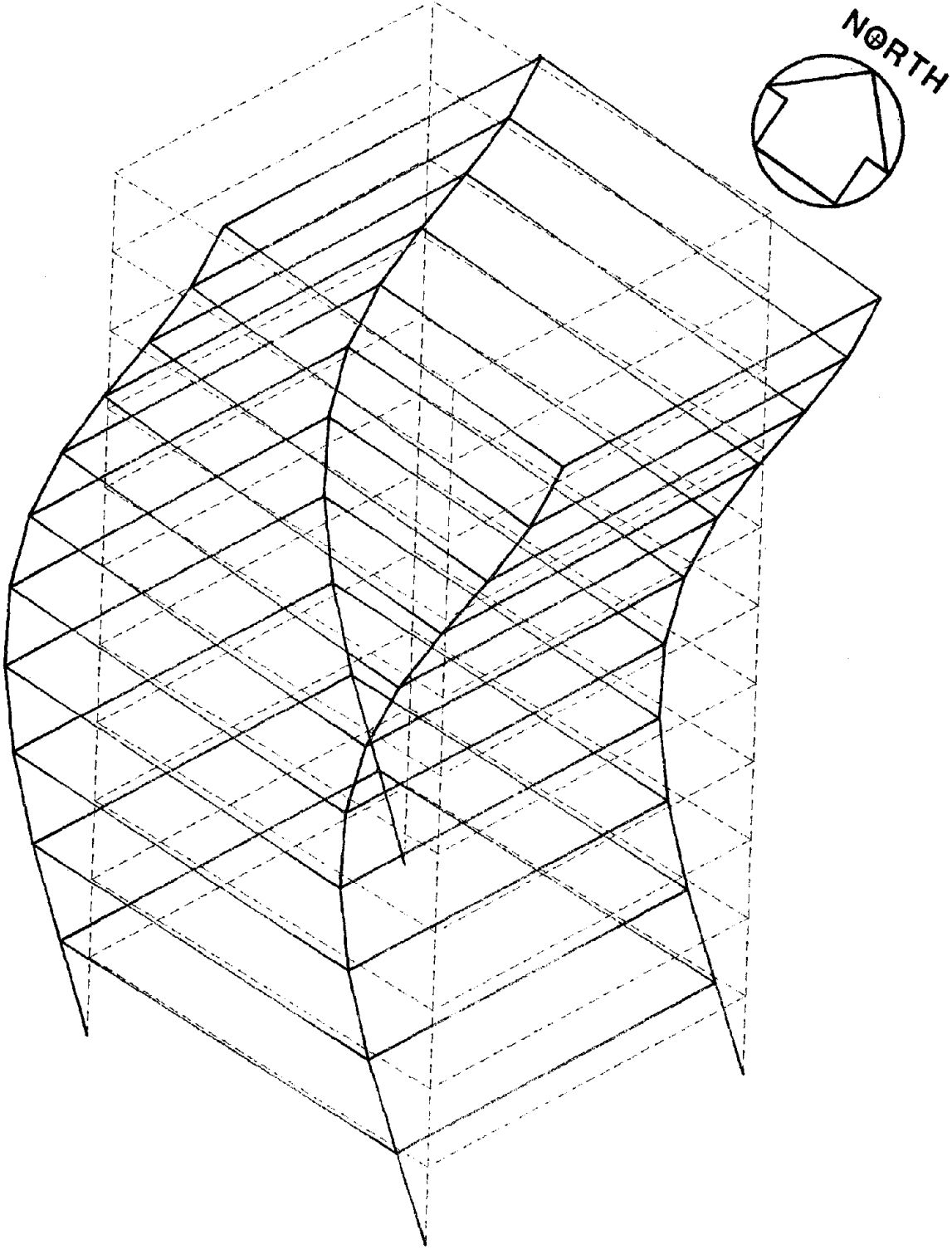


FIGURE 3.10 : COMPUTED MODE SHAPE - MODE 5 FREQUENCY = 4.78 Hz

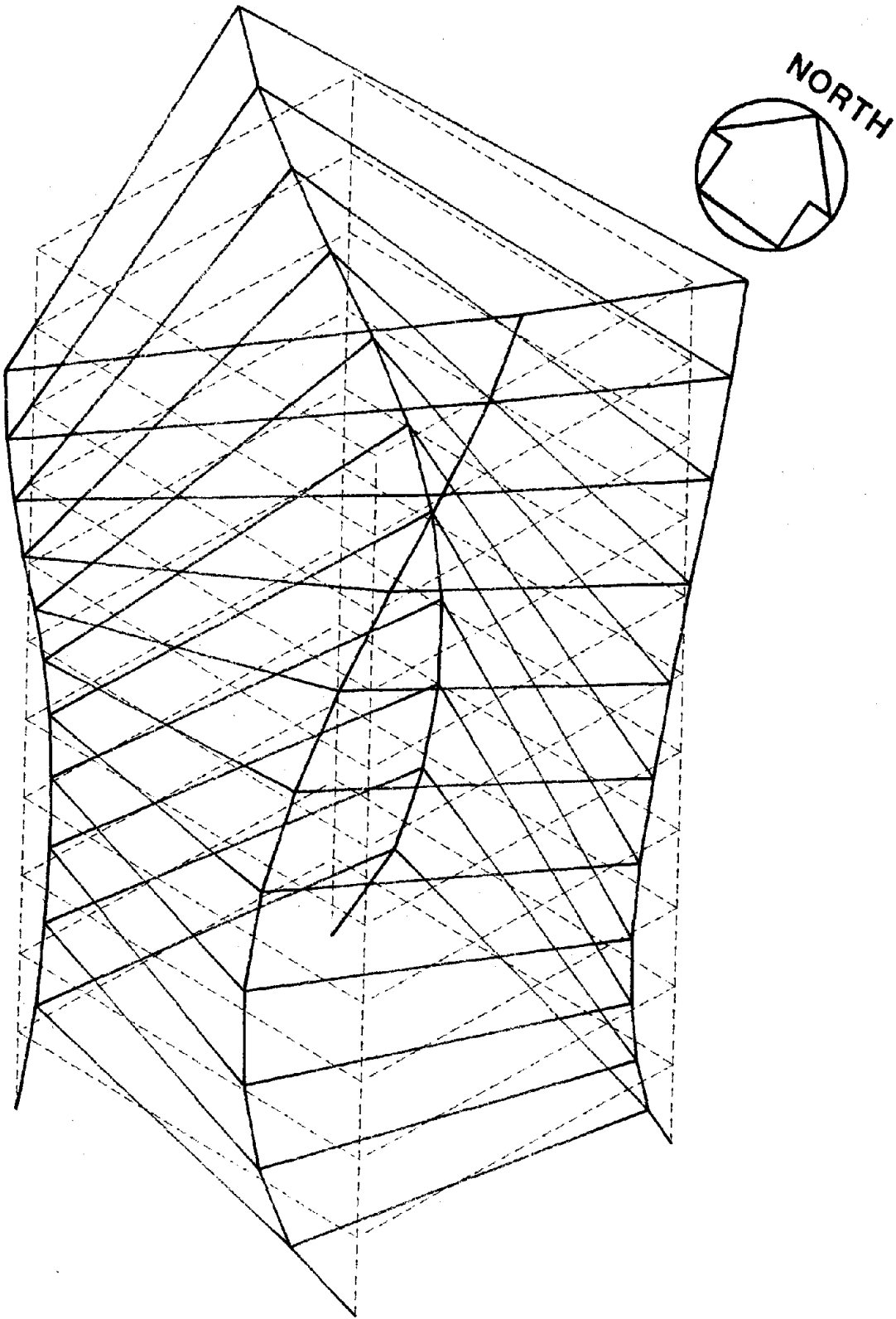


FIGURE 3.11 : COMPUTED MODE SHAPE - MODE 6 FREQUENCY = 5.81 hz

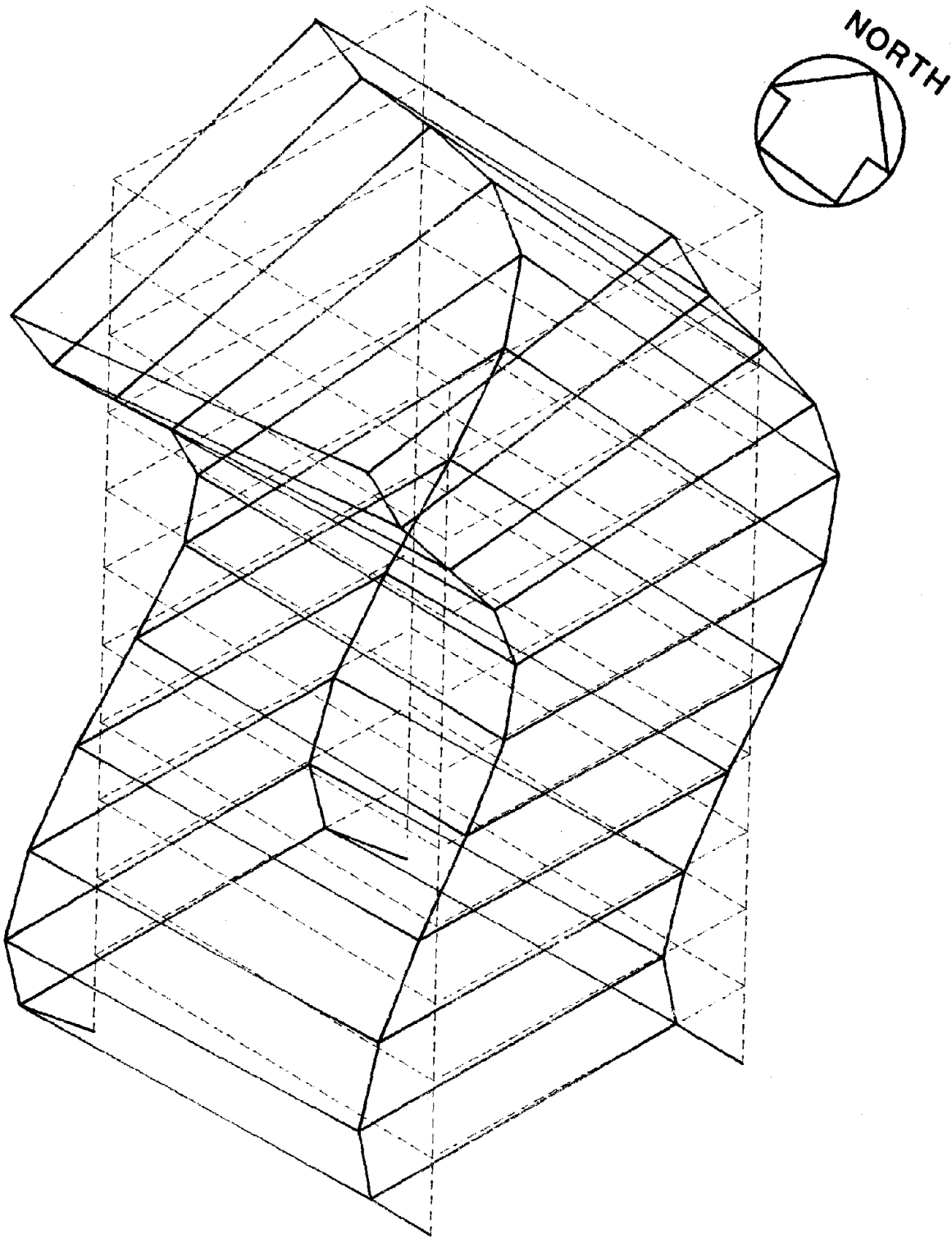


FIGURE 3.12 : COMPUTED MODE SHAPE - MODE 7 FREQUENCY = 8.35 hz

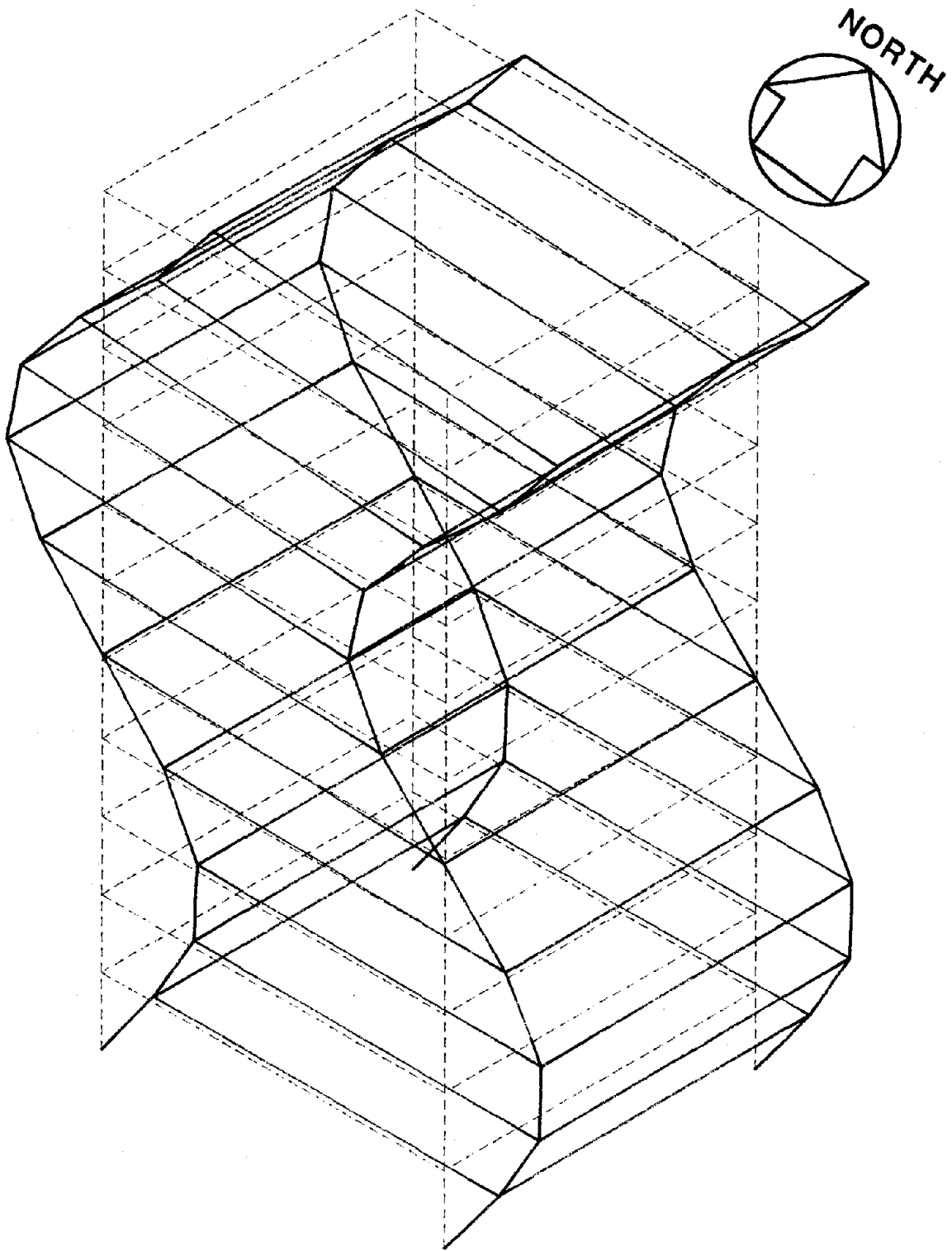


FIGURE 3.13 : COMPUTED MODE SHAPE - MODE 8 FREQUENCY = 8.85 hz

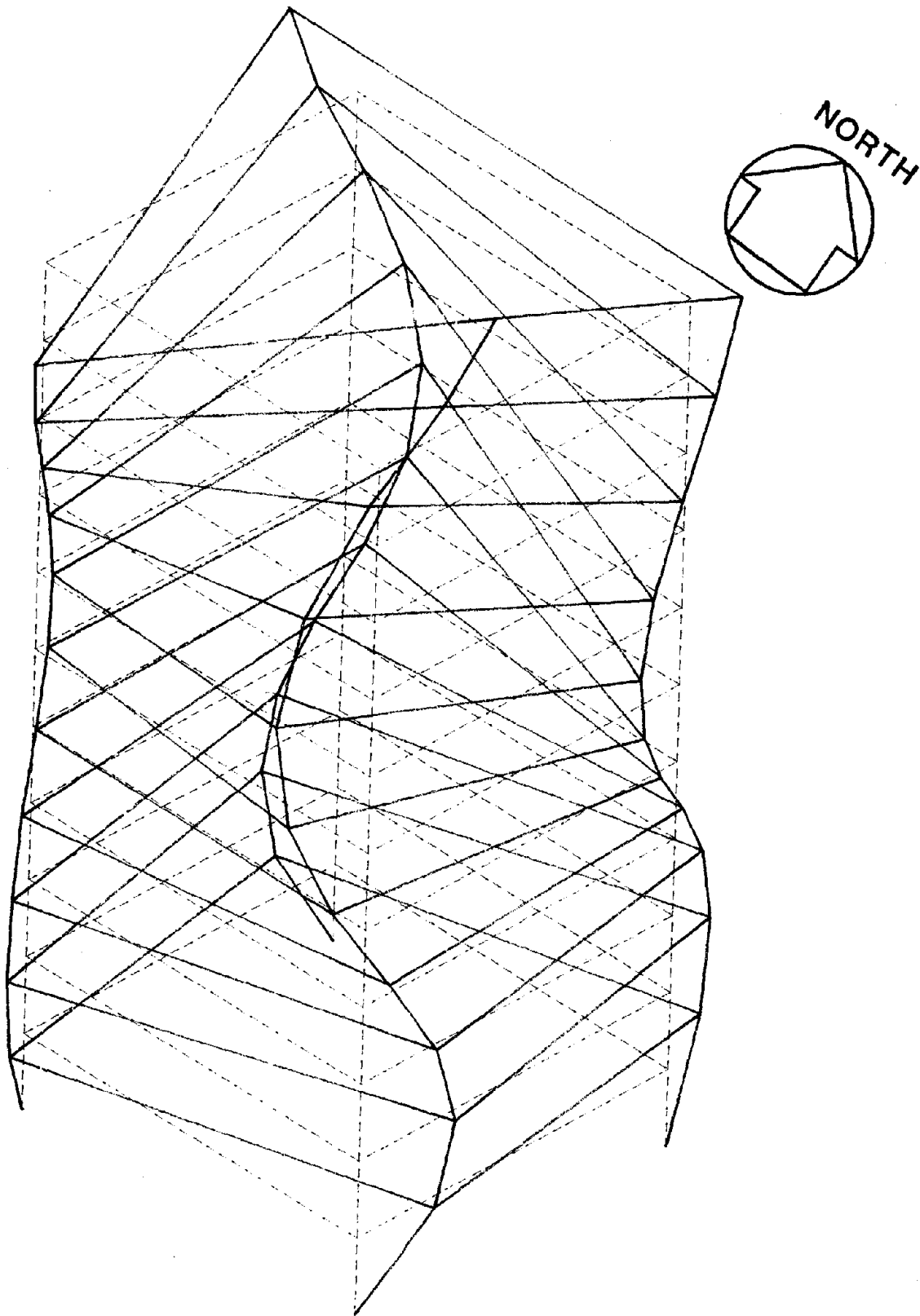
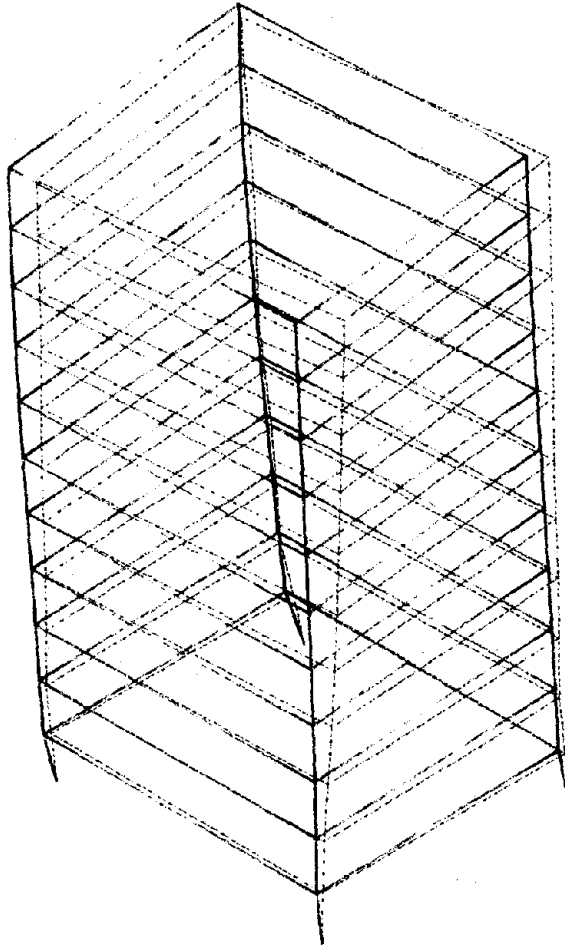
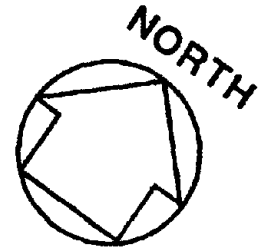
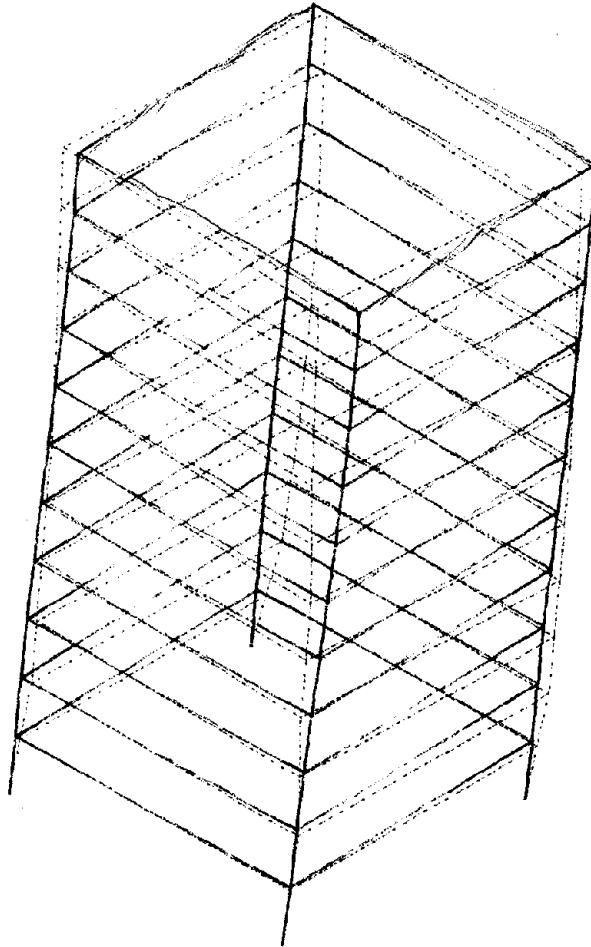
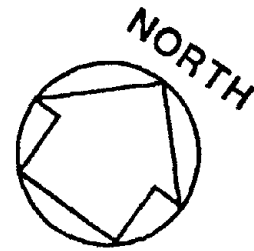


FIGURE 3.14 : COMPUTED MODE SHAPE - MODE 9 FREQUENCY = 10.38 hz



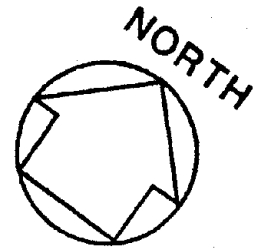
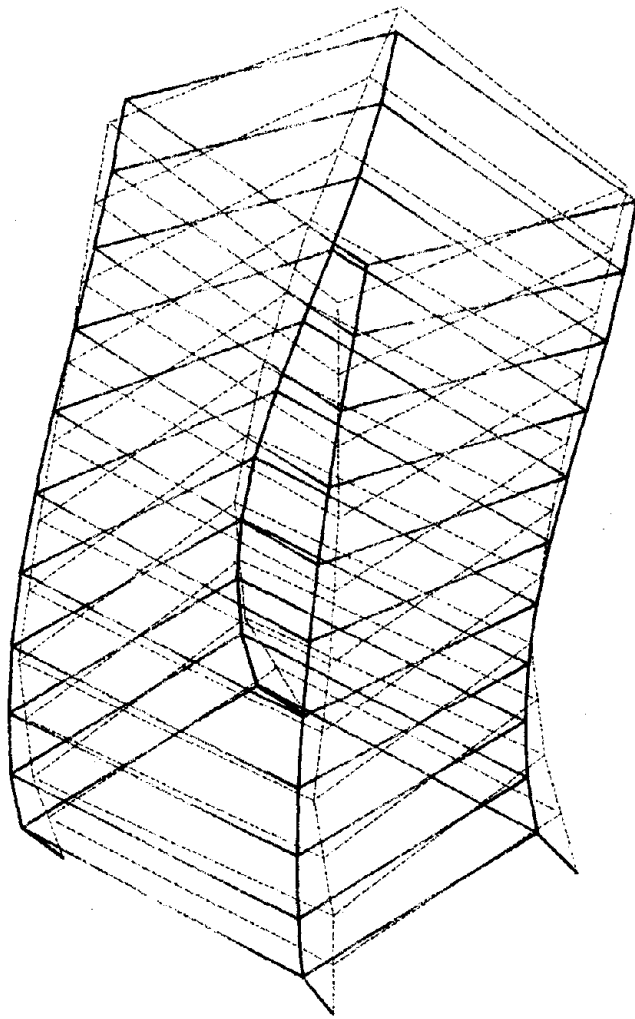
NOTE : Measured shapes are "best-fit" with N-S sign change.
Measured Frequency = 1.61 hz
Computed Frequency = 1.56 hz

FIGURE 3.15 : COMPUTED vs MEASURED MODE SHAPES - MODE 1



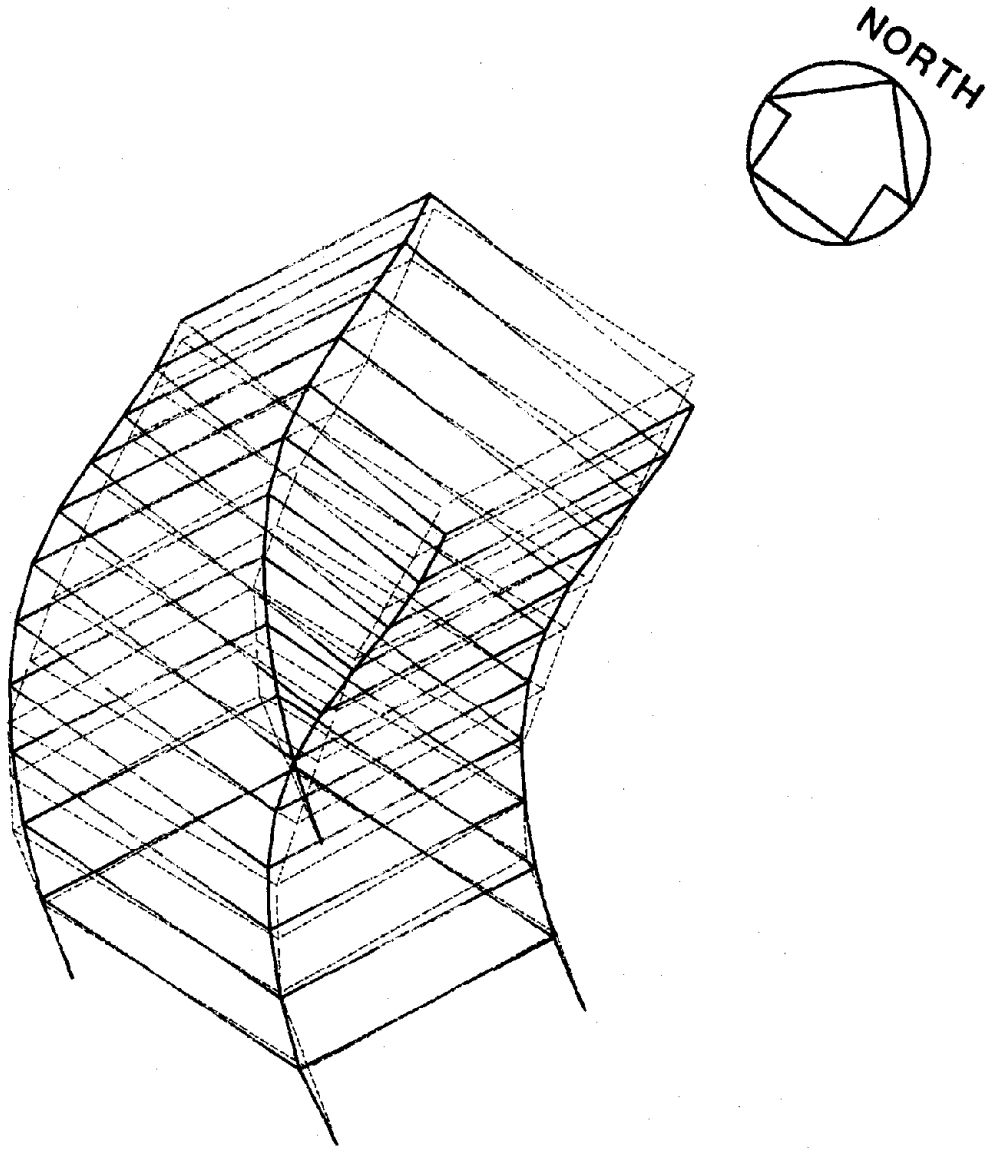
NOTE : Measured shapes are "best-fit" with N-S sign change.
Measured Frequency = 1.51 hz
Computed Frequency = 1.62 hz

FIGURE 3.16 : COMPUTED vs MEASURED MODE SHAPES - MODE 2



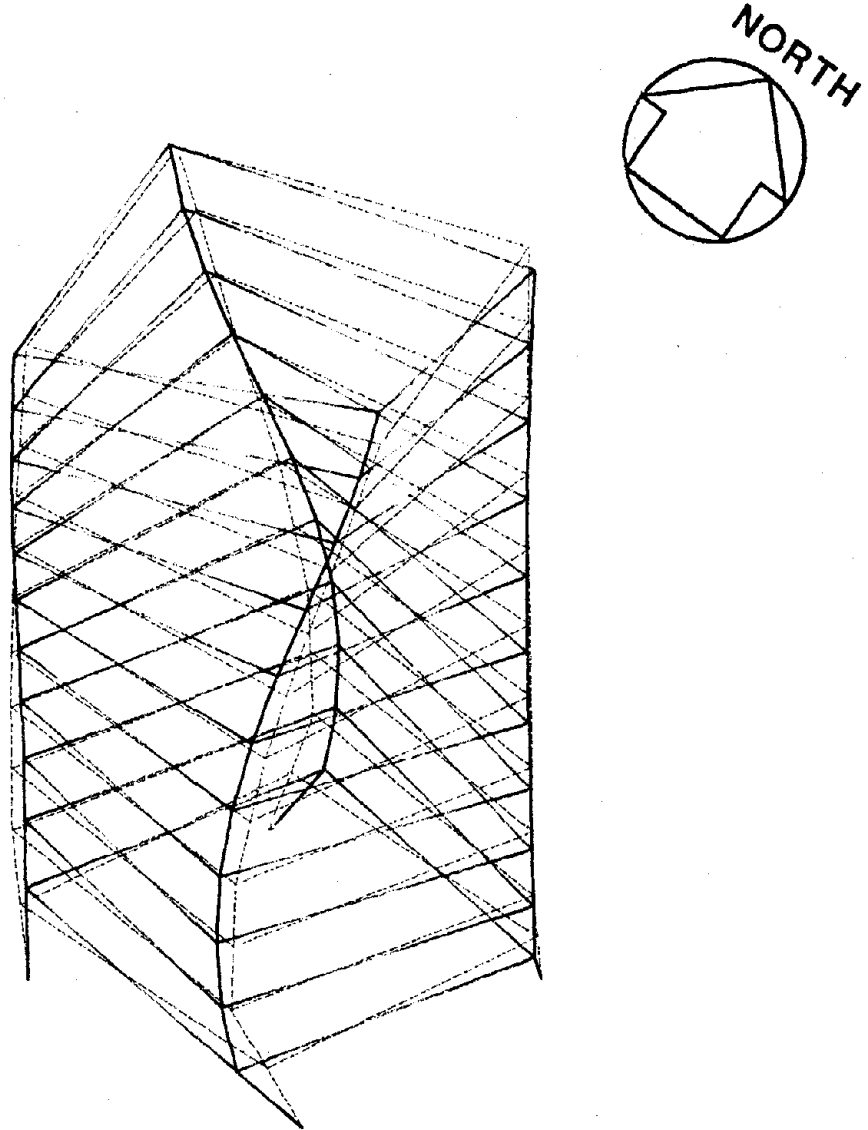
NOTE : Measured shapes are "best-fit" with N-S sign change.
Measured Frequency = 4.95 hz
Computed Frequency = 4.46 hz

FIGURE 3.18 : COMPUTED vs MEASURED MODE SHAPES - MODE 4



NOTE : Measured shapes are "best-fit" with N-S sign change.
Measured Frequency = 4.70 hz
Computed Frequency = 4.92 hz

FIGURE 3.19 : COMPUTED vs MEASURED MODE SHAPES - MODE 5



NOTE : Measured shapes are "best-fit" with N-S sign change.
Measured Frequency = 7.25 hz
Computed Frequency = 6.20 hz

FIGURE 3.20 : COMPUTED vs MEASURED MODE SHAPES - MODE 6

4 PROCEDURES FOR LARGE AMPLITUDE CORRELATION

This chapter of the report covers the correlation of the analytical results with the large amplitude shaking tests. Only the north-south large amplitude tests were used for the non-linear correlation study since they produced the largest displacements in the test program and reduced the number of variables that required consideration in the analytical model. Relevant details of the N-S large amplitude tests and a description of damage observed during the tests are summarized in Section 4.1. The scope of the correlation studies is defined in Section 4.2 and the computer programs and techniques developed to model the observed damage are presented in Section 4.3. Details of the modelling techniques and their application to the model of the test structure are presented in Section 4.4. Detailed results of the correlation study are given in Chapter 5.

4.1 NORTH-SOUTH TESTS

Two structural conditions affected what data was collected from the tests conducted in the North-South direction and subsequently correlated with the analytical results:

1. The tests in the North-South direction were performed with the external cladding removed from all but the top two floors.
2. The stairwell did not provide any significant stiffness to the frames in this direction.

As a result of these conditions, only the non-linearities that occurred in the reinforced concrete frame had to be considered in the correlation with the test results.

4.1.1 Summary of the N-S Large Amplitude Tests

A summary of all tests conducted is given in Chapter 2. The full sequence of tests performed in the N-S direction is given in Table 2.3. The N-S tests began with a series of tests at the 5,000 lbf level to determine the damping and mode shapes after the large amplitude E-W tests and prior to N-S tests.

The periods of the first four measurable modes in the N-S direction were 1.22, 1.06, 0.32 and 0.29 seconds, respectively. These modes were nominally called the first N-S translation, first N-S torsion, second N-S translation and second N-S torsion. It should be noted that each of the four modes contained both translation and torsional components. These tests were followed by damping tests at the two second mode periods (0.32 and 0.29 seconds) at force levels that increased in 5,000 lbf increments from 10,000 lbf to 25,000 lbf. Only minor stiffness degradation occurred in the structure during these tests. Standard damping tests at the 5,000 lbf force level were performed to determine the

changes that occurred in the periods and damping values as a result of these higher force level second mode tests. The changes in the periods were 1.22 to 1.32 seconds (+8%), 1.06 to 1.09 seconds (+3%), 0.32 to 0.37 seconds (+16%), and 0.29 to 0.30 seconds (+5%). The percentage changes are higher for the "translational" nodes than for the "torsional" modes, and are in both cases higher for the second mode than for the corresponding first mode.

The higher force level damping tests performed at the first mode periods were modified because of the continuing softening or stiffness degradation of the structure. As the period of the forcing function neared the first modal period of the structure, the displacement response of the structure increased, causing stiffness degradation at beam ends and in the exterior beam-column joints. This increased the period of the structure, and to obtain resonance, the period of the excitation force had to be increased. This resulted in further stiffness degradation until a steady-state condition was obtained for the force level of excitation. At the 10,000 lbf level, stiffness degradation occurred until the two first mode periods had increased from 1.09 to 1.22 seconds and 1.32 to 1.89 seconds, respectively. These periods were the upper bounds attained with the excitation force at 10,000 lbf. When the force level of the shaker increased to 15,000 lbf, the first torsional period increased from 1.22 to 1.47 seconds, and this appeared to be the steady state condition at this force level. The first translational period increased from 1.89 to 2.5 seconds, but did not reach a steady state condition. The building was severely damaged at this stage and it was decided to obtain the mode shapes and damping values before the final large amplitude tests were performed. During these first mode tests, the two second mode periods increased from 0.37 to 0.52 seconds and 0.30 to 0.34 seconds, respectively. Additional testing was performed after these mode shape tests until the structure appeared near collapse. Data was recorded but was not used in the correlation study.

4.1.2 Summary of Damage During N-S Tests

A description of the damage that was associated with the N-S tests is given in Section 2.3 and is summarized as follows:

1. The bottom reinforcing bars at beam ends were generally not anchored into the beam-column joints. As testing progressed, the bottom beam steel pulled out, providing a hinge under positive moment at the beam ends. Beam hinging gradually progressed up the height of the building as the force level of excitation increased.
2. The beam-column joints were without any confining reinforcement. This permitted the formation of diagonal shear cracks in the joints and was followed by spalling of the concrete in the joint. The

spalling was very severe on the two corner columns of the W face of the structure and became significant at the lower levels of the joints on column 42 towards the end of the 15,000 lbf test.

4.2 SCOPE OF THE CORRELATION STUDIES

The objectives of the correlation studies were as follows:

1. Evaluate the ability of existing non-linear analysis programs to predict, in a global sense, the structural behavior observed during the tests.
2. Evaluate appropriate methods of representing the non-linear behavior observed during the tests (i.e., beam hinging and joint degradation).
3. Develop a 'best fit' inelastic analytical model of the structure to evaluate the structure's capability to resist seismic ground motions representative of regions of varying seismic risk.

The major non-linearities observed in the tests [3] and typical of a non-seismically designed reinforced concrete structure, were bond failure of inadequately anchored beam reinforcement and shear failure of the inadequately reinforced beam-column joints. Both of these local failure modes prevented non-linear behavior from occurring within the beams and columns and restricted the non-linear behavior to the joints of the structure.

Unfortunately there is no cyclic test data available on poorly designed reinforced concrete joints and consequently, their analytical behavior could not be based on component test data.

4.2.1 Response Quantities for Correlation

The global response of the structure was of primary concern in the correlation because detailed measurements of localized structural behavior were not obtained. Thus, the major effort of the correlation studies was directed towards obtaining good matches with the structure's natural mode shapes and periods as the damage progressed.

It was decided to confine the correlation studies to the tests in the N-S direction for three reasons:

1. The removal of the external cladding and the insignificant stiffness contribution of the stairwell provided a "cleaner" test structure.
2. Structural degradation was more marked in this direction and provided a greater test of non-linear analysis programs.

3. There were two complete sets of mode shape tests conducted in this direction (before and after the bulk of the degradation), providing a more complete set of information with which to correlate the model's properties.

Triaxial accelerometers were placed on the 1st, 3rd, 5th, 7th, 9th, and 11th floors during the damping tests [3]. These were used to obtain the accelerations and displacements that occurred during the damping tests. During the mode shape tests, the 3-D acceleration response was obtained for a grid of 25 points on the 1st, 3rd, 6th, 7th, 9th, and 11th floors. This permitted a detailed determination of the mode shapes at every second floor level.

4.2.2 Structural Models

The essential feature of the test program the analytical model had to capture was the gradual stiffness degradation of the structure. This required that a non-linear model be used. The initial model incorporated the damage observed during the E-W tests. The results of an eigenanalysis at time step zero were correlated with the mode shapes and periods measured at the start of the N-S tests. The model was then subjected to a forcing function with the basic characteristics used in the tests (sinusoidal, with slowly increasing period), but of a shorter duration than was actually applied. The results of this analysis led to the calculation of a new set of stiffness parameters which reflected the damage induced by the N-S tests, and these stiffnesses formed the basis of the final model, from which the final analytical mode shapes and periods were calculated.

4.3 COMPUTER PROGRAMS

The computer program used was a version of DRAIN-TABS [5], developed by the Division of Structural Engineering and Structural Mechanics at the University of California, Berkeley, and adapted for a PRIME 750 computer by Computech. Three new features were developed for DRAIN-TABS specifically for this project. One was the "crimped hysteresis" beam element, which is described separately within the section on beam and joint models (Section 4.4.1). The other two are described in detail in Section 4.3.1.

4.3.1 New Features Developed for DRAIN-TABS

Two of the features developed on this project for DRAIN-TABS are described in the following two subsections.

4.3.1.1 Forced Vibration Response

The tests were performed using an applied forcing function distributed between the 10th and 11th floor levels. The original version of DRAIN-TABS (Berkeley v.9.1.76) was capable of handling only base acceleration as the dynamic excitation. The program was therefore extended to allow a series of dynamic force excitations to be applied to the structure at arbitrary locations on an arbitrary set of diaphragms. The scope of the modifications performed is presented following an overview of the solution procedure of the program.

The solution procedure in DRAIN-TABS involves two distinct phases:

1. Solution of the problem in terms of the condensed lateral stiffness matrix for the structure. This involves three degrees of freedom per diaphragm, namely two orthogonal horizontal translations and a rotation about a vertical axis through the center of mass of the diaphragm.
2. Solution for each frame independently, subject to the constraints imposed by the connected (i.e. diaphragm) degrees of freedom.

This dual solution strategy is of course nothing more than the substructure technique. Phase 1 requires the condensation of the structure load vector and the corresponding mass and stiffness matrices. In the original version of the program, the structure load vector is assembled from contributions from three sources: static concentrated loads applied at arbitrary points on the diaphragm, static loads applied at nodal points on the frames, and loads arising from the base acceleration input.

The implementation of the forced vibration solution involved the appropriate augmentation of the load vector to include effects from the forcing function as well as the other effects mentioned above. The procedure is as follows:

1. Input arbitrary function(s) of time.
2. At each diaphragm and for each location where dynamic loading is desired, specify the forcing function and scaling factors to be applied in the global X and Y directions. The coordinates, in the global X-Y system, of the point of application of the load are also required.
3. Compute the load increments corresponding to the solution time step at a given point in time, and transform them to the diaphragm degrees of freedom. Increment the condensed load vector accordingly.

A simple representative linear structural model was utilized to verify the new option. The results computed by the program were in excellent agreement with closed form analytical solutions.

4.3.1.2 Instantaneous Eigensolver

In order to keep a structural model with degrading stiffness (and changing period) at resonance, the ability to "follow" the degrading structural period with the period of the forcing function was required. The ability to alter the period of the forcing function interactively during any computer run was developed and implemented in DRAIN-TABS.

This required the ability to take the current global stiffness matrix at any point during an analysis (typically at response peaks or zero-crossings) and perform an eigensolution. This feature was added to facilitate the monitoring of the structural degradation during the forced vibration correlation.

4.3.2 Program Verification

As described in the previous two sections development work was required on DRAIN-TABS as part of this project. To test the program's new features without undue expense, a two-story, two-bay frame was modelled using beam-column elements for the columns and the new "crimped hysteresis" beam elements (Section 4.4.1) for the beams. A comprehensive series of load cases were run with this model to test the capabilities of both the load model and the new beam element. The parameters for the "crimped hysteresis" elements were adjusted to give a parallelogram-shaped loop as would be obtained from the beam-column elements. Beam-column elements were then substituted for the "crimped hysteresis" elements and results were compared and found to be in excellent agreement. Thus the crimped hysteresis elements were verified. The loading function was verified by performing hand calculations for a simple load case and comparing the results to those obtained from the program. Again the agreement was excellent. Finally, the eigenanalysis feature was tested by performing eigenanalyses on simple systems with known dynamic properties, and again DRAIN-TABS predicted these properties with a high degree of accuracy.

4.4 BEAM AND JOINT MODELS

To model the non-linearities that occurred in the test structure, a new element was developed for the non-linear beam behavior and is described in the following section. An existing column element was used to model the joint degradation as discussed in Section 4.4.2.

4.4.1 "Crimped Hysteresis" Beam Element

From studying the report on the large amplitude tests [3] and watching the movie of the structure's response during the tests, it was obvious that joint behavior played a large part in the overall response of the structure. Bottom beam steel was seen to pull out from the beam-column joint, and this was confirmed by inspection of the plans. The bottom beam steel was not continuous through the interior joint - rather bars came into the joint from both sides and lapped six inches within the column. On the exterior joints, the situation was no better. While the top steel had a hook detail, the bottom steel merely went straight into the joint. These details implied that the beam's full positive yield moment could not be developed at either the interior or exterior joints. Rather, the bottom steel would slip at a substantially smaller moment. Also, after the first cycle, the top steel would slip through the width of the column until the crack due to negative moment on the other side of the column closed, before the beam's full negative yield moment could be developed. The postulated hysteresis loop for this behavior of the beam end moment versus end rotation is shown in Figure 4.1. This is quite different from the loop available in any of the beam-type elements existing in either DRAIN-2D or DRAIN-TABS.

It was therefore decided to develop a new beam element with the required hysteresis loop. The reinforced concrete beam element available in DRAIN-2D was used as the starting point. This element is formulated in terms of a series of sub-elements: a linear elastic beam element, with non-linear rotational springs at each end. All plastic deformation effects, including the effects of the "crimped" hysteresis loop, are introduced by means of the moment-rotation relationships for the hinge springs. These moment-rotation relationships are specified by a set of six rules, the appropriate rule depending on the past history of element actions. The extra two degrees of freedom associated with the deformation of the two rotational springs are condensed out within the element, leaving it with six degrees of freedom, namely a rotation and two translations at each end. This series formulation for complex elements is now accepted as the most efficient way to form the stiffness for such elements, and supersedes the previously popular parallel element formulation.

The element was formulated in a rather general manner. By varying the input parameters, the shape of the hysteresis loop can be changed substantially. This generality required little extra development work, while providing a much more versatile element. The most general form for the hysteresis loop is shown in Figure 4.1, while the basic one used in this study is shown in Figure 4.2. The parameter α_1 controls the length of the plateau before hardening occurs, and the loop may be prevented from hardening on one or both sides by specifying the yield moment M_y and the slip moment M_s to be equal. The yield moments, slip moments and strain hardening ratios may each be different at each end of the beam. The initial stiffness of the hinge can either be automatically set by the program to a large value so that the hinge is essentially rigid until it slips or yields, or it can be input by the

user. The strain hardening ratio can be made to apply to just the hinge moment-rotation relationship, or to the overall moment-rotation relationship including the flexibility of the beam itself.

An element with a hardening portion in its hysteresis loop should use the so called "event-to-event" solution strategy. This strategy currently exists in the program DRAIN-2D, but does not in DRAIN-TABS. Because of the substructured nature of DRAIN-TABS, implementing the event-to-event solution strategy is a major development effort, and is well beyond the scope of work for this project. However, elements are interchangeable between the two programs. Thus the effect of not using the event-to-event strategy in DRAIN-TABS could be studied by running the same two-dimensional frame problem on both programs. The DRAIN-2D version would use event-to-event, but the DRAIN-TABS version would not. A two story, two bay frame was studied in this manner, and it was found that good agreement could be obtained between the two programs, providing the time step in DRAIN-TABS was reduced relative to that used with event-to-event in DRAIN-2D.

4.4.2 Degrading Stiffness Joint Element

The problem of modeling the joint stiffness degradation due to shear cracking and concrete spalling was open to several options. Three potential solutions were investigated as follows:

1. Use an inelastic rotational spring element and connect it to the beam and column members at each joint.
2. Model the joint degradation by a hinge at the top of the column using the non-linear beam-column element of DRAIN-TABS.
3. Model the joint degradation by a hinge at the top of the column using the extended version of the Takeda column element of DRAIN-TABS.

Option 1 was extensively investigated using a two-story two bay simplified model shown in Figure 4.3. Each joint is modelled by two nodes, both having the same translational degrees of freedom. The beam elements are connected to one node, the column elements to the other. Relative rotation is permitted between the two nodes, and it is this rotational degree of freedom for which the inelastic rotational spring provides stiffness. This rotation is intended to model the shear deformation of the joint.

Interaction between the beam hysteresis and the joint element led to a condition in the model which was not representative of the actual structural behavior. It was found that when the joint element yielded,

insufficient loads were transferred to the beams to cause them to yield or slip. Conversely, when the yield moment for the joint element was increased, slip and yield would occur in the beams, but the moments would not reach sufficiently large values to cause plastic rotation in the joint element. Also, as the value for the initial stiffness of the joint was decreased from a very large value to a rather small value, a trade-off was observed between rotation taking place in the joint element, and in the plastic hinge at the end of the beam. However, as these two rotations changed in relative magnitude, the overall structural displacements remained fairly constant. It was thus decided not to use the joint element as a means of modeling the joint degradation.

Option 2 was investigated using the full model of the structure. The characteristics of the beam-column model has only two stiffnesses that govern the hysteretic behavior of the model. Detailed investigation of the column element behavior revealed that the columns which yielded spent a relatively small proportion (less than 20%) of the total response time on the "soft", post-elastic slope of their hysteresis loops. The bulk of the response was governed by the initial stiffness. Thus in any one run, the initial elastic stiffness was unchanged from start to finish. This was not representative of what actually occurred in the test structure.

To correctly model the degradation that was occurring in the joint, it would have been necessary to adjust the initial stiffness of the model as the deformation in the joint increased. This would have been a tedious and inefficient procedure, and therefore, option 3 was investigated.

Option 3 used a degrading stiffness element to model the columns in the four exterior frames and a suitable element was available in DRAIN-TABS. The hysteresis loop available in this element is an extended version of the Takeda model, representing typical behavior of reinforced concrete members and its general shape is shown in Figure 4.4. The advantage of using this type of element is that stiffness degradation may take place during the course of a particular run. Two simplified models were studied, identical in every respect except that one had the columns modelled with degrading stiffness elements. The initial stiffness in each of these elements was exactly the same as that in the corresponding element modelled using the regular beam-column element. The response of the simplified model using the degrading stiffness element, when compared to the response of the model with the bi-linear column stiffnesses, indicated that the degrading stiffness element could model the observed behavior adequately.

In view of the advantages that the degrading column element offered for the earthquake phase of the study, considerable effort was spent in formulating a full structural model incorporating this element. It was tested extensively and was found to work very well in conjunction with the eigensolver, to monitor the degradation and "resonance" of the structure. This, then, was the approach used in matching the stiffness degradation of the joints observed during the tests.

4.4.3 Evaluation of Element Parameters

Having selected the element models to be used for the analysis, the problem of calculating appropriate parameters to define the elements' properties remained. For the "crimped hysteresis" beam element, the yield and slip moments were needed, and for the degrading column element the yield moments were required. The slip moments were the most crucial parameters, and were highly dependent on the bond stress assumed between steel and concrete.

After an extensive review of the relevant literature [10,11,12,13], a value of 625 psi was selected as a reasonable estimate of the bond stress between steel and concrete. Based on actual anchorage lengths, a set of moments were calculated using this value for the bond stress. Slip moments calculated in this way were invariably a high percentage of the yield moments (which were calculated assuming a yield stress for the steel of 60 ksi and concrete compressive strength of 8 ksi - these values coming from actual samples taken from surrounding buildings [1]). The percentage of slip moment was generally in excess of 50% of the yield moment. After watching the movie of the tests, it was obvious that these values for slip moments were much too high. After total loss of bond between steel and concrete, the frictional strength may be taken between 100 and 200 psi [14]. The slip moments were thus based on a bond strength equal to 200 psi. This assumption resulted in slip moments of the order of 10% of the corresponding beam yield moments, a value considered reasonable. It should be noted that the positive yield moment and the positive slip moment are set equal, due to the lack of anchorage for the bottom steel in all joints.

The yield moments for the columns were required to reflect damage in the beam-column joint rather than actual column hinges. Shear degradation of the joint does not allow sufficient load to be transferred to the columns for real column hinges to form. The column yield moments cannot therefore be calculated from the column section and the reinforcing steel as would normally be the case, but rather, must reflect the strength of the joint. Since the slipping of the beam steel was observed to occur during the tests at about the same time as the joints started to deteriorate, the column yield moments were related to the beam slip moments. It was noted during the tests that initial diagonal cracking of the joints occurred at approximately the 10,000 lbf load level of the first mode tests. Thus a linear static analysis was run with 10,000 lbf times the dynamic amplification factor as the load. The moments from this run were then examined as potential values for column yield moments. It was noted that the moments at the top of each column were of the same order as the beam slip moments at the corresponding joint. As already mentioned, the problem is really one of joint action, and the same parameters affect both beam and column as modelled here. It thus seemed reasonable to base both column and beam yield properties on the same parameters. This is effectively achieved by setting the column yield moment to the corresponding beam slip moment for corner columns, and to the sum of the beam slip moments on either side of the column for interior columns on exterior

frames. Corner columns were assumed to be elasto-plastic, while interior columns on exterior frames were assumed to have a bi-linear moment-rotation relationship, with a second slope equal to 30% of the elastic stiffness. This was because corner columns were observed to undergo more severe degradation than were interior columns. The interior frames have columns which remain elastic, as no damage was observed in these columns during the tests. However, the "crimped" beam model was used for the beams in all frames.

4.5 MODEL PRIOR TO NORTH-SOUTH TESTS

The starting point for the modelling of the structure for the N-S behavior was the "best" model from the small amplitude correlation studies. This model was described in Section 3.3 and used the program SAP IV. An equivalent DRAIN-TABS model was established and then modified to reflect the effects of the large amplitude E-W tests. In the real structure, the following had taken place between the end of the small amplitude tests and the start of the North-South large amplitude tests:

1. A substantial hole had been cut in the roof slab to enable the large amplitude test equipment to be positioned in the structure. Extra weight was present in the structure due to the test equipment and its lead weights.
2. The structure had undergone considerable shaking and consequent damage due to the large amplitude tests in the East-West direction.
3. After the completion of the East-West tests, the external cladding had been removed from all stories except the top two.

The following changes were thus made to the "best" model from the small amplitude correlation studies:

1. The masses from the external walls were removed from the model. This effected both the translational masses and the rotational inertia.
2. The mass of the shaking equipment was added at the appropriate level.
3. The mass corresponding to the portion of the roof slab which was removed, was removed from the model.
4. The stiffness contributions from the external walls, from the walls around the stair wells and from the stairs themselves were removed. The stiffness from the stairs and stair walls was removed because they were modelled as diagonal truss elements, and it was felt that they were contributing an artificially high vertical stiffness, which caused problems in matching the second mode frequencies. The stairs and stair walls contributed little to either the N-S translational stiffness, or to the rotational stiffness. They provided stiffness primarily in the E-W direction, and the structure's dynamic properties in that direction

were not of concern.

5. The damage observed during the E-W tests was confined mainly to the beams at levels 1 through 6. Plastic hinging was apparent at the ends of these beams in the exterior E-W frames. An estimate was made of the hinge length for these beams, and the cracked section moment of inertia was assigned in this region at each end of a typical beam. The gross moment of inertia was used for the remainder of the beam. A separate analysis was then conducted on a single beam, discretized as a series of beam elements to calculate the equivalent prismatic beam stiffness coefficients for use in DRAIN-TABS.

The E-W beam stiffness parameters were adjusted slightly from their initial values until reasonable correlation was obtained with the first 4 periods measured at the start of the large amplitude North-South tests. The "best fit" model compared to the test results follows:

Mode	Test Period	Model Period
North-South 1st	1.22 seconds	1.20 seconds
Torsional 1st	1.06 seconds	0.92 seconds
North-South 2nd	0.32 seconds	0.35 seconds
Torsional 2nd	0.29 seconds	0.27 seconds

4.6 MODEL FOR DEGRADING STRUCTURE

The three major aspects involved in modelling the degradation of the structure are described in the following three subsections.

4.6.1 Initial Modelling

The structure was idealized as a set of eight frames as shown in Figure 4.5. DRAIN-TABS assumes that these frames have stiffness only in their own planes. The frames are interconnected by rigid floor diaphragms, one diaphragm corresponding to each floor level. The model's natural periods were dependent only upon its elastic properties. Its post-yield properties were yet to be determined.

The columns in the model of the structure were initially constrained to remain elastic by specifying very high yield moments. Yield moments for the beams were calculated using the properties measured in the dimensional and material properties survey [1]. If the anchorage length provided did not permit the development of the full yield stress in the reinforcing bars, the bars were assumed to slip before yielding. This was universally the case for positive joint moments. The method of calculation for the slip and yield moments is described in Section 4.4.3.

This initial model was tested extensively to verify that the structural

configuration and properties were representative of the actual test structure. Initial computer runs were conducted using artificially high load levels to ensure that the beam elements cyclic behavior were working correctly. After careful study of the results from these runs, the model was deemed to be free of errors.

Considerable effort was made in the choice of a suitable integration time-step. A balance was sought between accuracy and economy. Initially a time step of 0.01 seconds was used. This is 0.0079 times the fundamental period of the model, and 0.0307 times the fourth natural period of the model (the highest mode of interest). An often-used rule of thumb is that the time step should be approximately 1% of the fundamental period, and no more than 10% of the period of the highest mode of interest. A time step of 0.01 seconds satisfies both of these guidelines with ease. For the sake of economy, a larger time step was investigated. A time step of 0.02 seconds was tested (this is 0.0158 times the fundamental period and 0.0613 times the fourth) but the solution with this time step tended to become unstable very suddenly (due to the stiffening branch of the beam element hysteresis loop). This is a consequence of not using the event-to-event solution strategy with a stiffening element. Thus an integration time step of 0.01 seconds was chosen for the correlation analyses, and no numerical instability was observed in the subsequent runs.

Mass proportional damping was provided in the structural model to give a damping ratio of 3% at a period of 2 seconds. This value was based on the damping tests on the structure [3].

4.6.2 Adjustment of Model Parameters

Due to constraints imposed by the modelling techniques, the model uses columns with appropriate end moment-rotation hysteresis loops to model what is essentially a joint phenomenon. While this model is satisfactory, appropriate properties must be specified for the column elements, as shear cracking and disintegration of the joints is equivalent to columns with a hinge at one end in this model. The overall column properties must be specified to include the effect of the hinge.

The top of each column in the four exterior frames was permitted to yield, with a hysteresis loop defined by the Takeda model with α and β both zero in Figure 4.4. This was justified by observations made during the tests. Thus, joint behavior is being modelled by element end behavior, and careful selection of member properties permits relatively accurate modelling. Yield levels for the columns were assigned based on observations made during the tests and described in Section 4.4.3.

The initial model was too stiff with regard to the action of the beams. The shape of the hysteresis loop is rather versatile, depending on the specification of its descriptive parameters. The early runs indicated that negative yield was never being reached in the main resisting frames. It is likely that this is in fact a realistic situation. Since there was

absolutely no confinement of concrete within the joint, the joints tended to break up before negative yield could occur. Thus top bars slip under negative rotation as the integrity of the joint is lost. However, the initial model of the beams had the negative moment increasing from the negative slip value to the negative yield value at zero hinge rotation, in all cycles, until negative yield was reached. In this case, negative yield was never reached. Consequently there was never any negative hinge rotation in the beams in the model. This was clearly not the case in the tests, as is easily seen by viewing the movie made during the tests. This difficulty was overcome by changing the value of α_1 for the hysteresis loop description from 1.0 to 1.5. The effect of this change on the shape of the loop is shown in Figure 4.2.

4.6.3 Load Level

The majority of the degradation observed during the test program was the result of a lengthy run with a slow change in the period of the excitation force from approximately 0.6 seconds to somewhat below the observed resonance at 2.5 seconds. This test was carried out at a nominal load level of 17,000 lbf.

In the early non-linear computer modelling, runs were made at this load level and indeed some degradation in the model stiffness (as indicated by changes in the eigenvalues) was obtained. However, the rate at which degradation occurred was such that the computer budget for the entire project could have been used in this phase of the project alone. With this in mind, it was decided to artificially increase the load level to expedite the degradation in the model. A load level of 50,000 lbf was thus used for all the forced vibration runs designed to degrade the structure.

As a check on the model properties at the end of the degradation, the degraded model was run under a realistic 17,000 lbf static load, and the order of the subsequent displacements (magnified by the dynamic load factor) were checked against those measured at the appropriate stage of the test program.

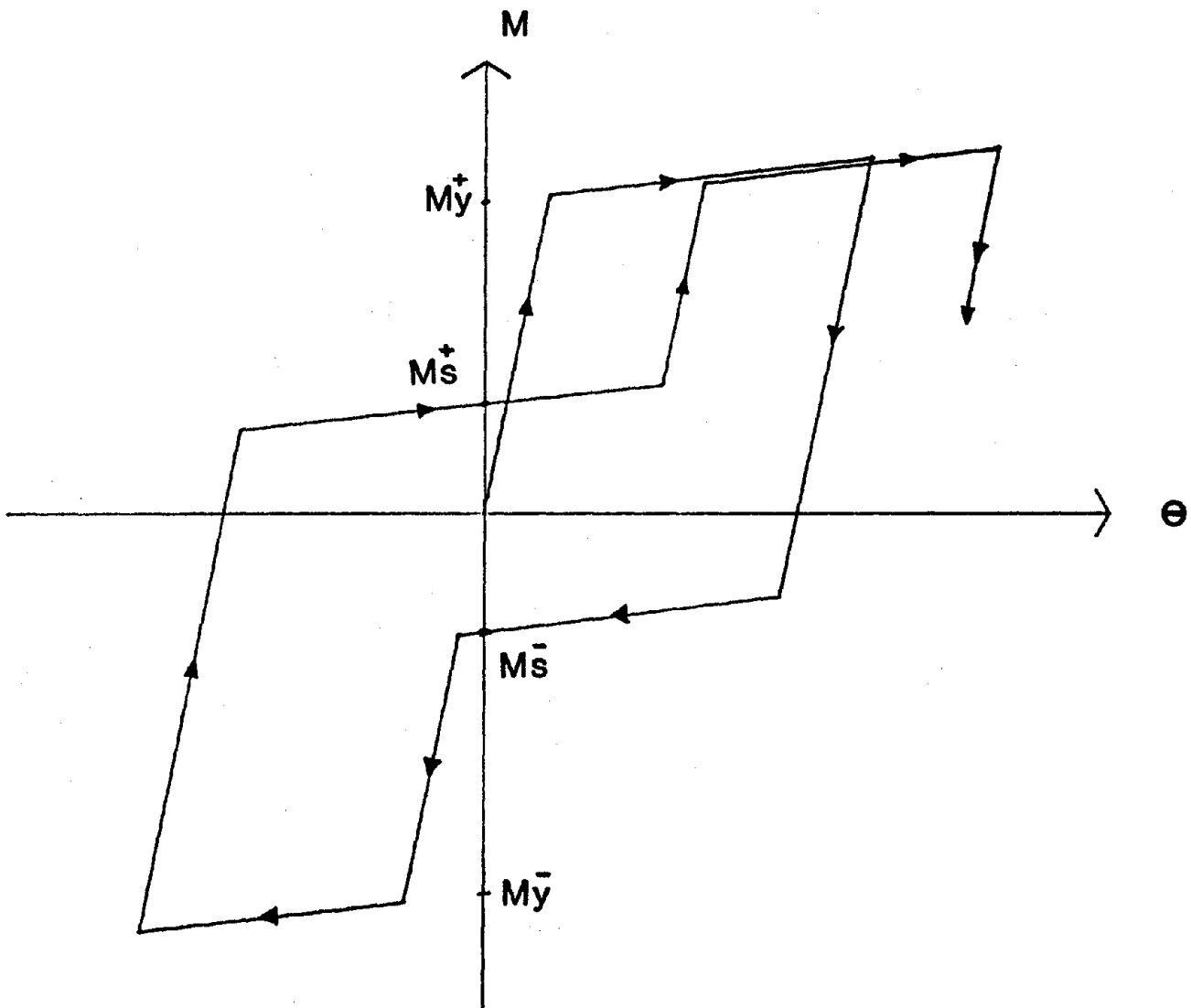


Figure 4.1 General Form of "Crimped" Hysteresis Loop

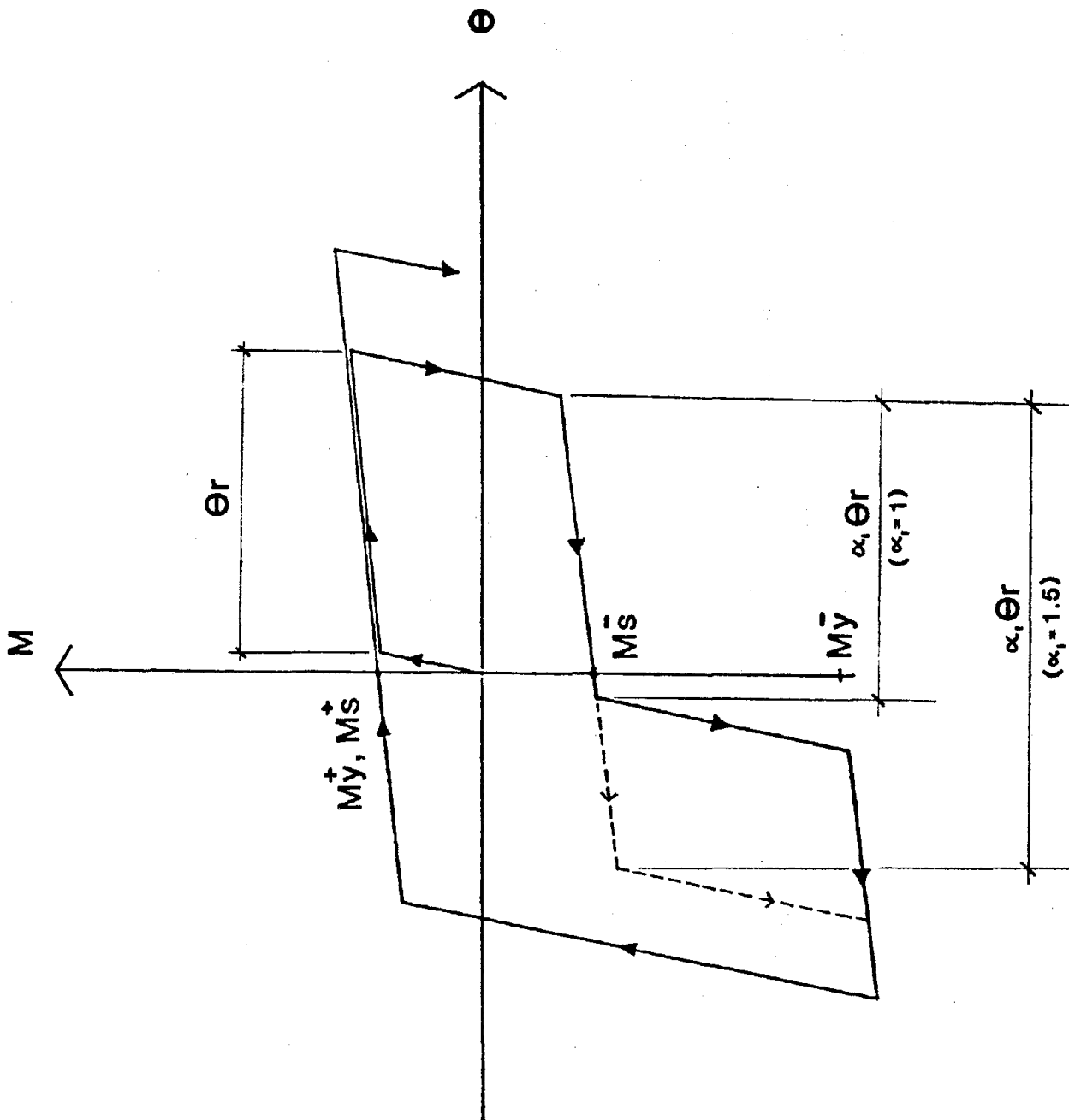


Figure 4.2 Specific Form of Beam Hysteresis Loop

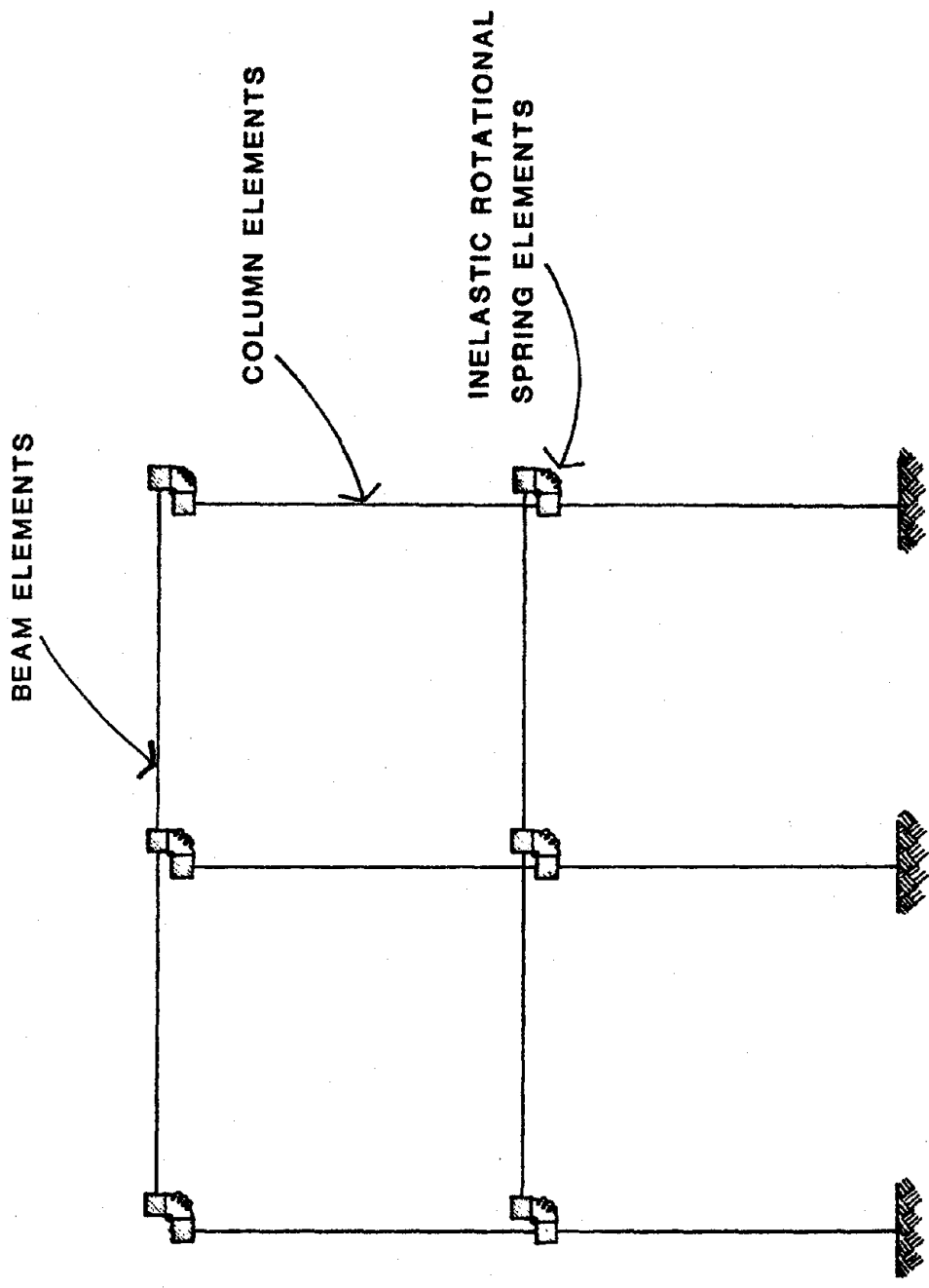


Figure 4.3 Structural Model Including Joint Element

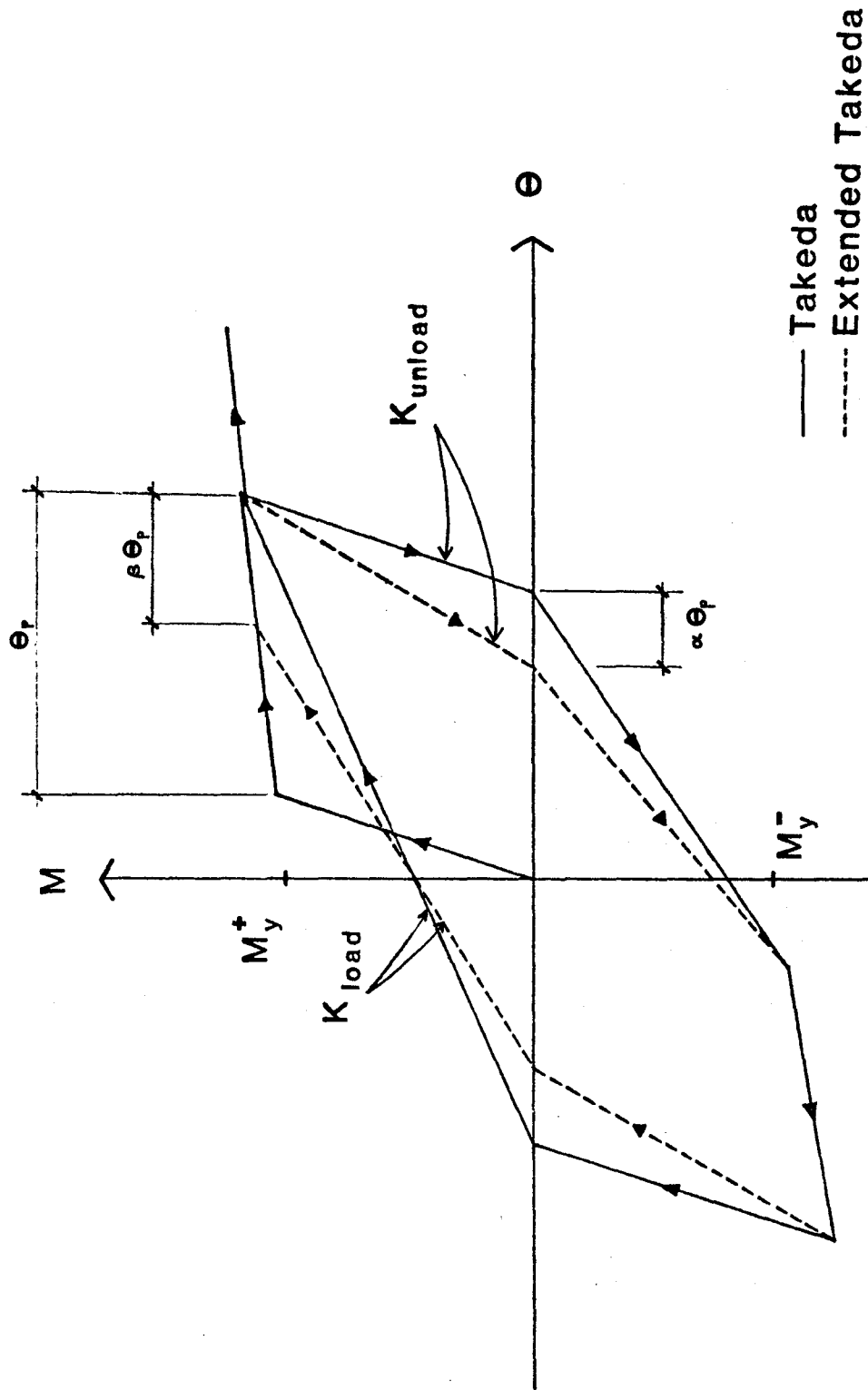


Figure 4.4 General Form of Takeda Hysteresis Loop

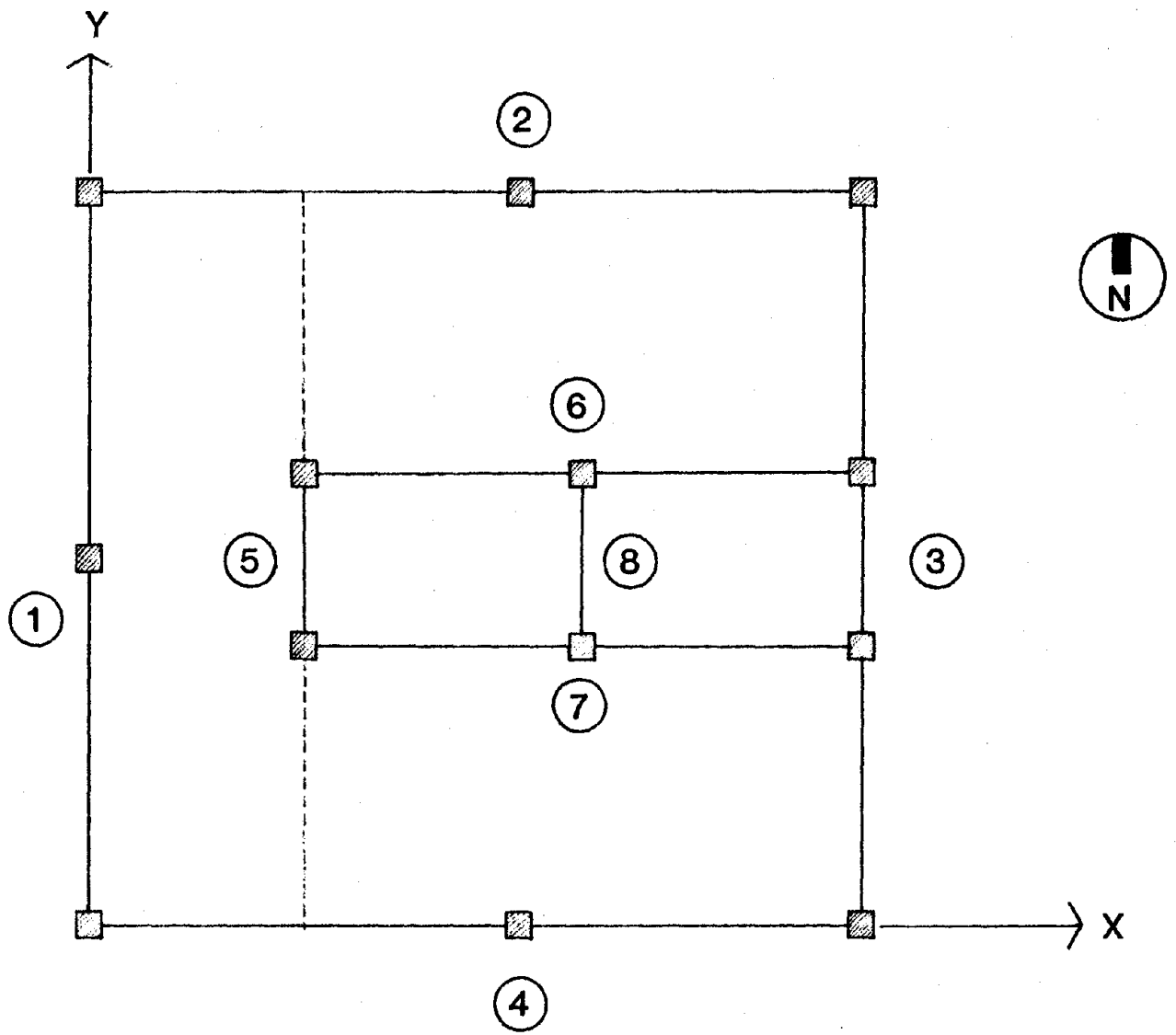


Figure 4.5 Plan of Model Showing Frame Numbers

5 RESULTS OF LARGE AMPLITUDE CORRELATION

This chapter presents the correlation of results from the analytical model with the observed response during the N-S large amplitude forced vibration testing. The correlation was performed in two distinct parts.

The first, presented in Section 5.1, consists of a comparison of the mode shapes and frequencies of the analytical model and test structure performed before and after large amplitude shaking. The second, presented in Section 5.2, consists of a comparison of the degradation observed during the large amplitude tests.

5.1 MODE SHAPES AND FREQUENCIES

Mode shape and frequency comparisons were made before and after the large amplitude shaking. The parameters of the analytical model used prior to the N-S large amplitude tests, discussed in Chapter 4, incorporated the degraded state of the beams following the E-W tests.

The four modes used for the comparison are nominally called the first and second north-south translational modes and the first and second north-south torsional modes. However, each of these modes has both translational and rotational components. The mode shapes and periods at the start of the north-south tests are shown in Figures 5.1 to 5.4. Those at the end of the test program are shown in Figures 5.5 to 5.8.

In general the agreement between experimentally measured mode shapes and those computed from the analytical models are very good. Figures 5.1 through 5.8 show both sets of mode shapes normalized with respect to the structure's mass matrix. The analytical mode shapes certainly capture the essence of the experimental shapes in every case.

The degree of correlation between the measured and computed natural periods is summarized in the table below.

TABLE 5-1

Mode	When	T (Test)	T (Model)	T_n/T_1 (Test)	T_n/T_1 (Model)
1st N-S	Start	1.22	1.20	1.00	1.00
1st Torsion	Start	1.06	0.92	0.87	0.77
2nd N-S	Start	0.32	0.35	0.26	0.29
2nd Torsion	Start	0.29	0.27	0.24	0.23
1st N-S	End	2.50	2.87	1.00	1.00
1st Torsion	End	1.33	1.70	0.53	0.59
2nd N-S	End	0.52	0.69	0.21	0.24
2nd Torsion	End	0.34	0.42	0.14	0.15

At the start of the N-S test the agreement between the fundamental periods is excellent, while the model is generally too stiff in the first torsional mode. Both second mode periods are in good agreement with those measured in the tests.

Considerable manipulation of the results was required before the final natural periods of the model could be calculated. The "instantaneous" eigensolver could not be used directly because the results are very sensitive to the location of each element on the hysteresis loop when the eigensolution is carried out. The degradation is permanent, however, as indicated by the small amplitude mode shape tests after the large amplitude degradation runs. Therefore, the maximum inelastic rotations were used for each member in frames 1, 3, 5 and 8 (the primary resisting frames for N-S response) to calculate an equivalent degraded stiffness which represented the structure at the end of the N-S tests. This was accomplished as follows. Using the plastic rotations, an equivalent linear EI for each hinge region (taken as the depth of the beams or the width of the columns) was calculated. The model for each beam or column then consisted of a section with the original EI in the central portion of the span and sections with a reduced EI at one or both ends, modelling the hinge region. Equivalent stiffness coefficients for a prismatic beam were then calculated. The structural model's final natural periods were based on these equivalent degraded stiffnesses.

While modelling of the considerable permanent degradation that occurred in the structure between the beginning and end of the N-S tests proved a real challenge, the correlation between the model periods and the test periods at the end of the test sequence is reasonable. The state of the structure predicted by the analytical model gave all four natural periods on the high side of the experimental values at the conclusion of the tests. This error may be due in part to the process used to derive the final equivalent degraded stiffness for use in the final eigensolution. However, when the results are normalized with respect to the first period, as shown in Table 5-1, the agreement between the test and model ratios is very good.

A difference of 15% between the first "translational" period and the first "torsional" period was observed at the start of the N-S tests. At the end of the tests, this difference had increased to 88%. The corresponding figures from the analytical model are 30%, increasing to 69% at the end of the tests. Thus the model predicted the increasing separation between these two modes although the magnitude predicted was not as large as that observed in the tests.

5.2 TIME HISTORY

The second set of results shows the time history of response obtained from the analytical model as the period of the shaker gradually changed from an initial value of 1.2 seconds to a final value of 2.85 seconds. The N-S, E-W and rotational responses to the forced vibration are shown in Figures 5.9, 5.10 and 5.11, respectively.

Figure 5.9 shows the gradual build-up of response in the N-S direction as the analytical model gradually degraded in stiffness. Figures 5.10 and 5.11 show the response in the E-W direction and the rotational response, respectively.

The analytical model did a good job of predicting the location of the major damage observed in the tests. The vast majority of the plastic rotations were restricted to the lower levels of frames 1 and 3 (the West and East frames, respectively). Frame 1 experienced greater degradation than did frame 3, and in each case, the plastic rotations were greatest at level 1. These results are entirely consistent with the damage observed during the tests.

The displacements predicted from the model, however, are lower than those observed during the tests. The model predicts approximately 4.5" maximum displacement. 5.4 inches was the measured displacement of frame 1 at the resonant period of 1.75 seconds. Displacements remained of this order until the very last test of the sequence when the resonant period was over 2.5 seconds. At this point, a displacement of 18 inches was observed in frame 1 and the structure was very close to collapse. Correlation with this displacement is given in the next section.

One aspect missing from the analytical model is strength degradation - the elements must reach the same force level each cycle before softening occurs. In a real structure, this force level would drop off as damage occurs, resulting in more time on the softer positions of the hysteresis loop. This artificially "late" decrease in stiffness in the model will effectively give low displacements in the model.

The model does indicate a gradual buildup in displacement as the system degrades and predicts the location of all major damage observed during the test program. It may therefore be stated that the analytical model captured the essence of test observations.

5.3 FINAL CORRELATION

As a final correlation, the model with the equivalent degraded stiffness properties (used to give the final mode shapes and periods) was loaded with a 17000 lbf static load, (the same load used at resonance during the latter part of the test program). Displacements from this analysis were then amplified by the dynamic load factor (calculated on the basis of 3% damping) to give a maximum displacement at the center of the 11th diaphragm of 16 inches. When the rotation of the structure is accounted for, the displacement at the top of frame 1 is 23.5 inches, and at the top of frame 3 it has a value of 8.5 inches. These are displacements at resonance for the model fundamental period of 2.87 seconds.

These displacements cannot be compared directly with actual measurements made during the tests, but steady state amplitudes were measured at a pair of fundamental periods shorter than the 2.87 seconds of the model.

During the course of degradation a large amplitude test was carried out when the structure had a fundamental period of 1.75 seconds. This test produced a maximum displacement of 5.4 inches in frame 1. A similar test performed with 17,000 lbf when the structure had a fundamental period of 2.5 seconds, produced maximum displacements in frame 1 of the order of 18 inches. At this point the structure was deemed to be perilously close to total collapse. This last value is to be compared with the 23.5" at the top of frame 1 predicted from the model at a resonant period of 2.87 seconds. The model also predicts a large torsional component of the displacement (as indicated by the 8.5" maximum displacement in frame 3), and this too is entirely consistent with the general response shape observed at the very end of the test program.

While not giving any absolute figures on the correlation with the displacements measured at the conclusion of the tests, the model displacement of 23.5 inches in frame 1 (at 2.87 seconds), is consistent with the observations made on the test structure.

ST LOUIS PRUITT-IGOE CORRELATION STUDY
NORTH-SOUTH FIRST TRANSLATIONAL MODE

———— MEASURED, $T = 1.22$ SECONDS
----- COMPUTED, $T = 1.20$ SECONDS

DATE 03/25/82

TIME 01:38:39

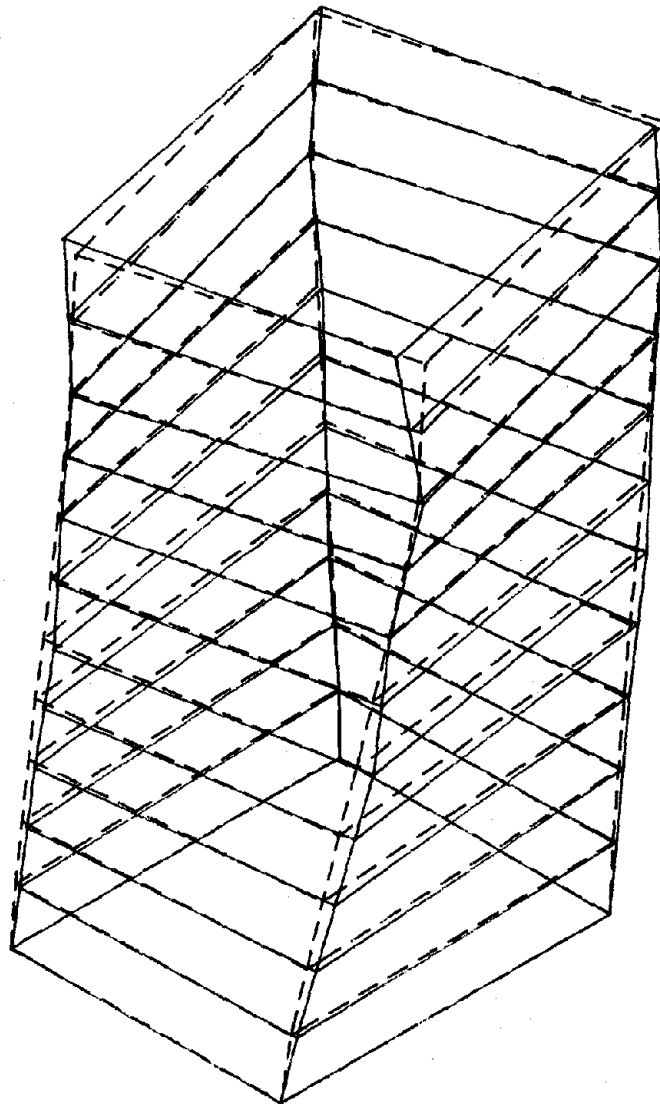


Figure 5.1 First N-S Translational Mode - Start of N-S Tests

ST LOUIS PRUITT-IGOE CORRELATION STUDY
NORTH-SOUTH FIRST TORSIONAL MODE

————— MEASURED, $T = 1.06$ SECONDS
----- COMPUTED, $T = 0.92$ SECONDS

DATE 03/25/82

TIME 01:39:29

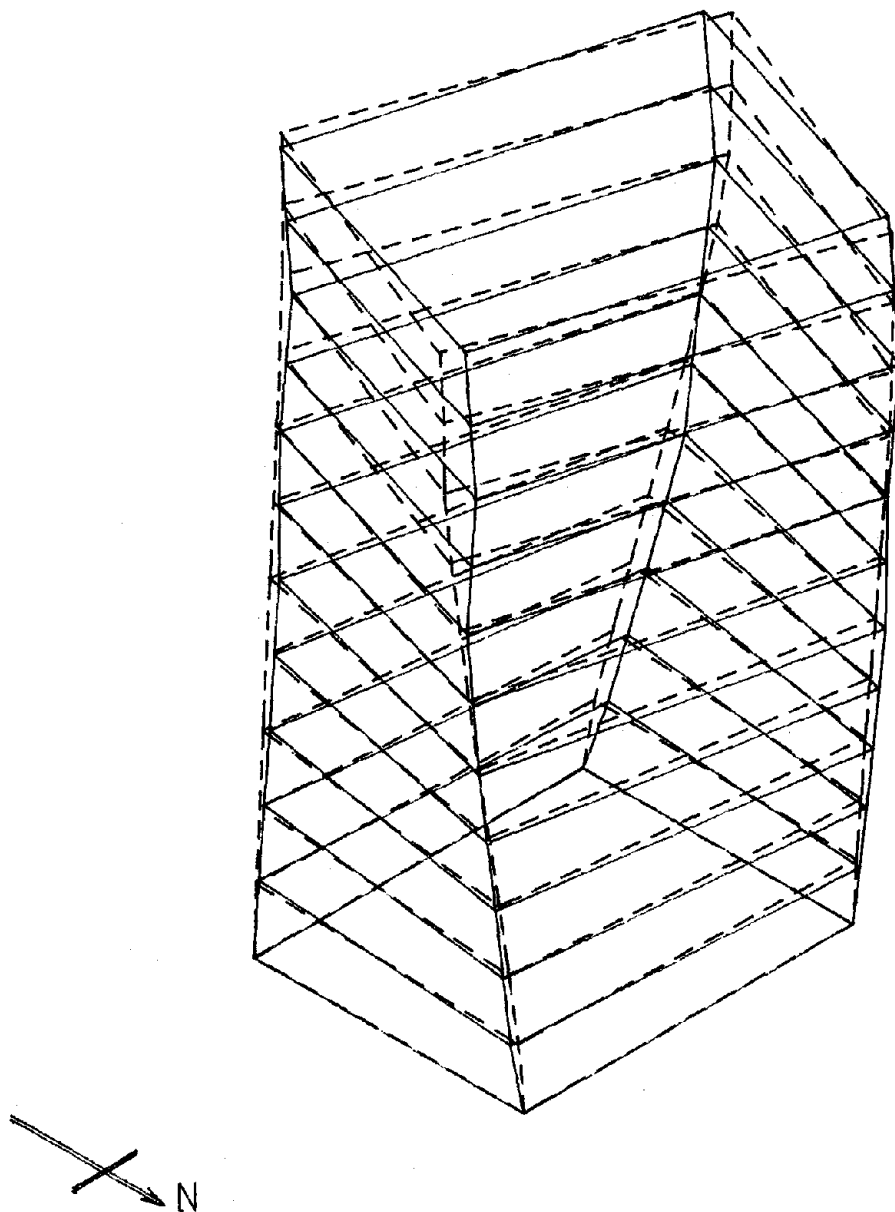


Figure 5.2 First N-S Torsional Mode - Start of N-S Tests

ST LOUIS PRUITT-IGOE CORRELATION STUDY
NORTH-SOUTH SECOND TRANSLATIONAL MODE

———— MEASURED, $T = 0.32$ SECONDS
----- COMPUTED, $T = 0.35$ SECONDS

DATE 03/25/82

TIME 01:39:06

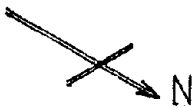
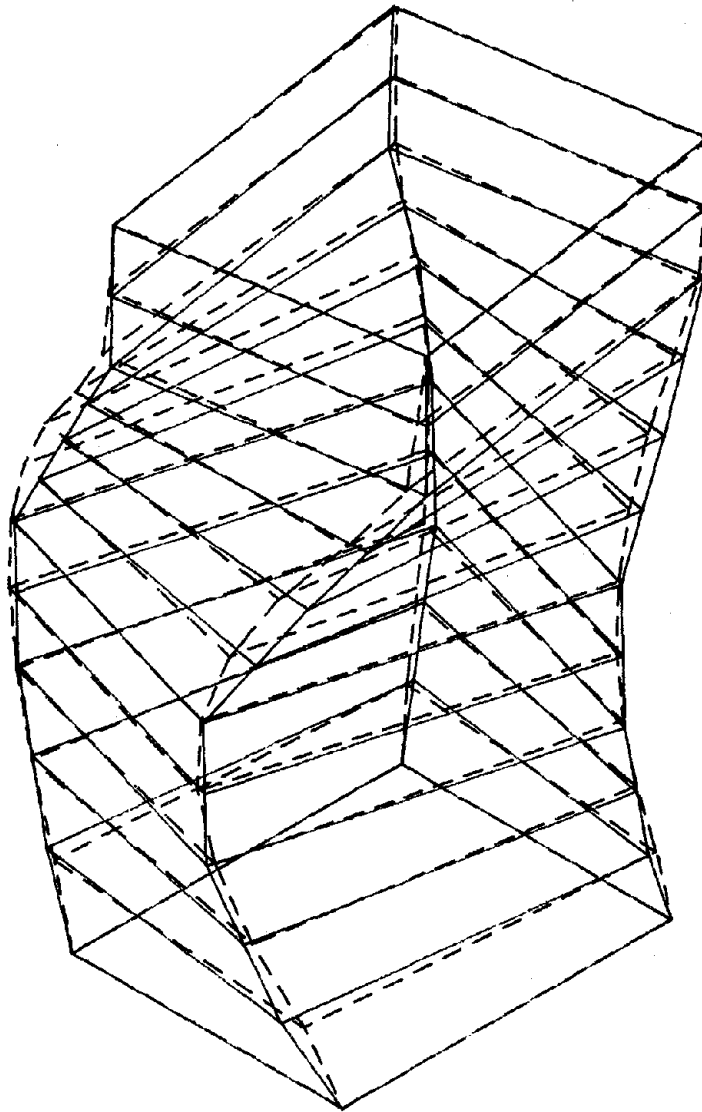


Figure 5.3 Second N-S Translational Mode - Start of N-S Tests

ST LOUIS PRUITT-IGOE CORRELATION STUDY
NORTH-SOUTH SECOND TORSIONAL MODE

———— MEASURED, $T = 0.29$ SECONDS

----- COMPUTED, $T = 0.27$ SECONDS

DATE 03/25/82

TIME 01:39:55

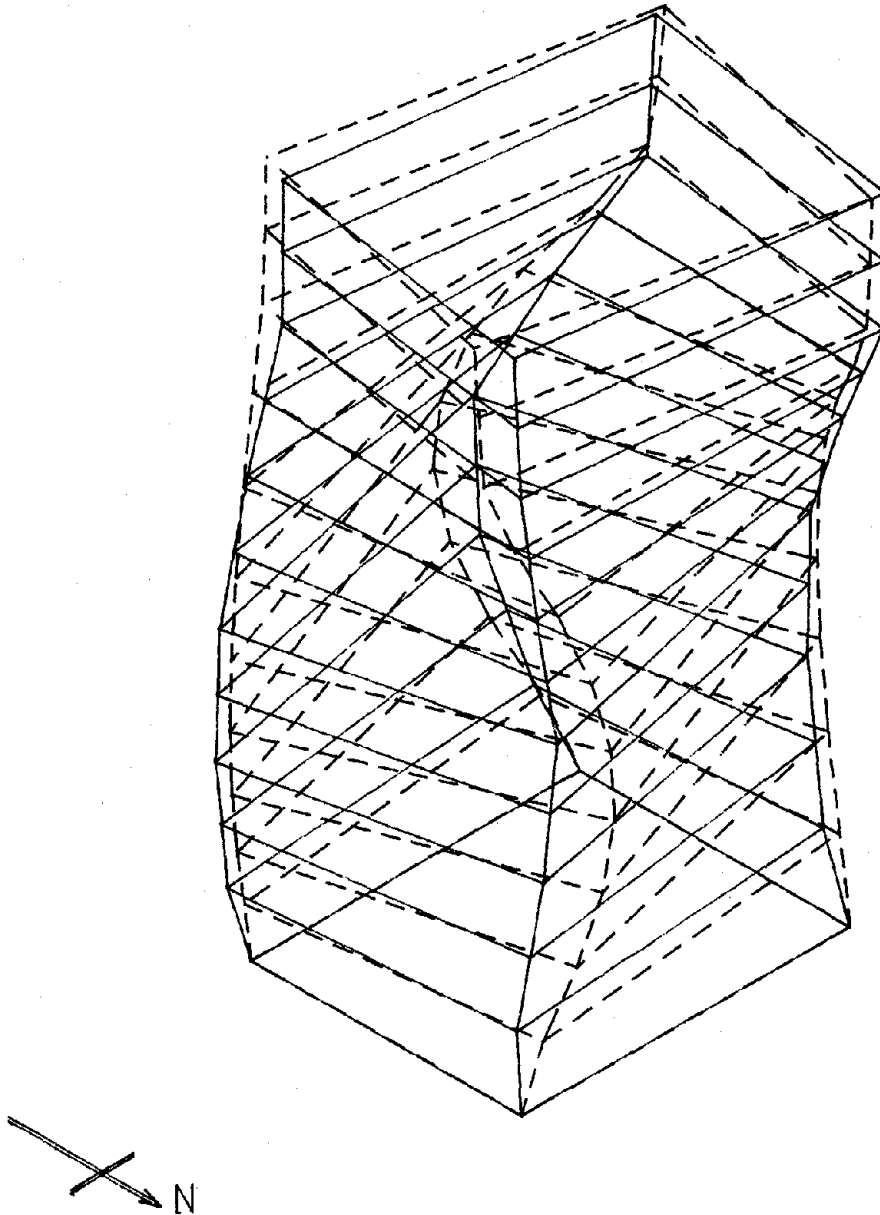


Figure 5.4 Second N-S Torsional Mode - Start of N-S Tests

ST LOUIS PRUITT-IGOE CORRELATION STUDY
NORTH-SOUTH FIRST TRANSLATIONAL MODE

———— MEASURED, $T = 2.50$ SECONDS

----- COMPUTED, $T = 2.87$ SECONDS

DATE 04/12/82

TIME 11:24:30

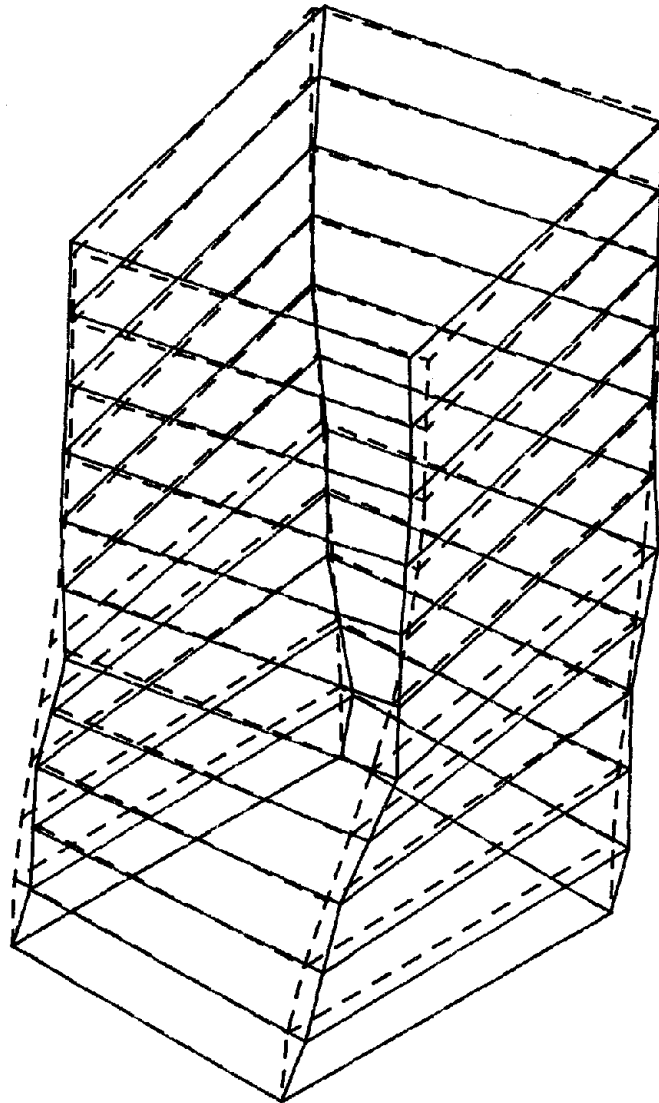


Figure 5.5 First N-S Translational Mode - End of N-S Tests

ST LOUIS PRUITT-IGOE CORRELATION STUDY
NORTH-SOUTH FIRST TORSIONAL MODE

———— MEASURED, $T = 1.33$ SECONDS
----- COMPUTED, $T = 1.70$ SECONDS

DATE 04/12/82 TIME 11:25:02

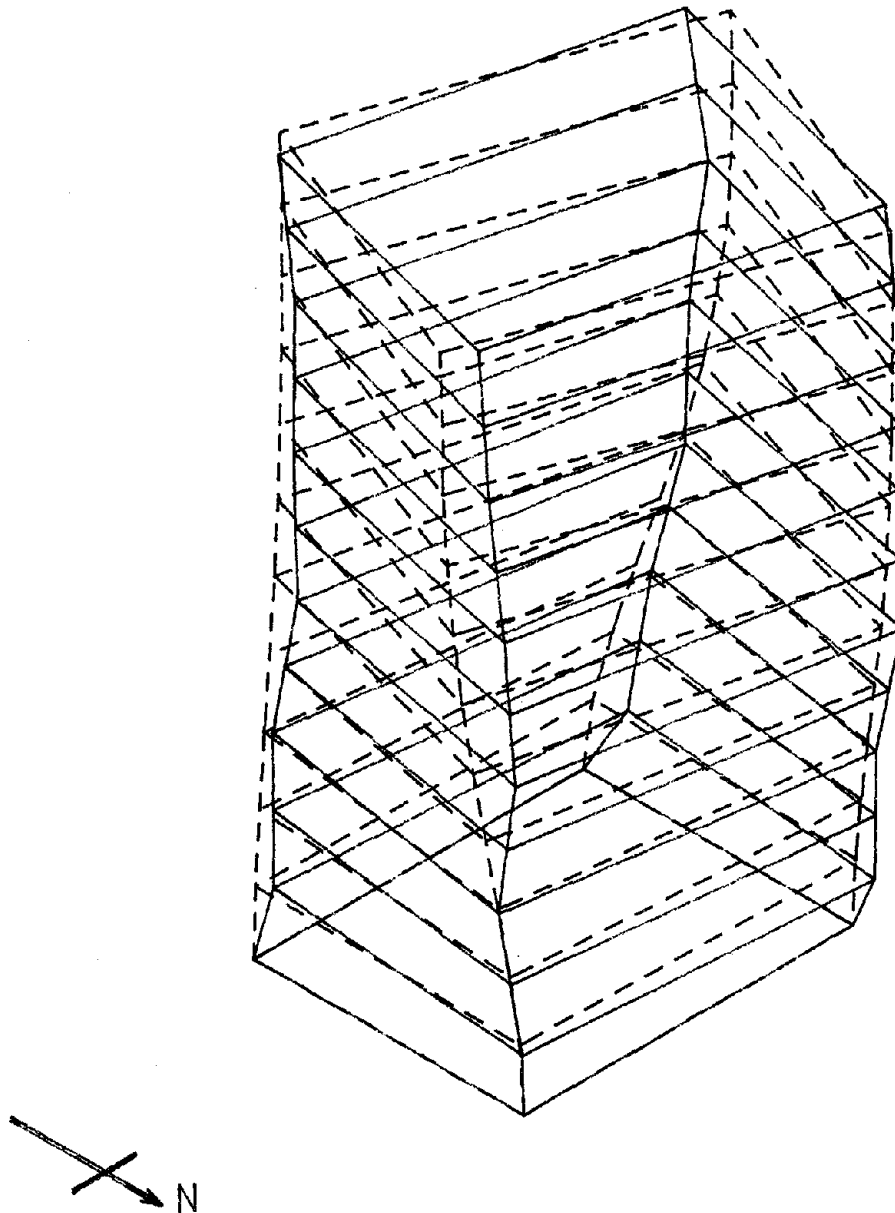


Figure 5.6 First N-S Torsional Mode - End of N-S Tests

ST LOUIS PRUITT-IGOE CORRELATION STUDY
NORTH-SOUTH SECOND TRANSLATIONAL MODE

————— MEASURED, $T = 0.52$ SECONDS

----- COMPUTED, $T = 0.69$ SECONDS

DATE 04/12/82

TIME 11:25:25

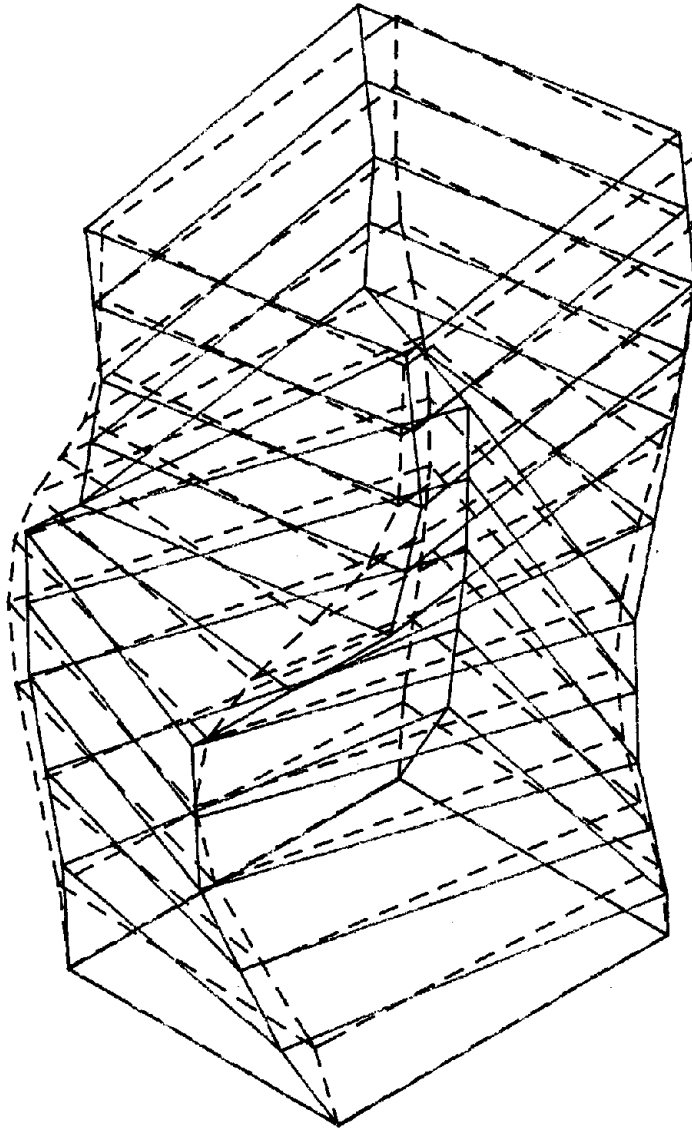


Figure 5.7 Second N-S Translational Mode - End of N-S Tests

ST LOUIS PRUITT-IGOE CORRELATION STUDY
NORTH-SOUTH SECOND TORSIONAL MODE

———— MEASURED, $T = 0.34$ SECONDS
----- COMPUTED, $T = 0.42$ SECONDS

DATE 04/12/82 TIME 11:25:49

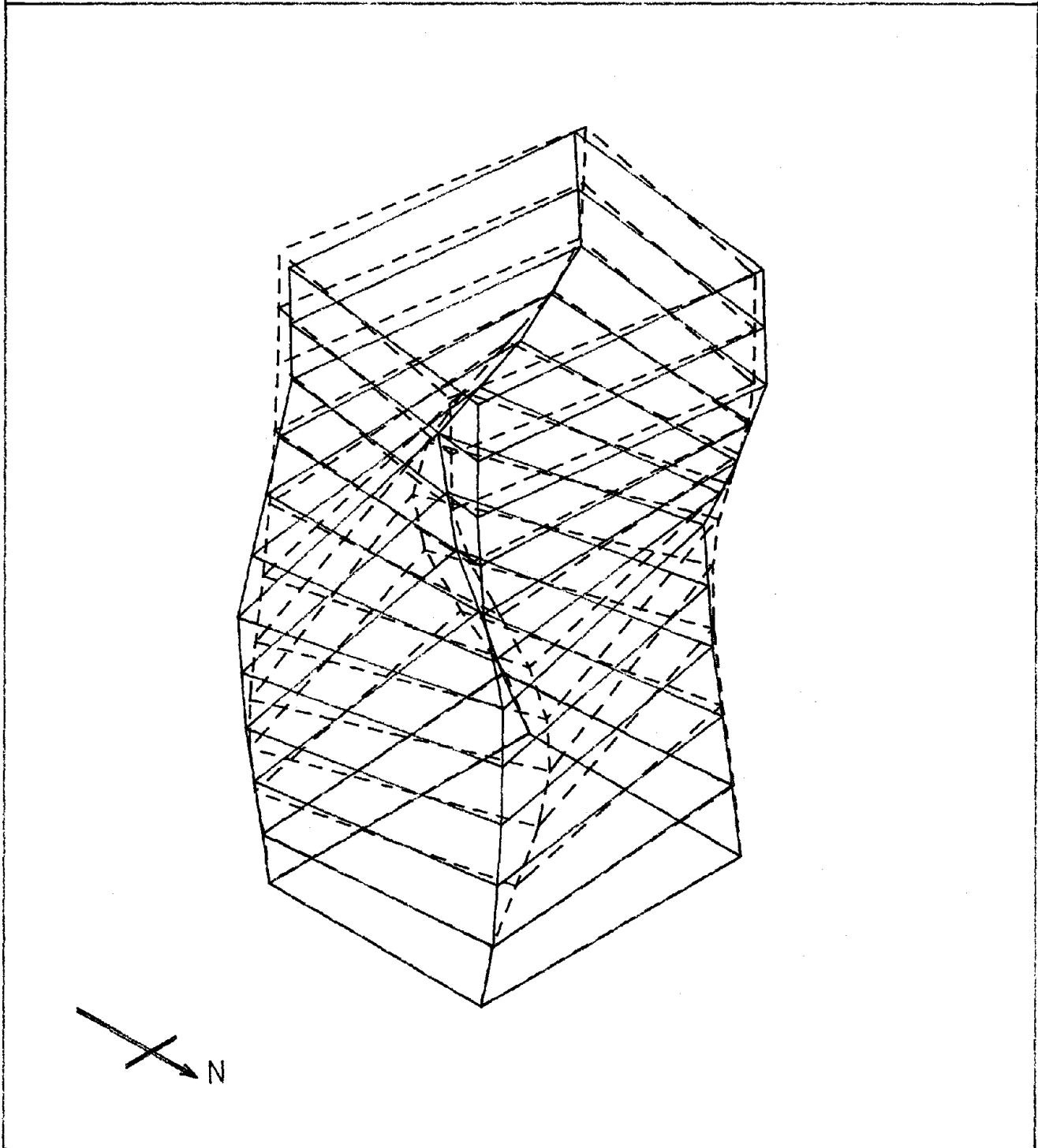


Figure 5.8 Second N-S Torsional Mode - End of N-S Tests

computech
 engineering services, inc.
 Berkeley, California

JOB NO.	DATE	TIME
J502	12/26/81	13:37:09

PROJECT : ST. LOUIS PRUITT-IGOE CORRELATION STUDY
CLIENT : NATIONAL SCIENCE FOUNDATION
SUBJECT : FORCED VIBRATION RESPONSE
 FRAME NO. 1 N-S RESPONSE AT LEVELS 5 AND 11

LEGEND
 — Y-RESP/D 5/(-263.0, 0.0)
 - - - Y-RESP/D 11/(-245.7, 0.0)

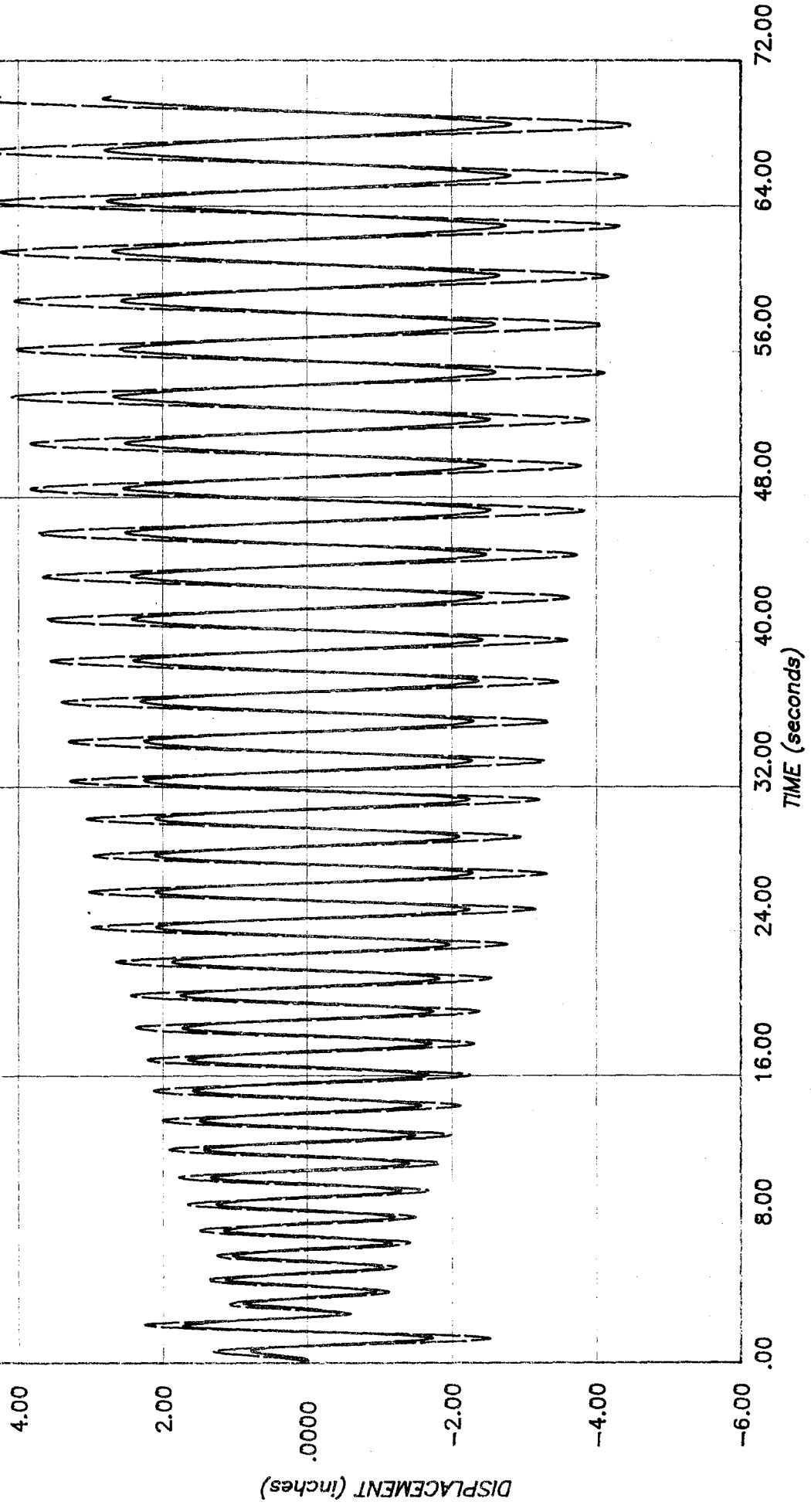
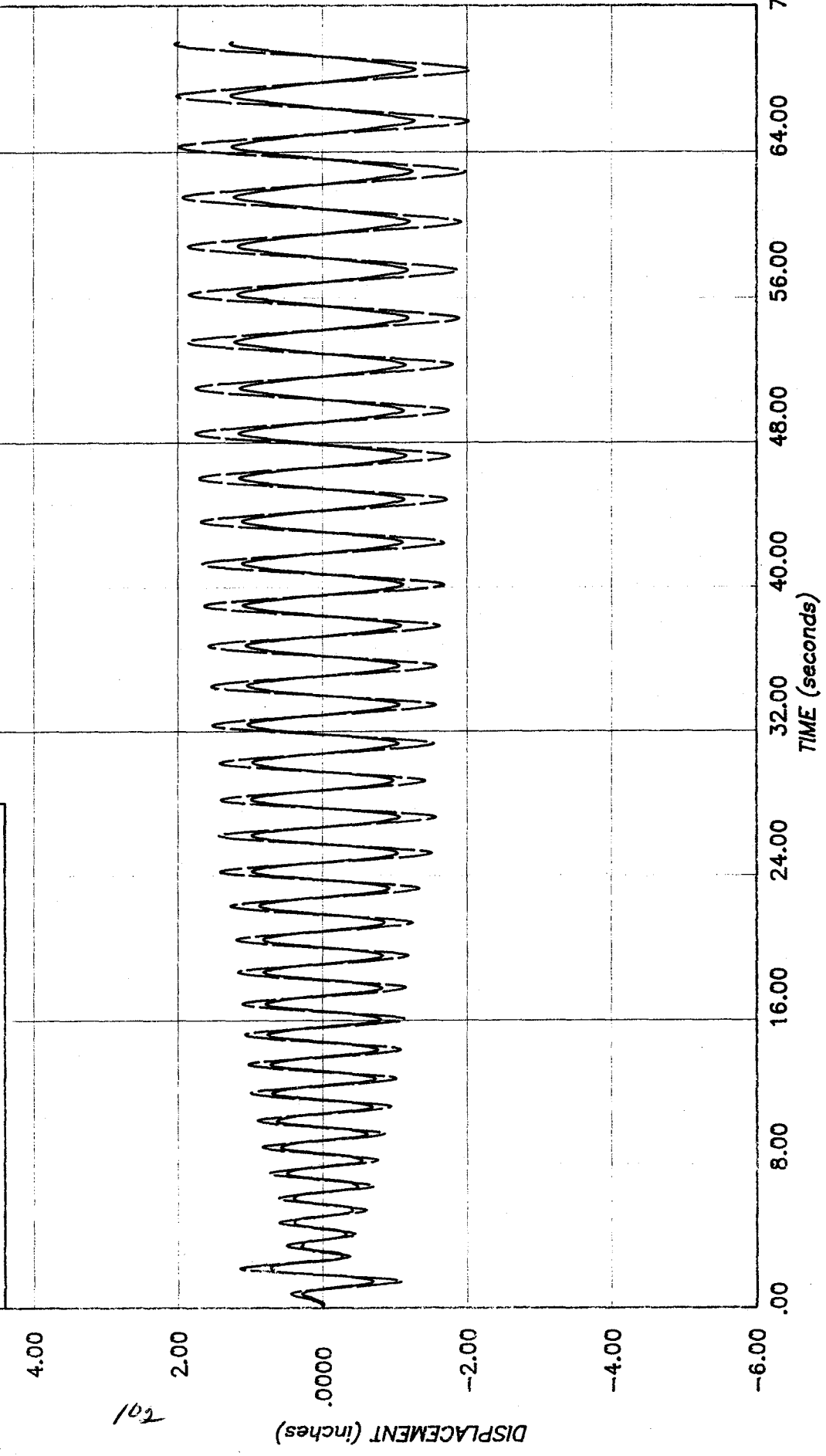


Figure 5.0

computech
 engineering services, inc.
 Berkeley, California
 JOB NO. J502
 DATE 12/26/81
 TIME 13:48:55

PROJECT : ST. LOUIS PRUITT-IGOE CORRELATION STUDY
CLIENT : NATIONAL SCIENCE FOUNDATION
SUBJECT : FORCED VIBRATION RESPONSE
 FRAME NO. 2 E-W RESPONSE AT LEVELS 5 AND 11

LEGEND
 — X-RESP/D 5/(0.0, 235.0)
 — X-RESP/D 11/(0.0, 215.4)



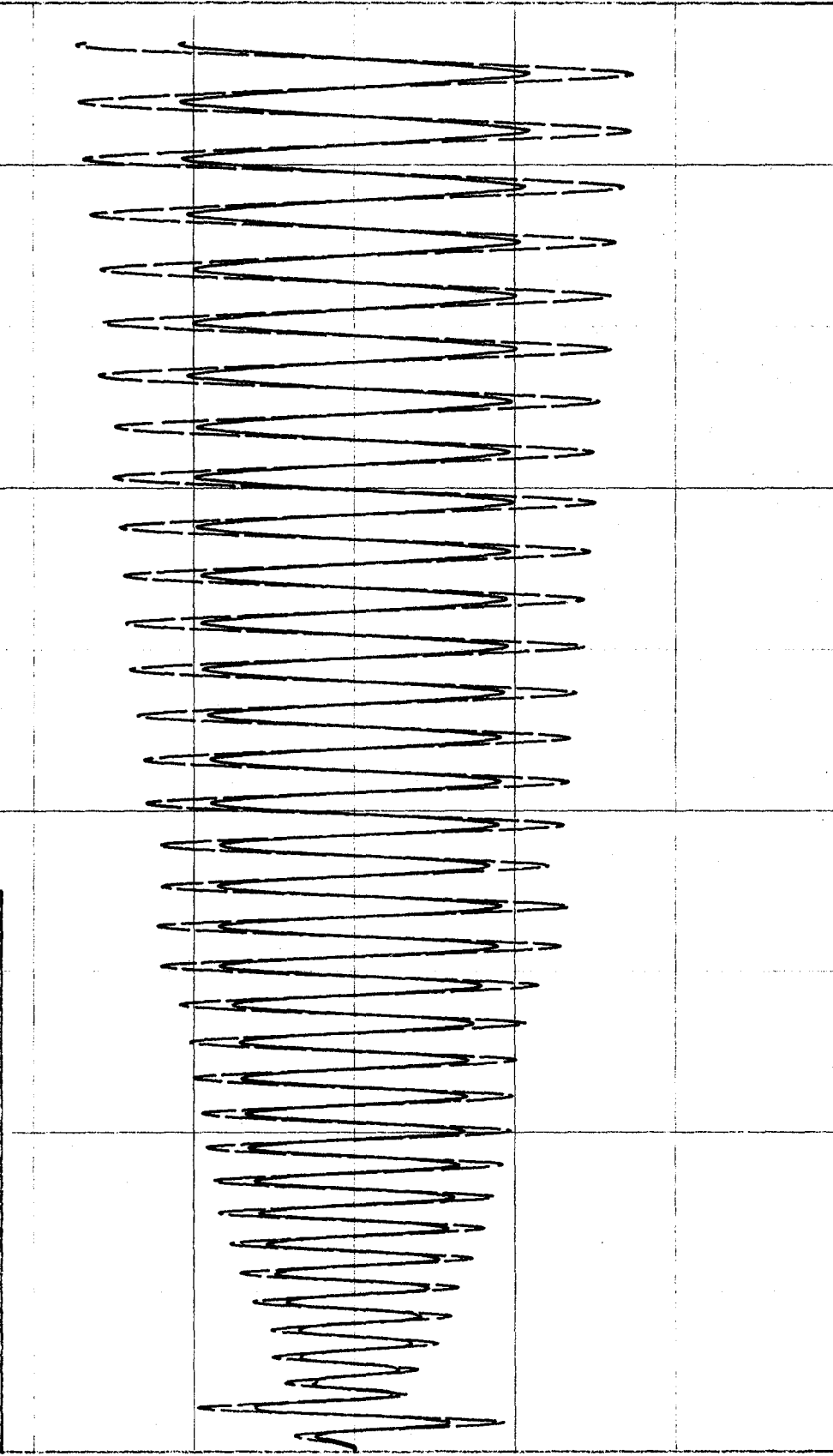
201

computech
 engineering services, inc.
 Berkeley, California

JOB NO.	DATE	TIME
J502	12/26/81	14:41:01

PROJECT : ST. LOUIS PRUITT-IGOE CORRELATION STUDY
CLIENT : NATIONAL SCIENCE FOUNDATION
SUBJECT : FORCED VIBRATION RESPONSE
 ROTATIONAL RESPONSE OF FLOORS 5 AND 11

LEGEND
 — R-RESP/D 5/(0.0, 0.0)
 - - - R-RESP/D 11/(0.0, 0.0)



0.01
 .0050
 .0000
 -.0050
 -.01
 -.02

ROTATION (radians)

0.00 8.00 16.00 24.00 32.00 40.00 48.00 56.00 64.00 72.00

TIME (seconds)

6 EARTHQUAKE RESISTANCE OF TEST STRUCTURE

This chapter presents the analytically predicted earthquake resistance of the test structure, and infers the seismic performance of non-seismically designed structures of this general type during ground motions representative of varying seismic risk regions in the United States. The base-shear forces developed during the tests are summarized in Section 6.1. A description of the analytical model is given in Section 6.2. Ground motions and the method of scaling the records to be representative of regions of varying seismic risk in the United States is described Section 6.3. The analyses performed are presented in Section 6.4, and their results in Section 6.5. A discussion of the results and the conclusions on the ability of a non-seismically designed reinforced concrete building to withstand earthquakes of varying intensity is given in Section 6.6.

6.1 TEST BASE-SHEAR FORCES

The base shear forces measured in the tests in many cases exceeded those base shears calculated from the 1976 UBC (see Table 6.1). The UBC base shears were exceeded for considerable periods of time (estimated at 70 minutes total during the north-south tests). Quoting from the report describing the tests [3],

"...this non-seismically designed building, both with and without external cladding, was able to withstand base shear forces greater than those demanded by recent UBC requirements when subjected to the sinusoidal type of motion induced by the moving mass shaker. Until further analysis of the results it cannot be inferred, however, that this structure would have resisted an earthquake which would have induced a base shear force of the same magnitude."

The purpose of this phase of the study was to determine if this inference could be made.

6.2 ANALYTICAL MODEL

The analytical model was similar to that used at the start of the N-S tests without the degradation due to the E-W tests. The earthquakes are applied as uni-directional excitations in the N-S direction of the structure.

The DRAIN-TABS model incorporates the "crimped hysteresis" beam elements to model the slip of the main steel in all beams. The columns of the four exterior frames use the Takeda model to represent joint degradation. The parameters for these elements are calculated as described in Section 4.4.3. The columns of the interior frames are permitted to yield, and have a bi-linear hysteresis loop.

It was necessary to perform the earthquake analyses with a time step of 0.005 seconds, due to the stiffening nature of the crimped hysteresis loop of the beams and the lack of an "event-to-event" solution strategy in DRAIN-TABS.

6.3 SELECTION OF GROUND MOTIONS

To perform the seismic evaluation of the test structure, recorded ground motions scaled to represent the expected intensity of different regions were used. Intensity of regions was based upon the design ground response spectra of the ATC publication, "Tentative Provisions for the Development of Seismic Regulations for Buildings" [6]. Three seismic regions were chosen, namely regions 7, 5 and 3 with effective peak accelerations (A_a) of 0.4g, 0.2g and 0.1g, respectively. Region 7 represents the highest risk areas and includes most of California ($A_a = 0.4$) and the area around Yellowstone National Park. Region 5 ($A_a = 0.2$) represents areas of moderate seismic risk, and includes areas such as Washington State, Utah and parts of Missouri and Arkansas. Region 3 ($A_a = 0.1$) is representative of areas of lower seismic risk and includes areas such as the North-Eastern States and South Carolina.

For each region, the ATC publication specifies two parameters to characterize the intensity of design ground shaking. These parameters are called the Effective Peak Acceleration (EPA), A_a , and the Velocity-Related Acceleration Coefficient, A_v . The following values of A_a and A_v apply for the selected regions.

Region	A_a	A_v	Cities
7	0.4	0.4	San Francisco, Los Angeles
5	0.2	0.2	Seattle, Salt Lake City, Memphis
3	0.1	0.1	Boston, Charleston, Knoxville

The normalized ground acceleration response spectra for values of the damping ratio equal to 2% and 5% is shown in Figure 6.1 for soil profile type S2 [6]. These are scaled by the appropriate value of the coefficient A_a to obtain the design ground response spectrum for each region.

The "Intensity" of an earthquake for our purposes is some measure of intensity over a relatively wide range of frequencies. Housner [7] has proposed the use of a spectral intensity based on the velocity spectrum. He considers the intensity to be the area under the velocity spectrum between the periods of 0.1 to 2.5 seconds (0.4 to 10 Hz). The value of this spectral intensity is readily hand-calculated for the ATC spectra, but for recorded ground motions, this calculation is much too cumbersome to be done by hand. A computer program was used to calculate velocity spectrum, and spectral intensity was calculated by numerical integration. The scaling factor applied to the particular ground motion is the ratio between the spectral intensity calculated for the ATC spectrum and the unscaled ground motion. The ATC spectra were available for damping ratio values equal to 2% and 5% only. When ground motion spectral intensities were calculated for these two damping ratios, the scaling factor was found to be very insensitive to which of the two values was used. As a consequence, scaling was based on the velocity spectra for 2% damping.

Three earthquakes were chosen, and the major component of each was used for the analyses. The three were the records measured at El Centro, 1940.

Taft, 1952, and Pacoima Dam, 1971. Although an attempt was made to obtain a record typical of "Eastern" type earthquakes (deep epicenter and large epicentral distance), no relatively strong motion record was readily available. Pacoima Dam is a somewhat controversial choice, but was used to study the effect of pulse-like disturbances on non-linear response. This record was used only for Region 7. The spectral intensities for the major components of these records, and for the ATC spectra are indicated below. All values are for 2% damping.

Ground Motion	Spectral Intensity (ft)
El Centro 1940	5.743
Taft 1952	3.022
Pacoima Dam 1971	14.815
ATC Aa = 0.4	8.219
Aa = 0.2	4.110
Aa = 0.1	2.055

Using these intensities, the following scale factors arise for each of the recorded motions.

	Region 7	Region 5	Region 3
El Centro	1.431	0.716	0.358
Taft	2.720	1.360	0.680
Pacoima	0.555	0.278	0.139

6.4 ANALYSES PERFORMED

A total of nine earthquake analyses were performed, using three earthquake records scaled to match the ATC spectra for three different seismic risk areas. Two models of the structure were considered, and the parameters of both are described in Section 6.2. The difference in the two models was the inclusion or exclusion of the weight of the external cladding. The stiffness contribution of the external walls was not included in either analysis. The first model had the walls removed on all floors except the top two. The second model had the same stiffness parameters as the first model, but included added mass and rotational inertia due to the exterior walls. In the table that follows, the model without the wall masses is referred to as Model 1. Model 2 includes the wall masses. An entry in the table indicates the time duration for which seismic response was calculated. No entry indicates that a particular combination was not considered.

Model	Earthquake	Region 7	Region 5	Region 3
1	Taft	20 secs	12 secs	12 secs
1	El Centro	20 secs	10 secs	
1	Pacoima	20 secs		
2	Taft	16 secs	8 secs	8 secs

Each model had mass proportional damping, set to give 3% of critical damping at a response period of 2 seconds.

6.5 RESULTS

The maximum N-S displacement (in inches) at the top of frame 1 (Figure 4.5) for each analysis is indicated in the table below. Model 1 is structure without the walls. Model 2 includes wall masses but does not include any stiffness contribution from the walls.

Model	Earthquake	Aa=0.4	Aa=0.2	Aa=0.1
1	Taft	10.34	3.96	1.68
1	El Centro	10.59	4.12	
1	Pacolima	11.27		
2	Taft	12.32	5.02	2.22

Selected response time histories for each earthquake are shown in Figures 6.2 through 6.10. Each figure has two parts: the first indicates the N-S response of frames 1 and 3, and the second gives the E-W response of frames 2 and 4 (see Figure 4.5).

As well as giving the time history of displacement response, the analyses produced maximum values for plastic rotation in the beams and in the columns (representing the joint deformations). Rotations from non-linear analyses are often converted to ductilities, and presented as such. This approach has not been used because expressing results in terms of ductilities implies that some ductility exists in the structure. This is not the case in a non-seismically designed reinforced concrete structure such as the test structure. In the beams, instead of the main steel yielding (giving rise to some rotational ductility), the bars pull out or slip long before their yield stresses are reached. Thus, beam rotations were converted into crack widths and presented in that manner.

The discrete hinges at the column ends model the joint degradation. In a similar fashion to that described above for the beams, these column rotations were converted to lateral shear displacement of the joint zones. Detailed results were calculated only for frames 1 and 3. These were the primary lateral resisting frames in the N-S direction, although some inelastic action was observed in frames 5 and 8.

To facilitate the presentation of a large amount of information, each frame was divided into three regions. Region I included the beams on the first 3 levels, and the columns of the first 3 stories. Region II included the beams on levels 4 through 7 and the columns of stories 4 through 7. Region III is the structure above level 7 (see Figure 6.11). Within each region, 4 response quantities were monitored, namely, the maximum beam crack widths at the faces of the exterior and interior columns and the maximum shear deformation in the exterior and interior beam-column joints. This information is presented for frame 1 in Table 6.2, and for frame 3 in Table 6.3. The number in parentheses in the case of the beam crack

widths is the approximate percentage of beams in that particular region with crack widths within 20% of the maximum value. In the case of joint shear deformation, the parenthetical number represents the equivalent number of cycles of the maximum magnitude that the joint undergoes. This quantity is defined as the ratio of accumulated secondary rotation to maximum primary rotation (see reference [5] for a definition of these terms). When examining the equivalent number of cycles, it must be remembered the duration of analysis is different between $A_a = 0.4$ (generally 20 seconds) and $A_a = 0.2$ and 0.1 (generally 10 seconds).

6.6 DISCUSSION OF RESULTS

This section presents a discussion of the results presented in Section 6.5. Throughout this section, Model 1 refers to the analytical model without the wall masses, and Model 2 includes the wall masses. Neither model includes the stiffness of the exterior cladding.

6.6.1 Time History Response

The time history responses shown in Figures 6.2 through 6.10 reveal much information about the ability of the structure to withstand earthquakes of varying intensity. The initial fundamental period of the structure is 1.26 seconds for Model 1 and 1.57 seconds for Model 2.

In all cases with the earthquake scaled to $A_a = 0.4$, the predominant period of the response is considerably longer (of the order of 2.5 seconds for Model 1, and 3.5 seconds for Model 2) than the initial fundamental period. This alone indicates extreme damage and loss of stiffness. It is interesting to note that 2.5 seconds was the fundamental period of the test structure at the conclusion of the N-S tests, and at that stage the structure was grossly unstable and very close to collapse. The results indicate the structure tended to oscillate about a non-zero displacement, indicating that permanent set is likely if the structure does not collapse. This is more severe for the Pacoima record, where approximately 2 inches of permanent deformation remain at the end of the ground shaking. The time history plots for Region 7 indicate that such a structure would be likely to collapse, or if it remained standing, would be an extreme risk and have to be demolished. This observation is supported by evidence of the damage sustained during this intensity of shaking (see Tables 6.2 and 6.3). These results are discussed in section 6.2.

For the case of earthquakes scaled to $A_a = 0.2$ (Region 5), the situation is improved. The predominant response periods are from 1.8 to 1.9 seconds for Model 1, and slightly over 2 seconds for Model 2. These periods indicate significant degradation, but do not suggest total instability or loss of structural integrity. Unfortunately, due to restricted computer funds, these analyses considered 10-12 seconds of response only. It is difficult to infer whether significant permanent displacements would

exist at the end of an earthquake of this intensity. However, the increase in fundamental period, and maximum displacements of 4" to 5" indicate that for Region 5, such a structure would be unlikely to collapse during an earthquake, but would, for safety reasons, very likely need to be demolished after the earthquake or would require a substantial amount of repair for the cracks that developed during the earthquake. This is discussed further in Section 6.6.2.

Perhaps the most important result of this study is the ability of this non-seismically designed structure to withstand earthquakes typical of Region 3 intensities. With earthquakes scaled to this intensity, Models 1 and 2 give maximum displacements of 1.68 inches and 2.22 inches, respectively. The predominant response period for Model 1 is about 1.6 seconds, and that of Model 2 is about 1.8 seconds. Thus, there is some inelastic behavior, and this is confirmed by inspection of Tables 6.2 and 6.3. However, at these displacements, the structure would retain its structural integrity, and in all likelihood would be functional after such an earthquake. Infill walls would no doubt contribute significantly to the stiffness of the structure at these displacements and improve the structural performance. This is discussed further in Section 6.6.2.

6.6.2 Structural Damage

As explained in Section 6.5, the structural damage is summarized in Tables 6.2 and 6.3. The information in these tables confirms the conclusions drawn from analysis of the displacement time history plots. There is a marked increase in the levels of damage as the intensity of the earthquake increases from Region 3 to 5 to 7.

As a general observation, damage in the beams decreased up the height of the building. However, shear degradation of the beam-column joints was relatively constant between Regions I and II of the test structure and decreased slightly in Region III. The damage in the joints, therefore, was more constant over the height of the structure than the damage in the beams. Thus, poorly reinforced joints should be avoided in the earthquake resistant construction of reinforced concrete structures.

Both Models 1 and 2 predict that for Region 7 ($A_a = 0.4$) the building is grossly unsafe. Crack widths of the order of 0.2" to 0.34" in the majority of the lower floor beams indicate that the structure's lateral load resisting system is severely degraded. This, coupled with approximately 10 cycles of shear deformations of 0.1" in the corner joints and 0.15" to 0.2" in the interior joints of the main lateral load resisting frames, indicates that all structural integrity would be lost and collapse of the building would be likely. In the event of no collapse, the post-earthquake structure would be highly unstable and an extreme risk to public safety. It is interesting to note that the Pacoima record, while inducing higher joint deformations, subjects the joints to less cyclic action and may not be as damaging as earthquakes that produce more cycles of deformation.

In Region 5 ($A_a = 0.2$) the test structure would be expected to suffer considerable cracking in the beams in Regions I and II of the structure (0.1" to 0.13" crack widths) with subsequent stiffness degradation. The beams towards the top of the structure would experience only moderate cracking (widths less than 0.05"). For this intensity, the joint shear deformations would be significantly less than for Region 7 (0.06" to 0.08" maximum in Region I, 0.05" maximum in Region II and 0.02" maximum in Region III.) The equivalent number of cycles shown in Tables 6.2 and 6.3 are based on 10 or 12 seconds of response, thus the number would be expected to be higher if the full duration of the earthquakes were used in the analysis. However, at this amplitude of deformation, the joints should retain some integrity, and total structural collapse is unlikely. The damage would be such, however, that the structure would possibly require demolition or a substantial amount of repair for the cracks that developed during the earthquake.

In Region 3 ($A_a = 0.1$), the results indicate that the test structure would survive with little or minor damage to ground motions typical of that region. The major basis for this statement comes from the fact that no joint damage is indicated by the results. Beam crack widths are less than 0.04" throughout the entire structure, and approximately half the beams in Regions I and II will have cracks much smaller than this value. Beam cracking towards the top of the structure is very minor. The predicted crack widths for this region may be considered an upper bound as the infill walls will contribute significantly to the building stiffness and relieve the beams somewhat at these predicted test structural displacements. It can therefore be stated that structures of this general type in Region 3 have a good chance of surviving an earthquake without the need for subsequent major repair or demolition.

Test No.	Period of Test (sec)	V_T Test Base Shear (Kips)	V_T/W	V_T/V_C for Code Period			V_T/V_C for Measured Period		
				Zone 4, S=1	Zone 4, S=1.5	Zone 4, S=1	Zone 4, S=1	Zone 4, S=1.5	Zone 4, S=1.5
1E-SD	0.74	115	0.038	0.60	0.40	0.49	0.33		
10E-SD	0.84	168	0.056	0.88	0.59	0.78	0.52		
22E-D	1.18	238	0.080	1.26	0.84	1.30	0.87		
23E-D	1.30	460	0.154	2.42	1.61	2.63	1.75		
23E-D	1.60	320	0.107	1.68	1.12	2.03	1.35		
24E-D	1.71	460	0.154	2.42	1.61	3.02	2.01		
10N-SD	1.25	60	0.027	0.42	0.28	0.45	0.30		
29N-D	1.75	160	0.072	1.13	0.75	1.43	0.95		
31N-D	2.38	300	0.135	2.12	1.41	3.12	2.08		
41N-D	2.38	210	0.094	1.45	0.97	2.18	1.45		

TABLE 6.1 Comparison of Test Induced Base Shear Forces with 1976 UBC

TABLE 6.2
FRAME I RESPONSE

QUANTITY	REGION	Aa = 0.4			Aa = 0.2		Aa = 0.1
		Taft	EI Centro	Pacoima	Taft	EI Centro	
<u>NO WALL MASS</u>							
Exterior Beam Crack Width ("") (% Beams)	I II III	0.29 (100%) 0.20 (80%) 0.18 (25%)	0.35 (100%) 0.31 (80%) 0.19 (25%)	0.37 (85%) 0.33 (75%) 0.19 (25%)	0.10 (85%) 0.10 (85%) 0.04 (25%)	0.09 (85%) 0.09 (50%) 0.06 (25%)	0.04 (85%) 0.03 (100%) 0.02 (25%)
Interior Beam Crack Width ("") (% Beams)	I II III	0.28 (80%) 0.21 (100%) 0.12 (25%)	0.29 (100%) 0.27 (50%) 0.11 (25%)	0.28 (75%) 0.24 (75%) 0.10 (25%)	0.10 (100%) 0.10 (75%) 0.04 (25%)	0.10 (100%) 0.09 (75%) 0.04 (25%)	0.05 (100%) 0.04 (75%) 0.02 (25%)
Exterior Joint Shear Deformation ("") (Equiv # Cycles)	I II III	0.10 (9) 0.16 (7) 0.15 (10)	0.10 (9) 0.13 (6) 0.19 (6)	0.12 (5) 0.20 (3) 0.16 (5)	0.03 (5) 0.04 (4) 0.02 (4)	0.02 (5) 0.02 (3) 0.03 (4)	0.01 (2) -- --
Interior Joint Shear Deformation ("") (Equiv # Cycles)	I II III	0.11 (10) 0.16 (7) 0.15 (10)	0.11 (10) 0.15 (7) 0.19 (6)	0.17 (4) 0.21 (4) 0.16 (5)	0.03 (6) 0.03 (5) 0.01 (7)	0.02 (5) 0.02 (4) 0.02 (5)	0.001 (3) -- --
<u>WITH WALL MASS</u>							
Exterior Beam Crack Width ("") (% Beams)	I II III	0.38 (75%) 0.34 (75%) 0.20 (50%)			0.14 (75%) 0.12 (85%) 0.07 (25%)		0.06 (85%) 0.04 (50%) 0.03 (10%)
Interior Beam Crack Width ("") (% Beams)	I II III	0.29 (75%) 0.30 (75%) 0.11 (35%)			0.12 (85%) 0.11 (75%) 0.06 (35%)		0.06 (85%) 0.05 (50%) 0.03 (20%)
Exterior Joint Shear Deformation ("") (Equiv # Cycles)	I II III	0.14 (9) 0.17 (7) 0.14 (6)			0.06 (3) 0.06 (2) 0.02 (2)		0.01 (2) -- --
Interior Joint Shear Deformation ("") (Equiv # Cycles)	I II III	0.18 (9) 0.22 (7) 0.14 (8)			0.06 (3) 0.06 (3) 0.03 (3)		0.01 (2) -- --

TABLE 6.3

FRAME 3 RESPONSE

QUANTITY	REGION	Aa = 0.4				Aa = 0.2			Aa = 0.1
		Taft	EI Centro	Pacoima	Taft	EI Centro	Taft	EI Centro	Taft
<u>NO WALL MASS</u>									
Exterior Beam Crack Width ("") (% of Beams)	I	0.22 (85%)	0.26 (85%)	0.31 (65%)	0.07 (75%)	0.09 (75%)	0.02 (50%)		
	II	0.21 (85%)	0.26 (65%)	0.28 (65%)	0.07 (75%)	0.06 (85%)	0.03 (65%)		
	III	0.12 (25%)	0.13 (25%)	0.10 (25%)	0.03 (25%)	0.03 (25%)	0.01 (25%)		
Interior Beam Crack Width ("") (% Beams)	I	0.21 (95%)	0.23 (100%)	0.24 (85%)	0.13 (50%)	0.09 (85%)	0.03 (75%)		
	II	0.16 (75%)	0.24 (75%)	0.21 (75%)	0.10 (75%)	0.06 (85%)	0.03 (65%)		
	III	0.09 (25%)	0.13 (25%)	0.10 (25%)	0.04 (25%)	0.05 (25%)	0.02 (25%)		
Exterior Joint Shear Deformation ("") (Equiv # Cycles)	I	0.10 (11)	0.11 (8)	0.12 (4)	0.03 (4)	0.03 (3)	---		
	II	0.12 (34)	0.14 (4)	0.13 (3)	0.02 (4)	0.02 (2)	---		
	III	0.09 (9)	0.13 (5)	0.10 (4)	0.01 (4)	0.02 (3)	---		
Interior Joint Shear Deformation ("") (Equiv # Cycles)	I	0.15 (45)	0.14 (8)	0.22 (3)	0.04 (4)	0.06 (3)	---		
	II	0.15 (22)	0.15 (5)	0.17 (3)	0.03 (4)	0.05 (2)	---		
	III	0.10 (9)	0.14 (6)	0.12 (4)	0.02 (4)	0.02 (3)	---		
<u>WITH WALL MASS</u>									
Exterior Beam Crack Width ("") (% Beams)	I	0.34 (85%)			0.13 (50%)		0.04 (35%)		
	II	0.26 (75%)			0.10 (75%)		0.02 (35%)		
	III	0.14 (40%)			0.03 (25%)		0.01 (10%)		
Interior Beam Crack Width ("") (% Beams)	I	0.30 (75%)			0.10 (75%)		0.04 (50%)		
	II	0.28 (65%)			0.09 (50%)		0.03 (65%)		
	III	0.13 (35%)			0.04 (30%)		0.01 (10%)		
Exterior Joint Shear Deformation ("") (Equiv # Cycles)	I	0.13 (18)			0.06 (2)		---		
	II	0.18 (9)			0.04 (2)		---		
	III	0.09 (5)			0.01 (2)		---		
Interior Joint Shear Deformation ("") (Equiv # Cycles)	I	0.21 (61)			0.08 (3)		---		
	II	0.17 (38)			0.05 (3)		---		
	III	0.09 (6)			0.01 (2)		---		

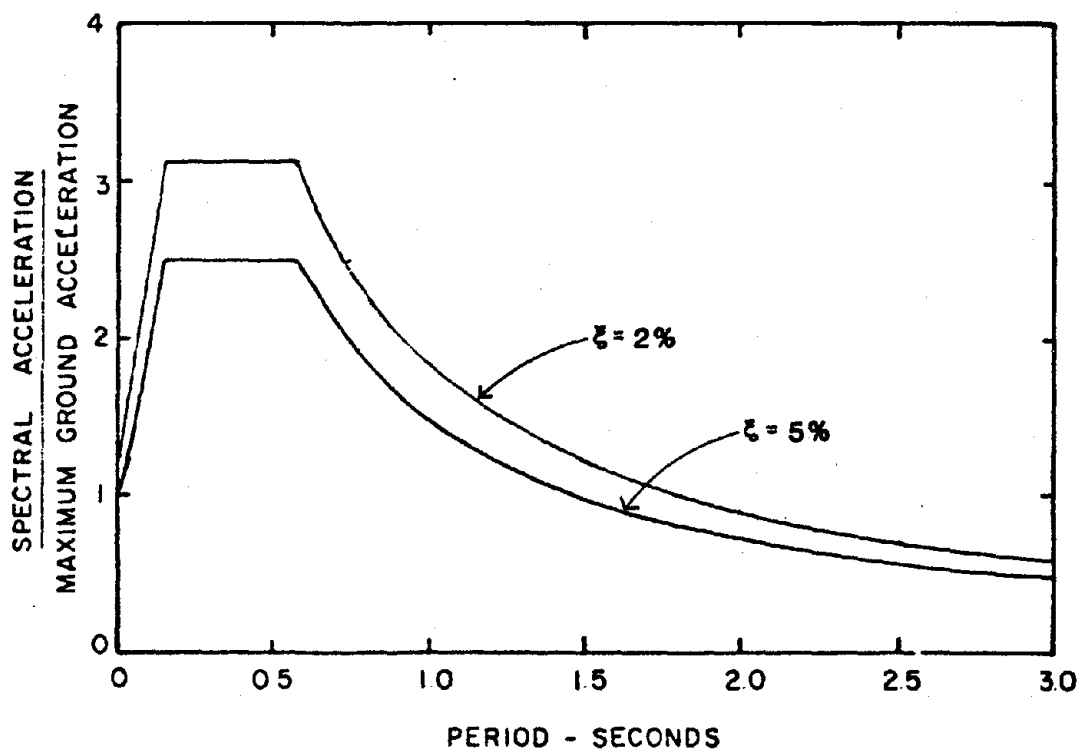


Figure 6.1 Normalized Design Response Spectra [6]

computech
 engineering services, inc.
 Berkeley, California

JOB NO.	DATE	TIME
J 502	01/10/82	13:30:18

PROJECT : ST. LOUIS PRUITT-IGOE CORRELATION STUDY
CLIENT : NATIONAL SCIENCE FOUNDATION
SUBJECT : SEISMIC RESPONSE : TAFT '52 E/Q, S69E COMPONENT, Aa = .4
 N-S RESPONSE OF FRAMES 1 AND 3, AT LEVEL 11

LEGEND

- Y-RESP/D 11/(-245.7, 0.0)
- - - Y-RESP/D 11/(273.8, 0.0)

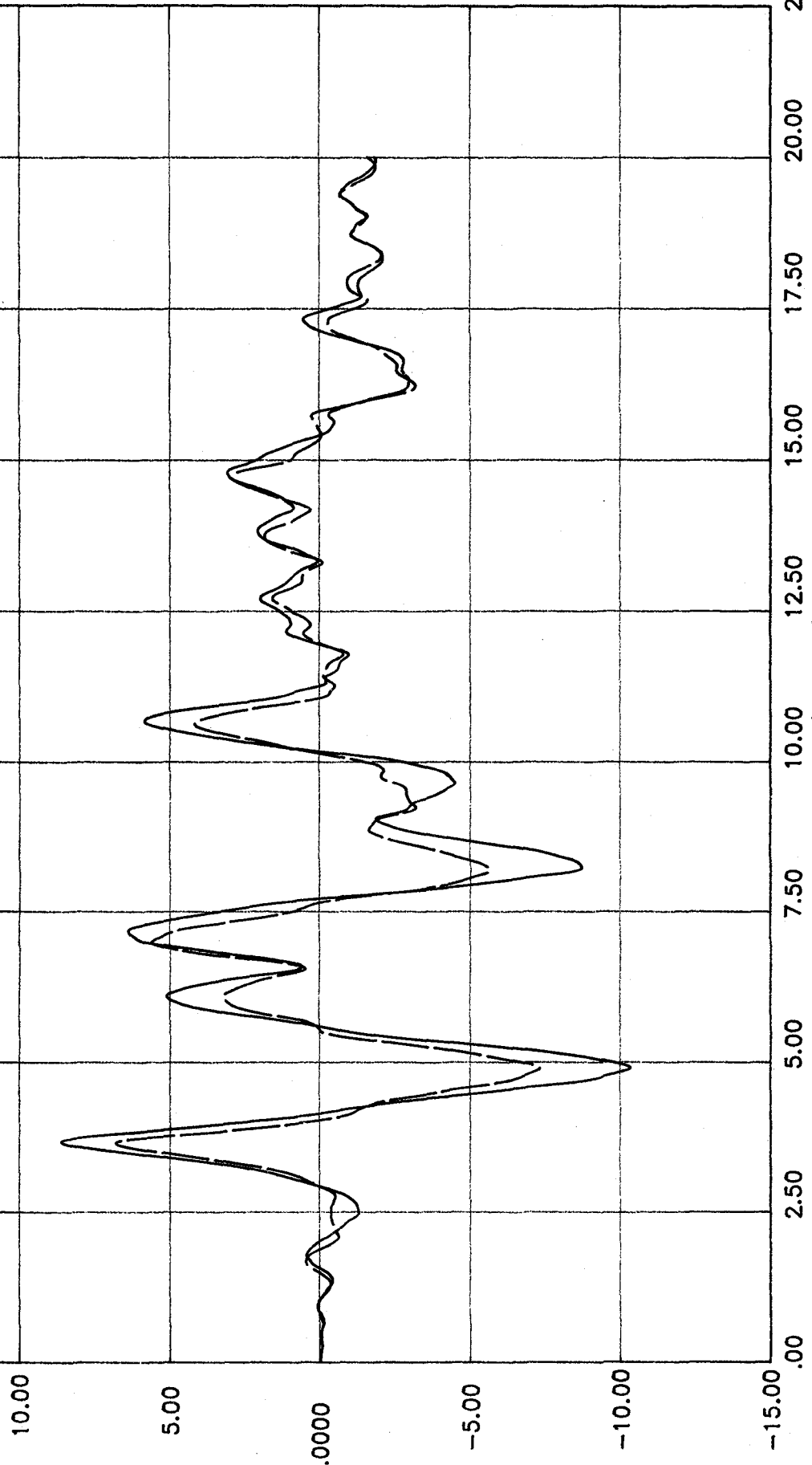


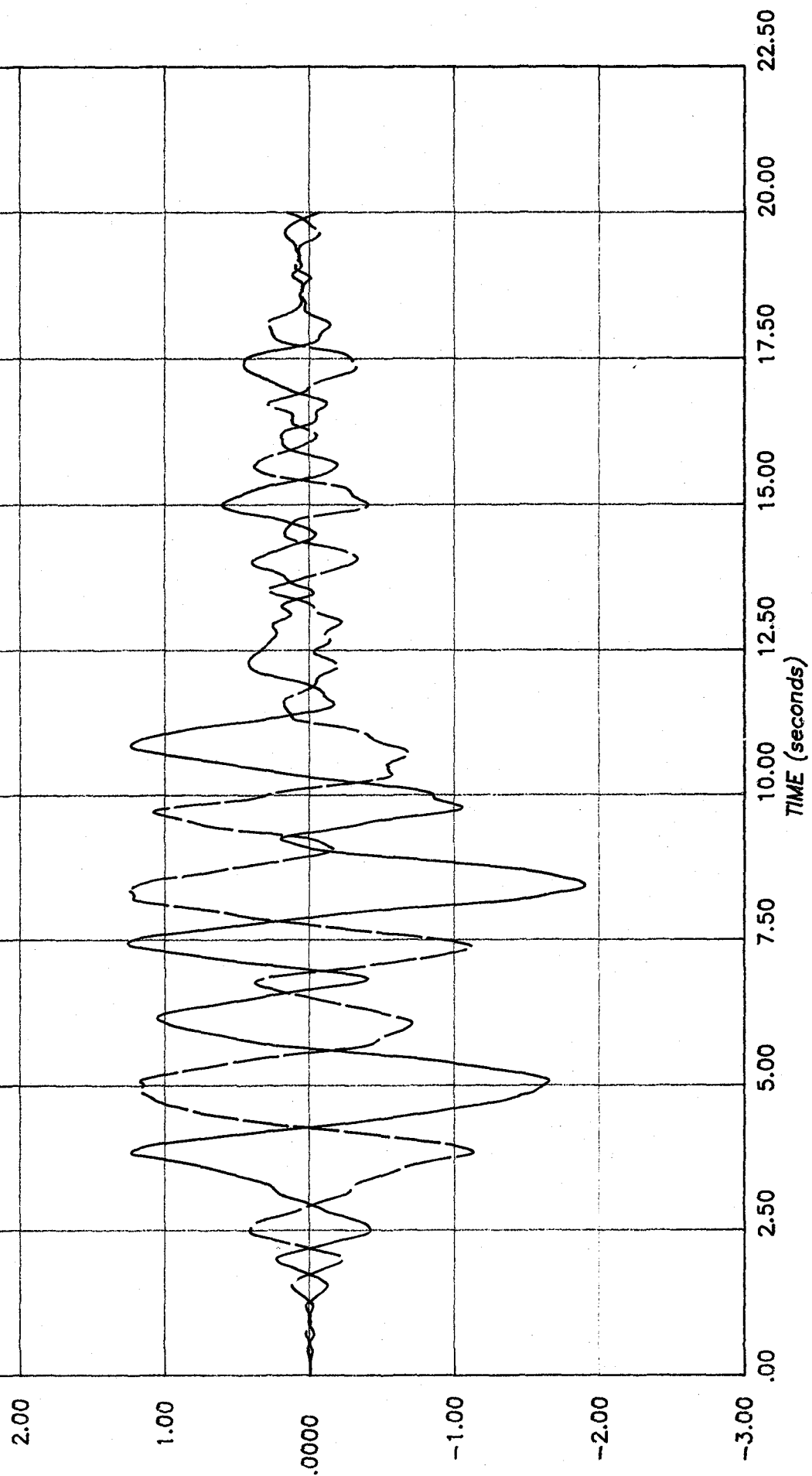
Figure 6.2(a) N-S Response, Taft Scaled to Aa = 0.4

computech
 engineering services, inc.
 Berkeley, California

JOB NO.	DATE	TIME
J 502	01/10/82	13:30:18

PROJECT : ST. LOUIS PRUITT-IGOE CORRELATION STUDY
CLIENT : NATIONAL SCIENCE FOUNDATION
SUBJECT : SEISMIC RESPONSE : TAFT '52 E/Q, S69E COMPONENT, A_g = .4
 E-W RESPONSE OF FRAMES 2 AND 4, AT LEVEL 11

LEGEND
 — X-RESP/D 11/(0.0, 215.4)
 - - - X-RESP/D 11/(0.0, -254.6)



PROJECT : ST. LOUIS PRUITT-IGOE CORRELATION STUDY
CLIENT : NATIONAL SCIENCE FOUNDATION
SUBJECT : SEISMIC RESPONSE : EL CENTRO '40 E/Q, N-S COMPONENT, Ad=.4
 N-S RESPONSE OF FRAMES 1 AND 3, AT LEVEL 11

LEGEND
 — Y-RESP/D 11/(-245.7, 0.0)
 - - - Y-RESP/D 11/(273.8, 0.0)

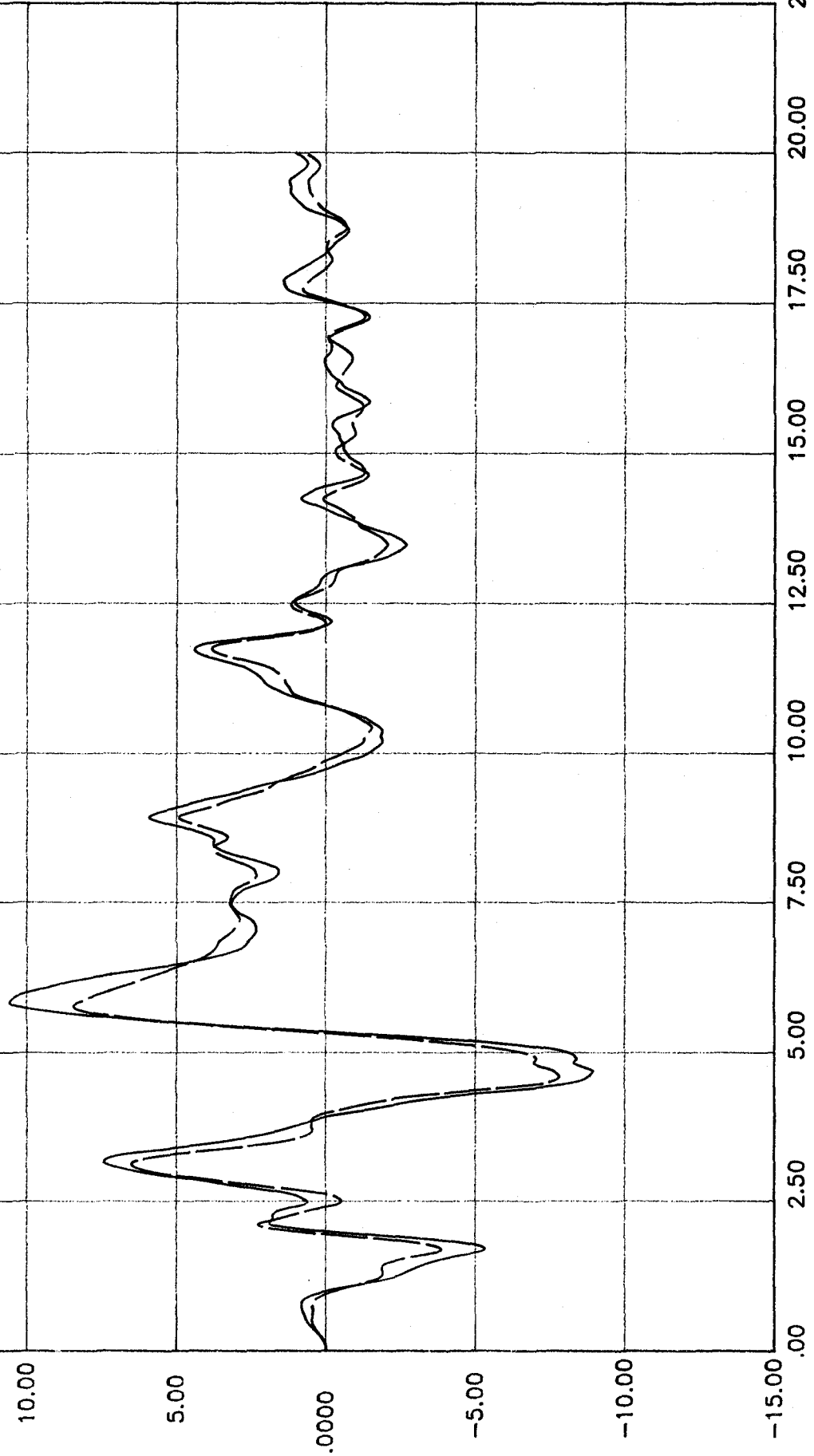


Figure 6.3(a) N-S Response, El Centro Scaled to $A_a = 0.4$

computech
 engineering services, inc.
 Berkeley, California

JOB NO.	DATE	TIME
J 502	01/10/82	12:05:12

PROJECT : ST. LOUIS PRUITT-IGOE CORRELATION STUDY
CLIENT : NATIONAL SCIENCE FOUNDATION
SUBJECT : SEISMIC RESPONSE : EL CENTRO '40 E/Q, N-S COMPONENT, $A_a = 0.4$
 E-W RESPONSE OF FRAMES 2 AND 4, AT LEVEL 11

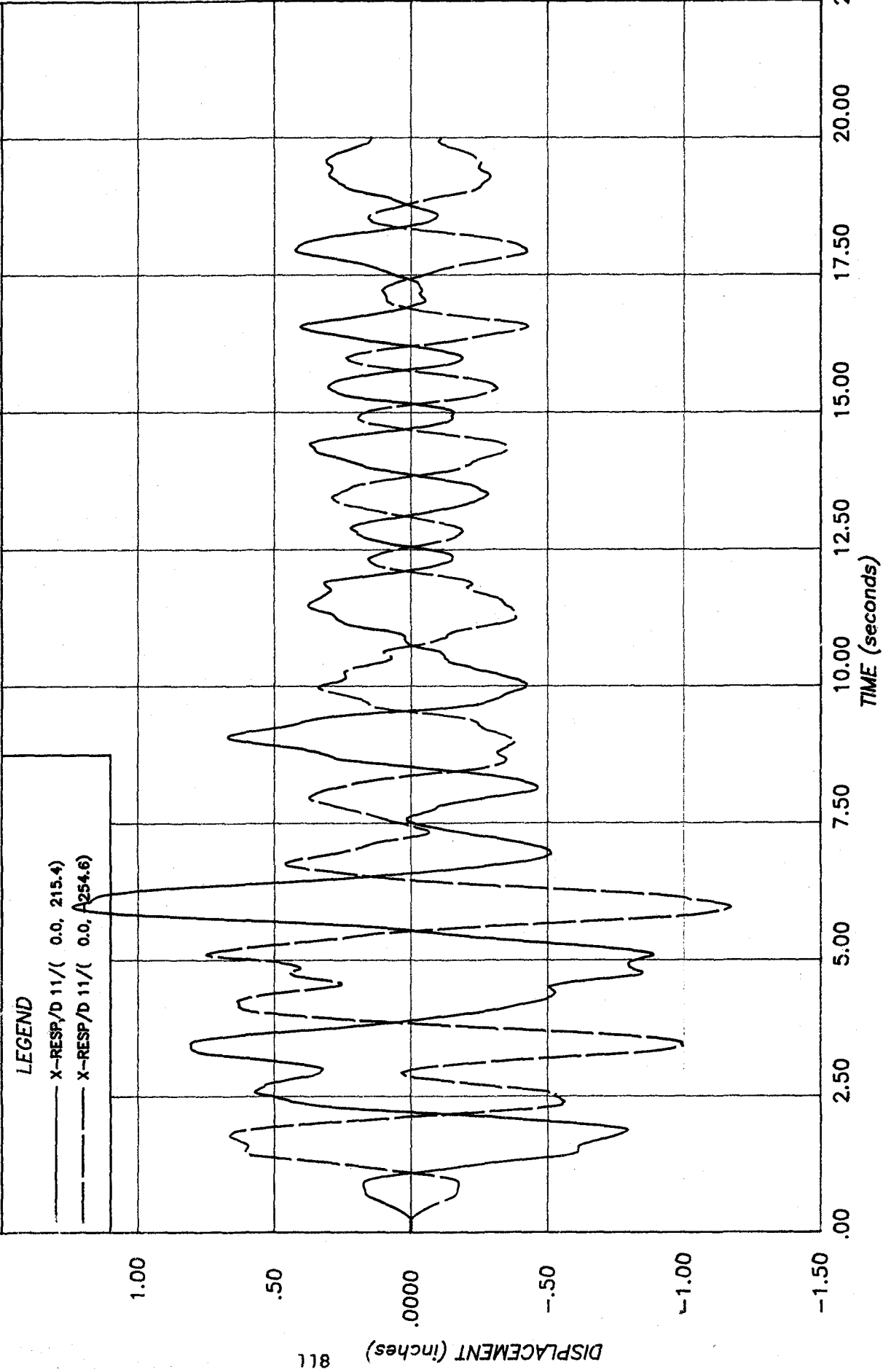


Figure 6.3(b) E-W Response, El Centro Scaled to $A_a = 0.4$

computech
 engineering services, inc.
 Berkeley, California

JOB NO.	DATE	TIME
J 502	01/10/82	14:18:54

PROJECT : ST. LOUIS PRUITT-IGOE CORRELATION STUDY
CLIENT : NATIONAL SCIENCE FOUNDATION
SUBJECT : SEISMIC RESPONSE : PACOIMA '71 E/Q, S16E COMPONENT, A_g = .4
 N-S RESPONSE OF FRAMES 1 AND 3, AT LEVEL 11

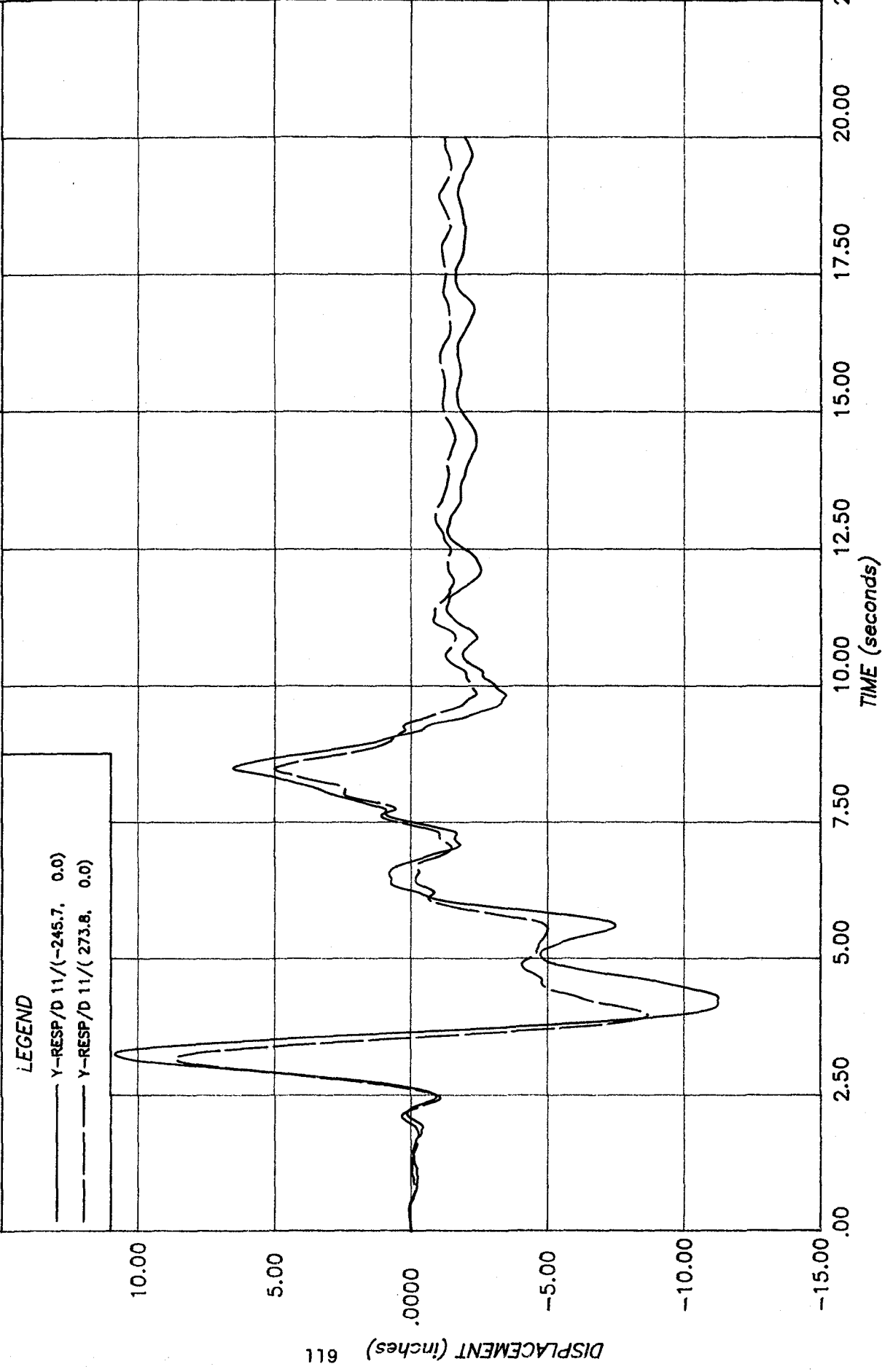


Figure 6.4(a) N-S Response. Pacoima Scaled to A_g = 0.4

computech
 engineering services, inc.
 Berkeley, California

JOB NO.	DATE	TIME
J 502	01/10/82	14:18:54

PROJECT : ST. LOUIS PRUITT-IGOE CORRELATION STUDY
CLIENT : NATIONAL SCIENCE FOUNDATION
SUBJECT : SEISMIC RESPONSE : PACOIMA '71 E/Q, S16E COMPONENT, Aa =.4
 E-W RESPONSE OF FRAMES 2 AND 4, AT LEVEL 11

LEGEND

— X-RESP/D 11/(0.0, 215.4)
 - - - X-RESP/D 11/(0.0, -254.6)

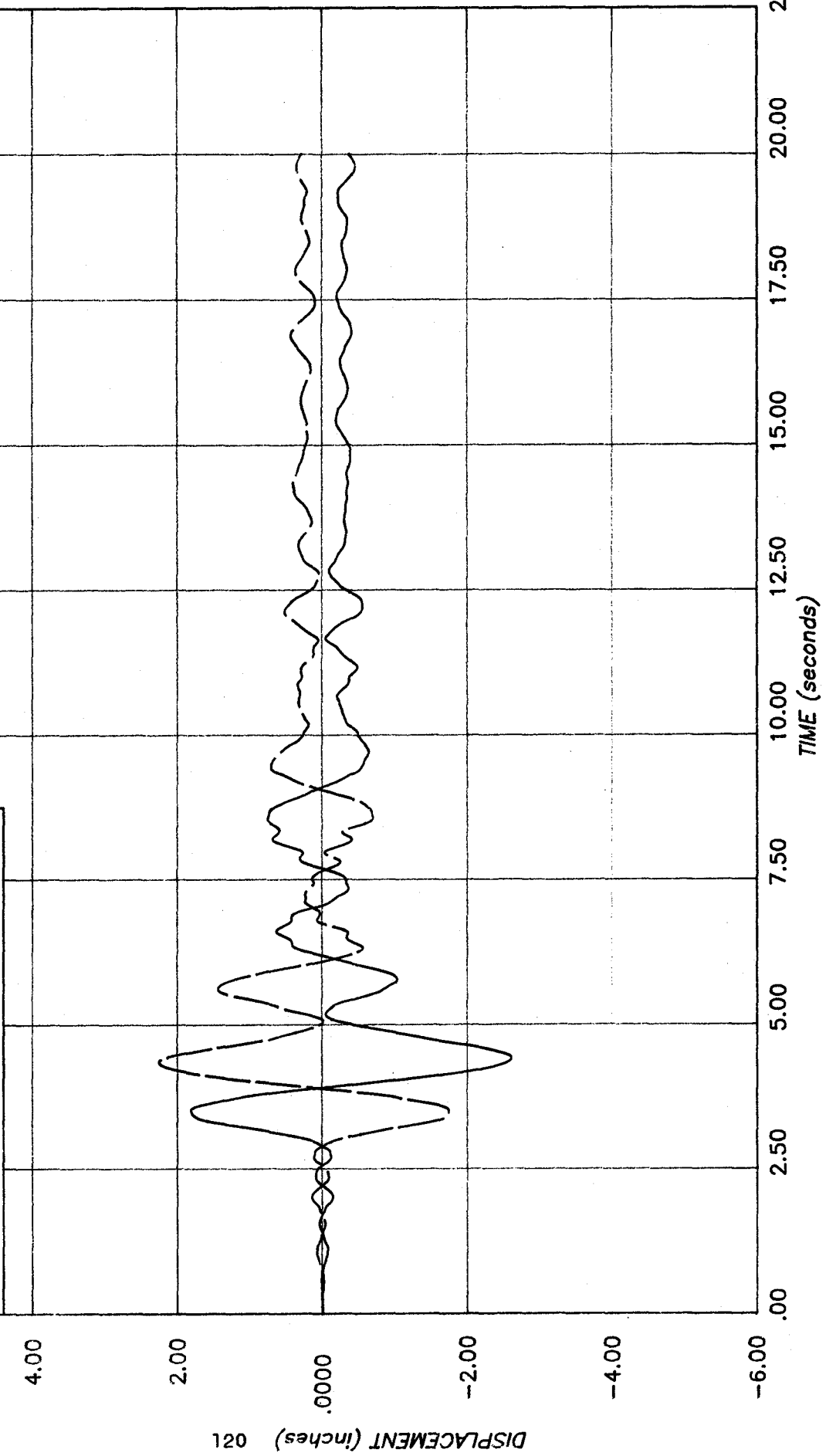


Figure 6.4(b) E-W Response, Pacoima Scaled to Aa = 0.4

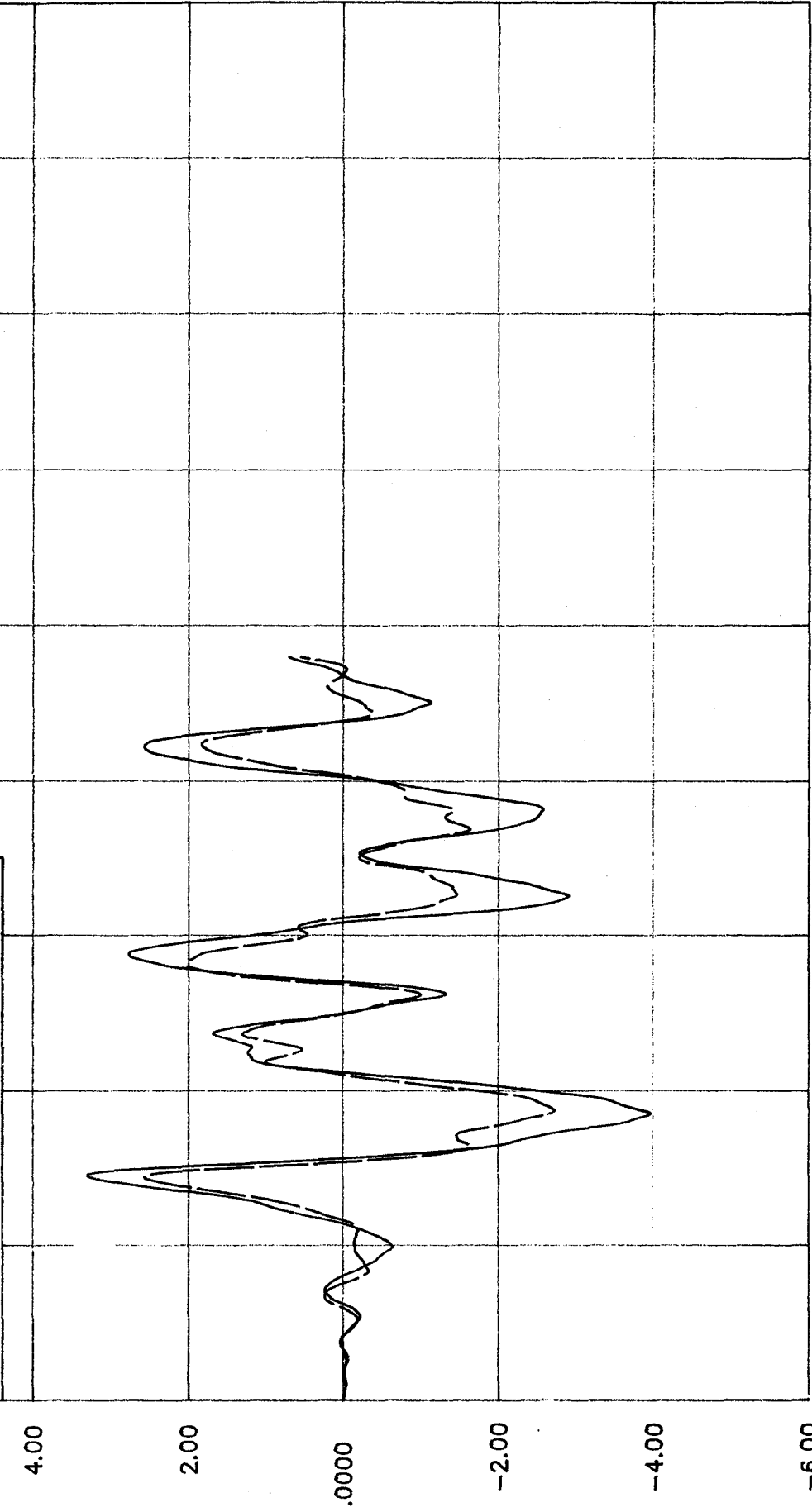
computech
 engineering services, inc.
 Berkeley, California

JOB NO.	DATE	TIME
J 502	01/10/82	13:25:53

PROJECT : ST. LOUIS PRUITT-IGOE CORRELATION STUDY
CLIENT : NATIONAL SCIENCE FOUNDATION
SUBJECT : SEISMIC RESPONSE : TAFT '52 E/Q, S69E COMPONENT, Aa = .2
 N-S RESPONSE OF FRAMES 1 AND 3, AT LEVEL 11

LEGEND

— Y-RESP/D 11/(-245.7, 0.0)
 - - - Y-RESP/D 11/(273.8, 0.0)



DISPLACEMENT (inches) 121

TIME (seconds)

0.00 2.50 5.00 7.50 10.00 12.50 15.00 17.50 20.00 22.50

Figure 6.5(a) N-S Response. Taft Scaled to Aa = 0.2

computech
 engineering services, inc.
 Berkeley, California

JOB NO.	DATE	TIME
J 502	01/10/82	13:25:53

PROJECT : ST. LOUIS PRUITT-IGOE CORRELATION STUDY
CLIENT : NATIONAL SCIENCE FOUNDATION
SUBJECT : SEISMIC RESPONSE : TAFT '52 E/Q, S69E COMPONENT, Aa = .2
 E-W RESPONSE OF FRAMES 2 AND 4, AT LEVEL 11

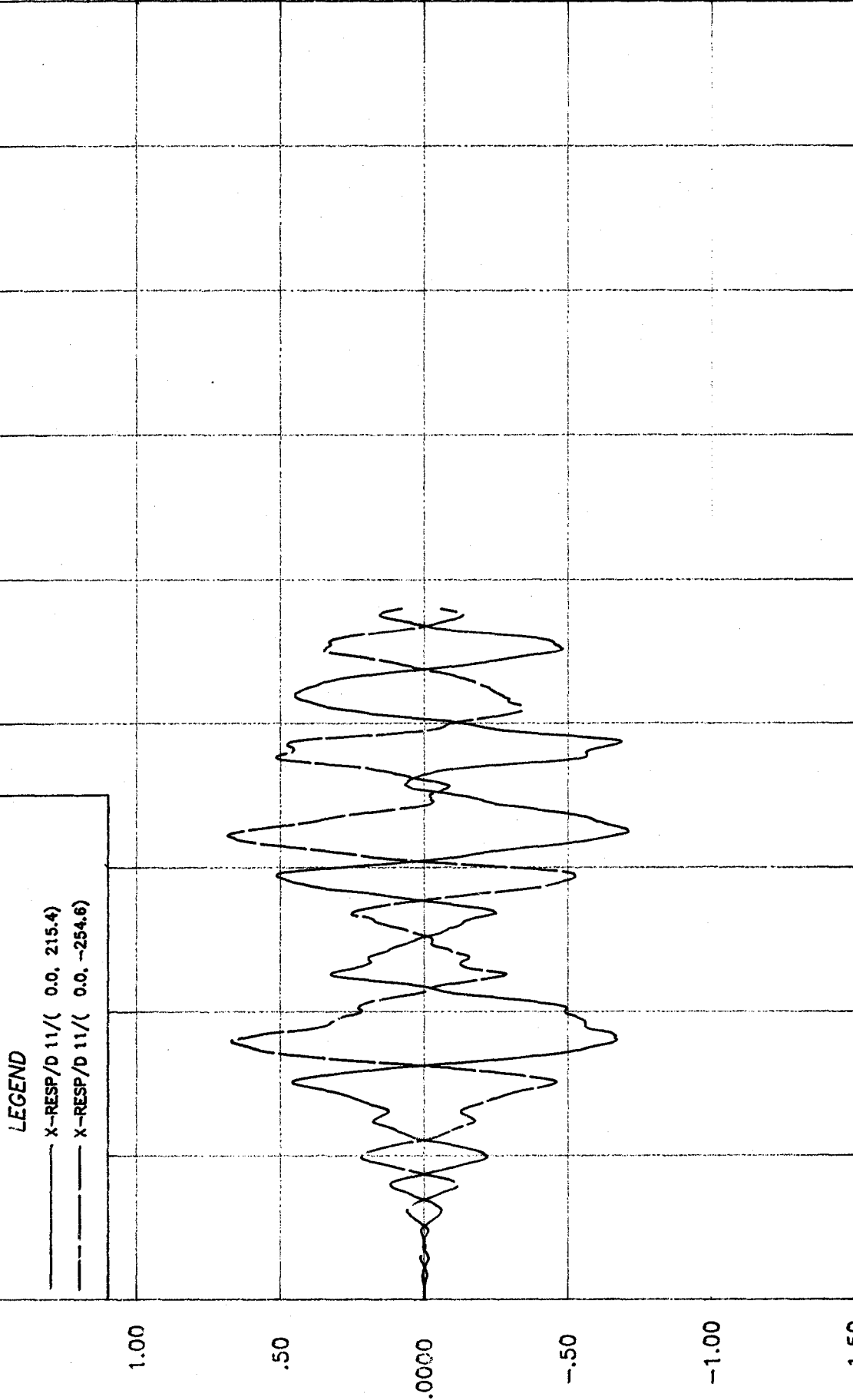


Figure 6.5(b) E-W Response, Taft Scaled to Aa = 0.2

computech
 engineering services, inc.
 Berkeley, California

JOB NO.	DATE	TIME
J 502	01/10/82	11:58:48

PROJECT : ST. LOUIS PRUITT-IGOE CORRELATION STUDY
CLIENT : NATIONAL SCIENCE FOUNDATION
SUBJECT : SEISMIC RESPONSE : EL CENTRO '40 E/Q, N-S COMPONENT, $A_a = .2$
 N-S RESPONSE OF FRAMES 1 AND 3, AT LEVEL 11

LEGEND
 — Y-RESP/D 11/(-245.7, 0.0)
 - - - Y-RESP/D 11/(273.8, 0.0)

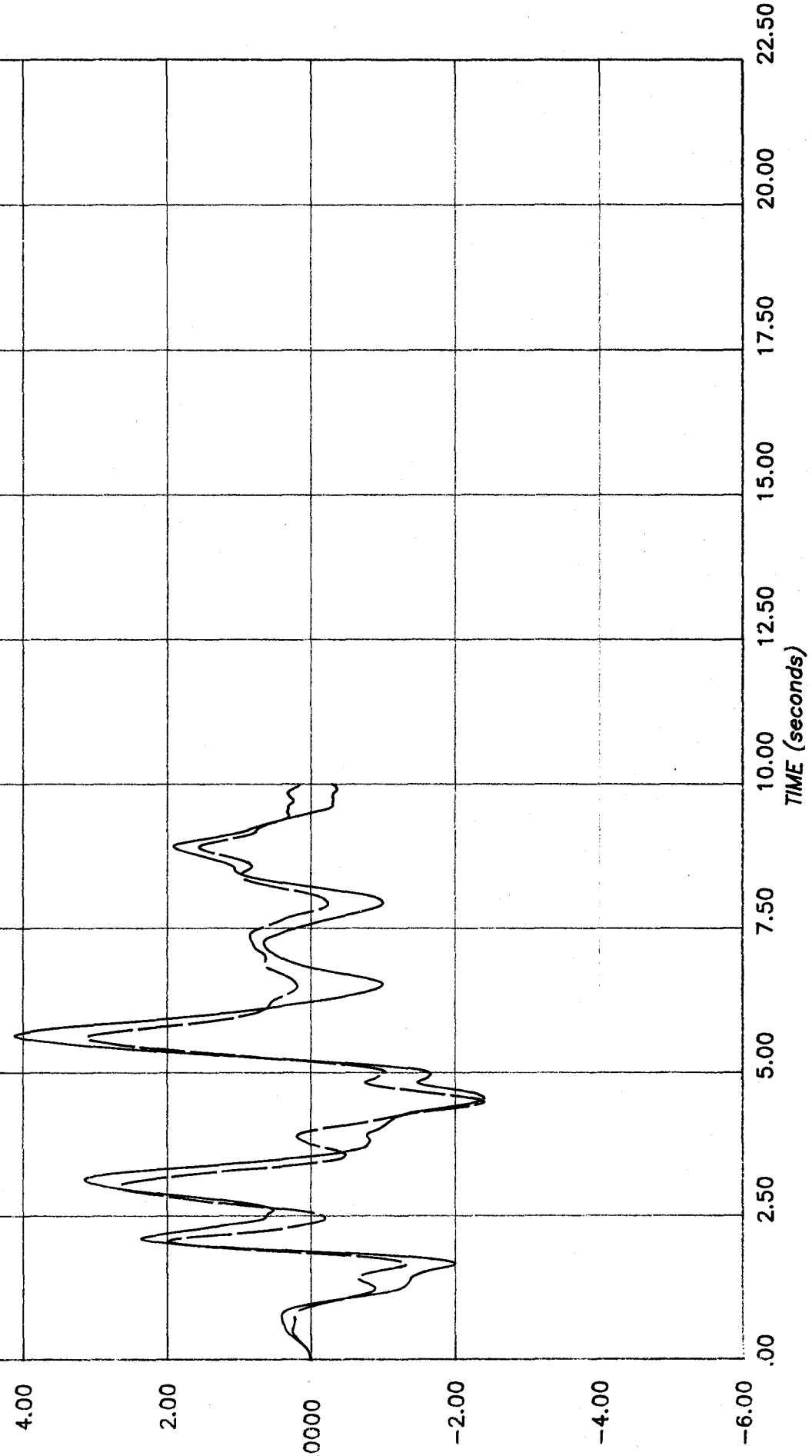


Figure 6.6(a) N-S Response. El Centro Scaled to $A_a = 0.2$

computech
 engineering services, inc.
 Berkeley, California

JOB NO.	DATE	TIME
J 502	01/10/82	11:58:46

PROJECT : ST. LOUIS PRUITT-IGOE CORRELATION STUDY
CLIENT : NATIONAL SCIENCE FOUNDATION
SUBJECT : SEISMIC RESPONSE : EL CENTRO '40 E/Q, N-S COMPONENT, $A_g = .2$
 E-W RESPONSE OF FRAMES 2 AND 4, AT LEVEL 11

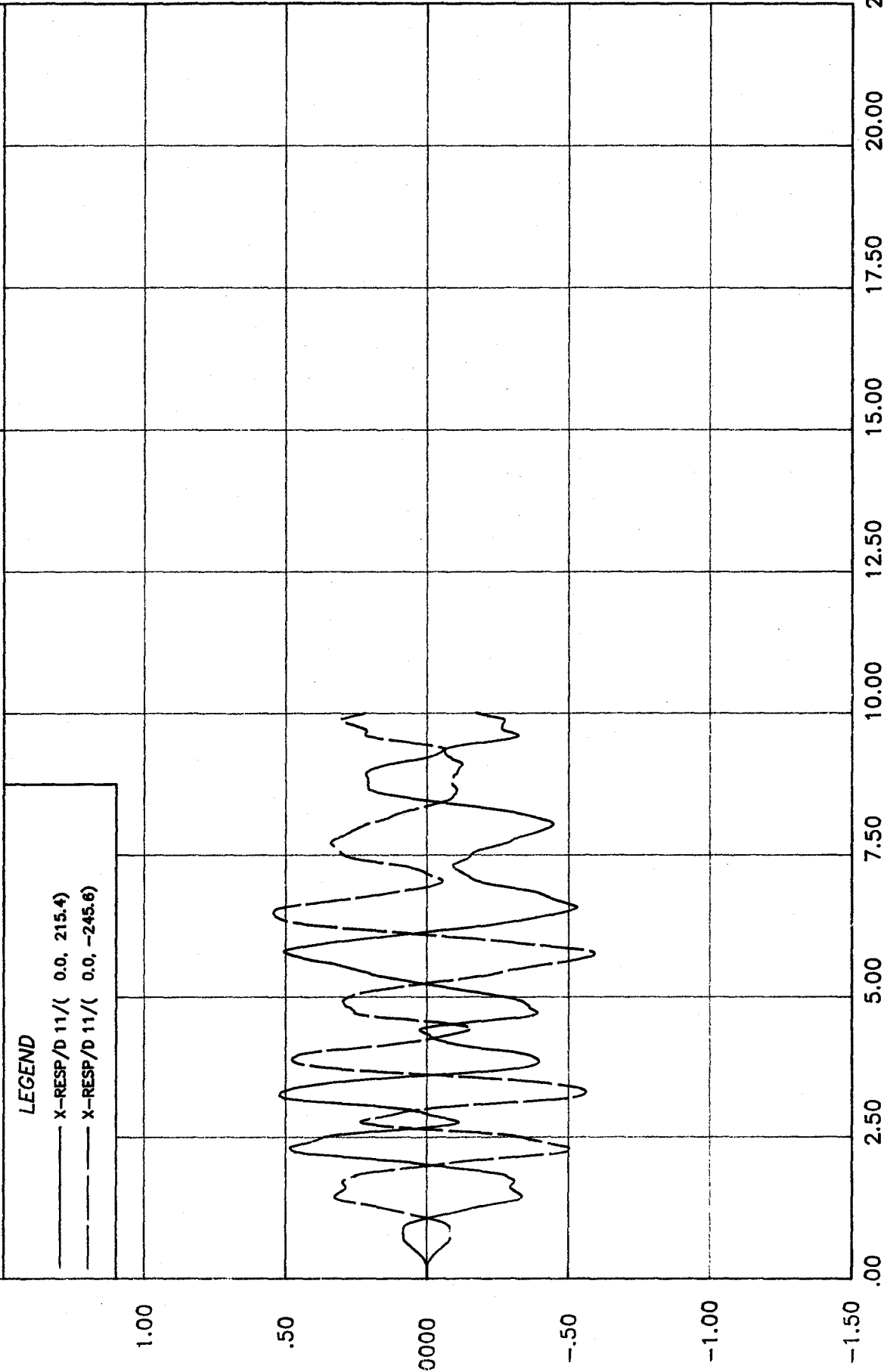


Figure 6.6(h) E-W Response El Centro Scaled to $A_g = 0.2$

computech
 engineering services, inc.
 Berkeley, California

JOB NO.	DATE	TIME
J 502	01/10/82	13:13:21

PROJECT : ST. LOUIS PRUITT-IGOE CORRELATION STUDY
CLIENT : NATIONAL SCIENCE FOUNDATION
SUBJECT : SEISMIC RESPONSE : TAFT '52 E/Q, S69E COMPONENT, Aa = .1
 N-S RESPONSE OF FRAMES 1 AND 3, AT LEVEL 11

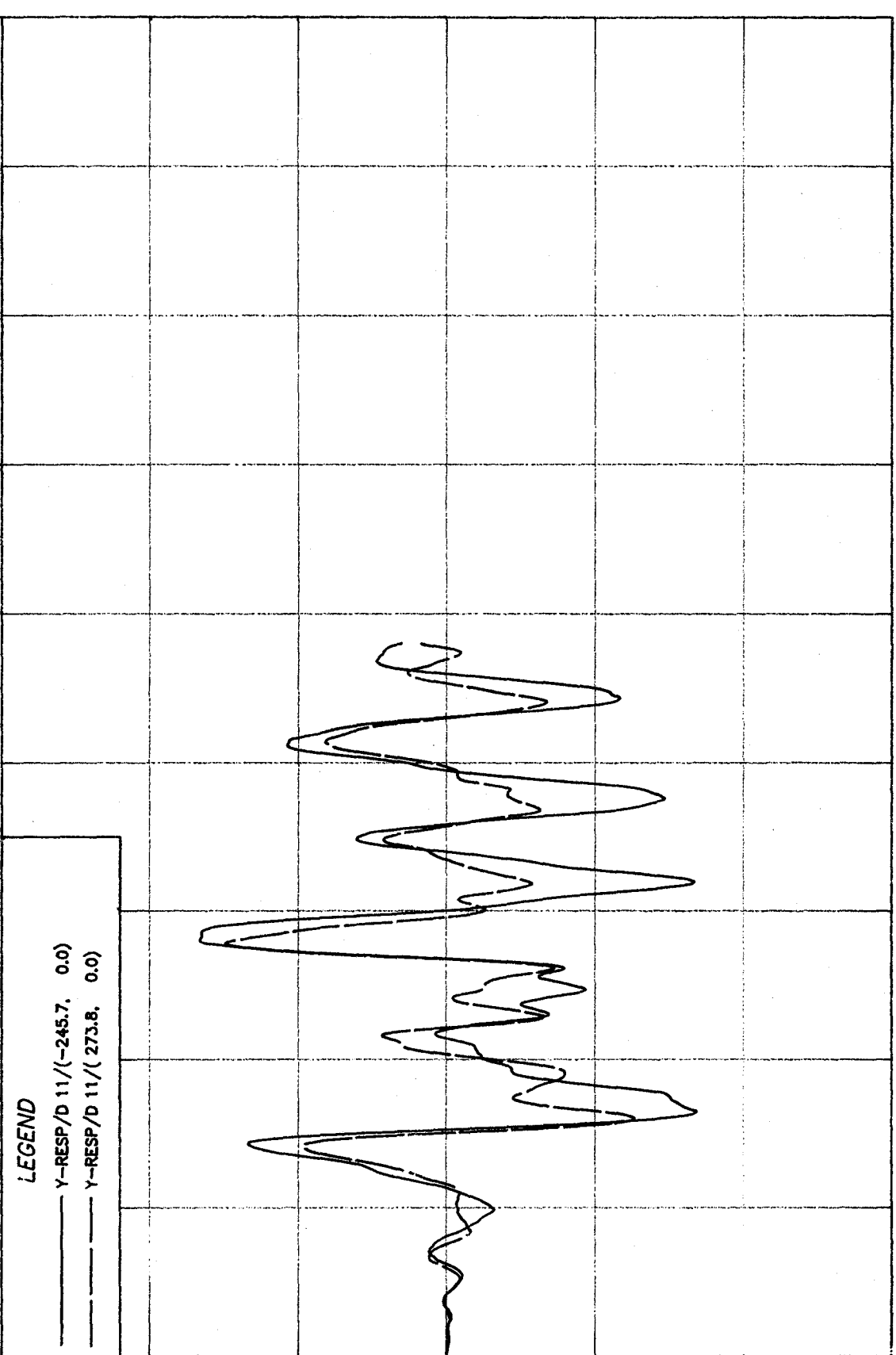


Figure 6.7(a) N-S Response, Taft Scaled to Aa = 0.1

computech
 engineering services, inc.
 Berkeley, California

JOB NO.	DATE	TIME
J 502	01/10/82	13:13:21

PROJECT : ST. LOUIS PRUITT-IGOE CORRELATION STUDY
CLIENT : NATIONAL SCIENCE FOUNDATION
SUBJECT : SEISMIC RESPONSE : TAFT '52 E/Q, S69E COMPONENT, $A_g = .1$
 E-W RESPONSE OF FRAMES 2 AND 4, AT LEVEL 11

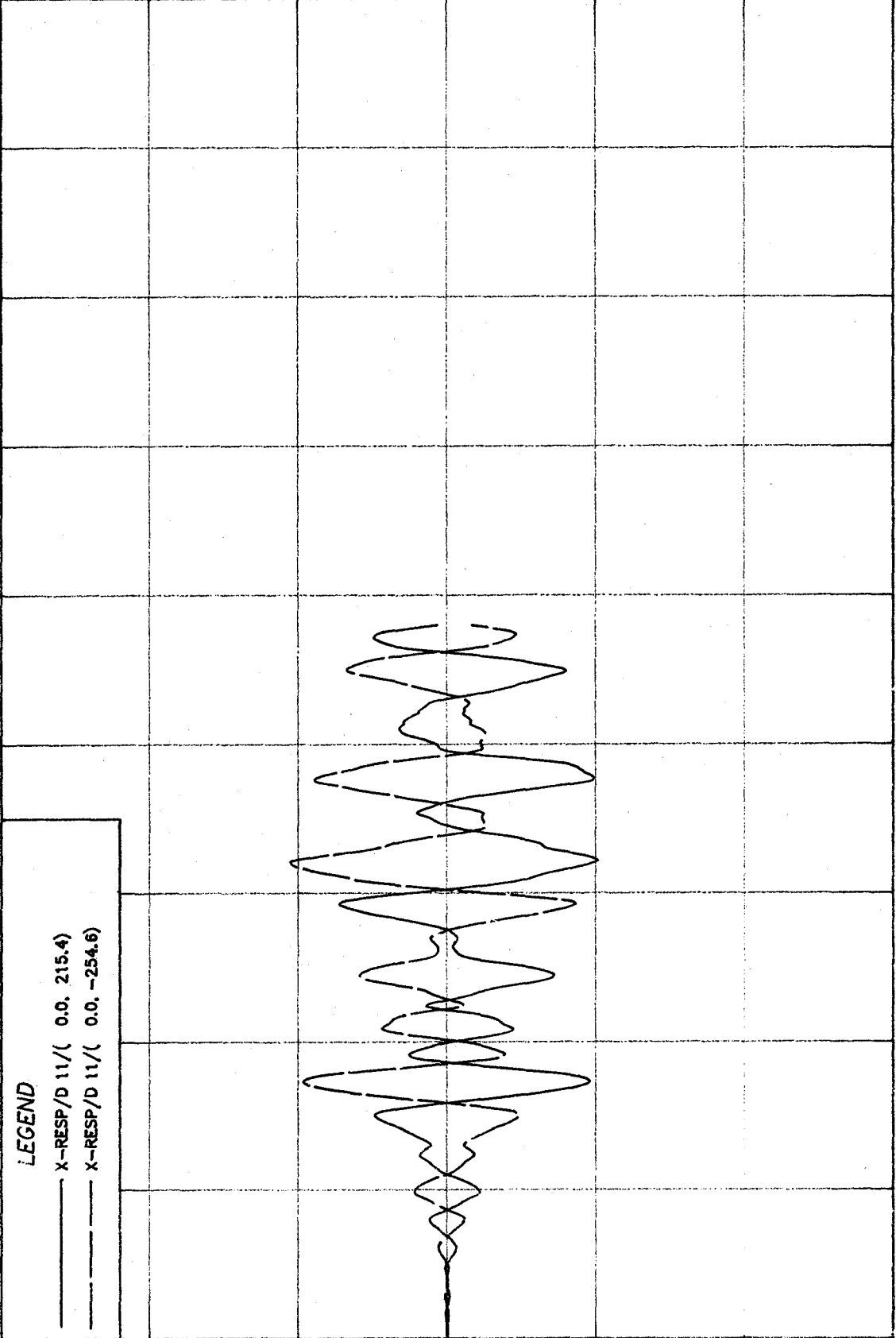


Figure 6.7(b) E-W Response, Taft Scaled to $A_g = 0.1$

computech
 engineering services, inc.
 Berkeley, California

JOB NO.	DATE	TIME
J 502	01/10/82	13:07:07

PROJECT : ST. LOUIS PRUITT-IGOE CORRELATION STUDY
CLIENT : NATIONAL SCIENCE FOUNDATION
SUBJECT : SEISMIC RESPONSE : TAFT '52 E/Q, S69E COMPONENT, $A_g = .4$
 N-S RESP. OF FRAMES 1 AND 3 (w/ WALL MASSES), AT LEVEL 11

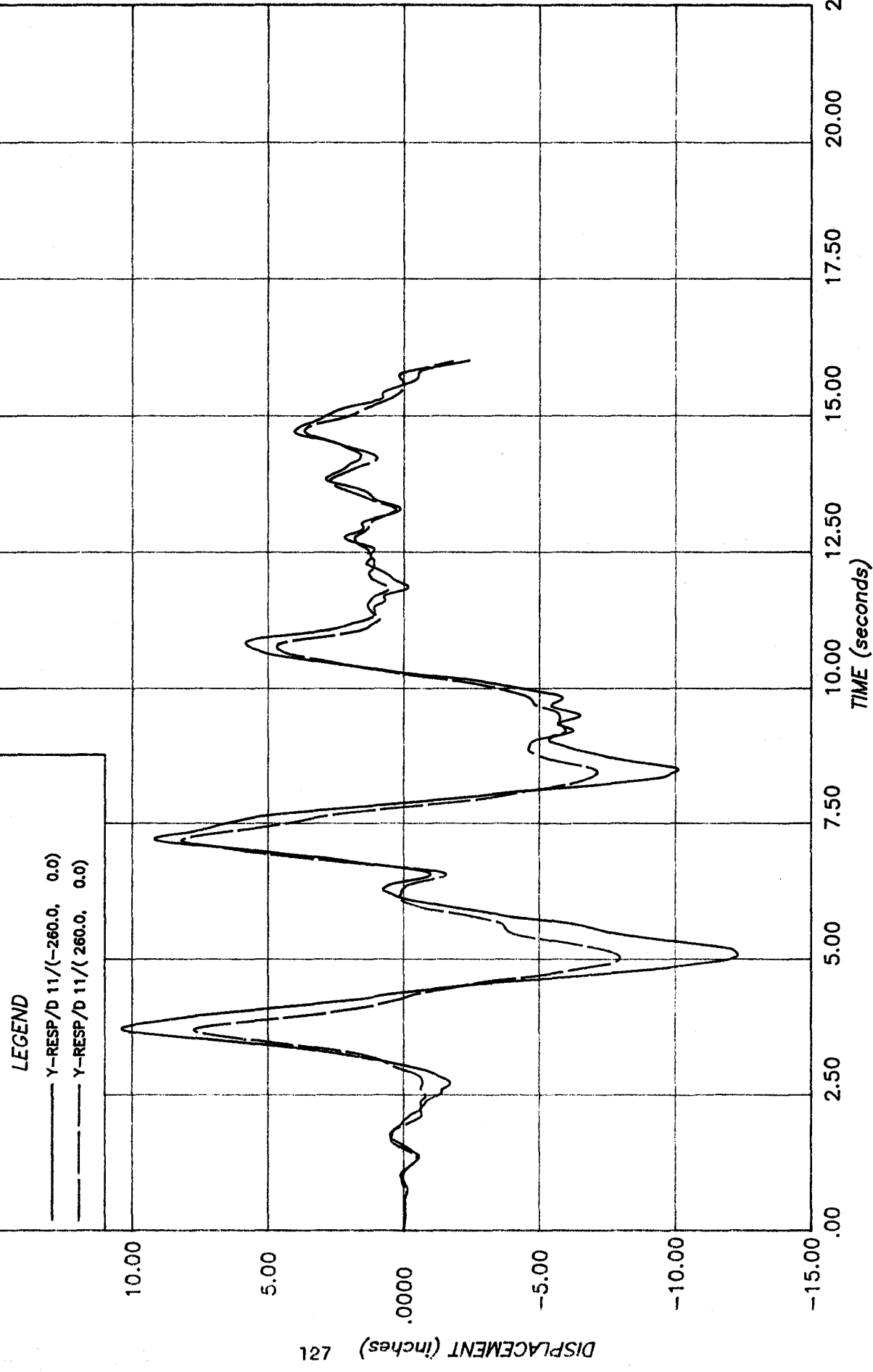


Figure 6.8(a) N-S Response, Wall Masses Included, Taft Scaled to $A_a = 0.4$

computech
 engineering services, inc.
 Berkeley, California

JOB NO.	DATE	TIME
J 502	01/10/82	13:07:07

PROJECT : ST. LOUIS PRUITT-IGOE CORRELATION STUDY
CLIENT : NATIONAL SCIENCE FOUNDATION
SUBJECT : SEISMIC RESPONSE : TAFT '52 E/Q, S69E COMPONENT, $A_d = .4$
 E-W RESP. OF FRAMES 2 AND 4 (w/ WALL MASSES), AT LEVEL 11

LEGEND

- X-RESP/D 11/(0.0, 235.0)
- - - X-RESP/D 11/(0.0, -235.0)

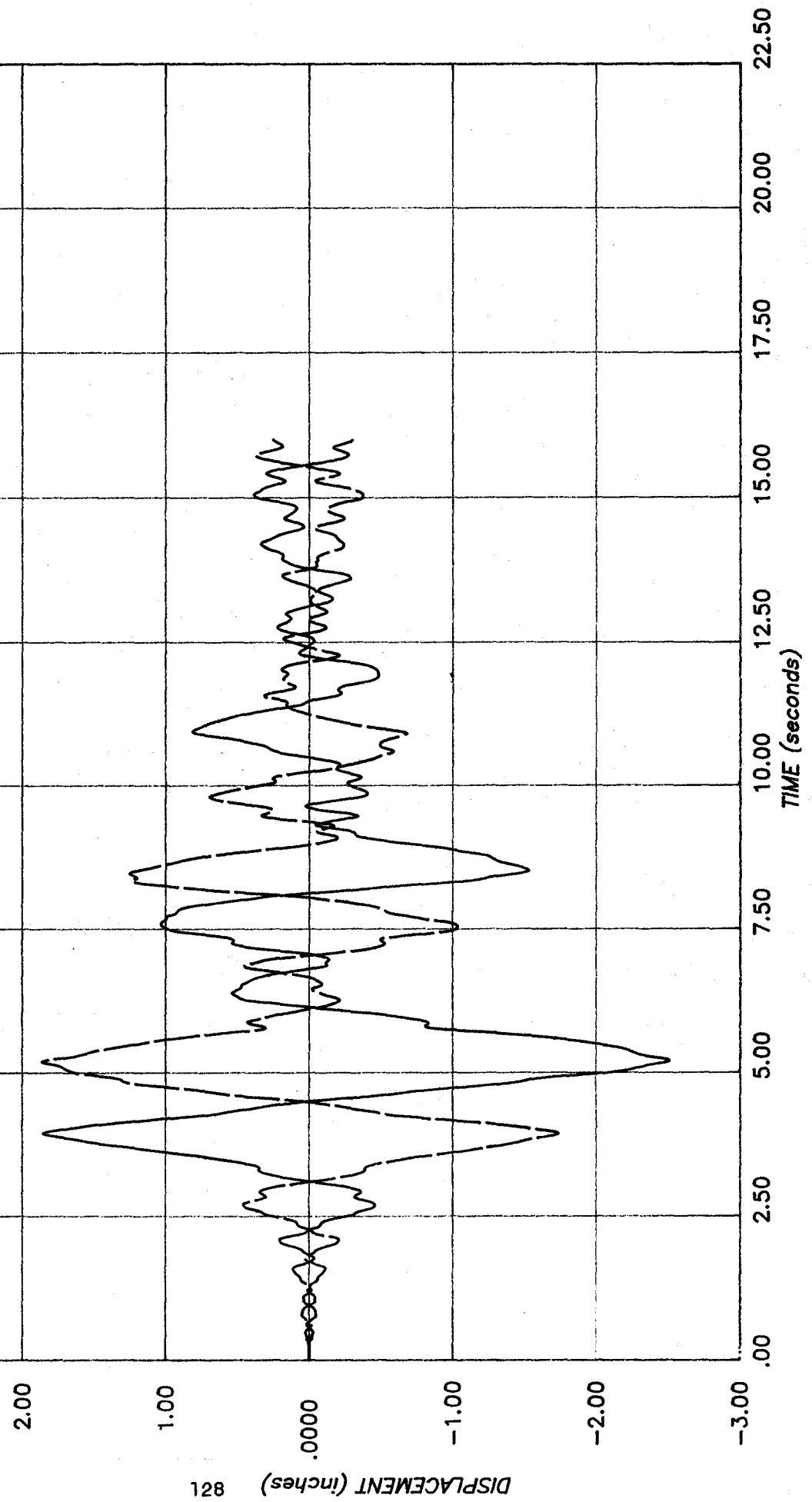


Figure 6.8(b) E-W Response, Wall Masses Included, Taft Scaled to $A_a = 0.4$

computech
 engineering services, inc.
 Berkeley, California

JOB NO.	DATE	TIME
J 502	01/10/82	13:02:45

PROJECT : ST. LOUIS PRUITT-IGOE CORRELATION STUDY
CLIENT : NATIONAL SCIENCE FOUNDATION
SUBJECT : SEISMIC RESPONSE : TAFT '52 E/Q, S69E COMPONENT, $A_g = .2$
 N-S RESP. OF FRAMES 1 AND 3 (w/ WALL MASSES), AT LEVEL 11

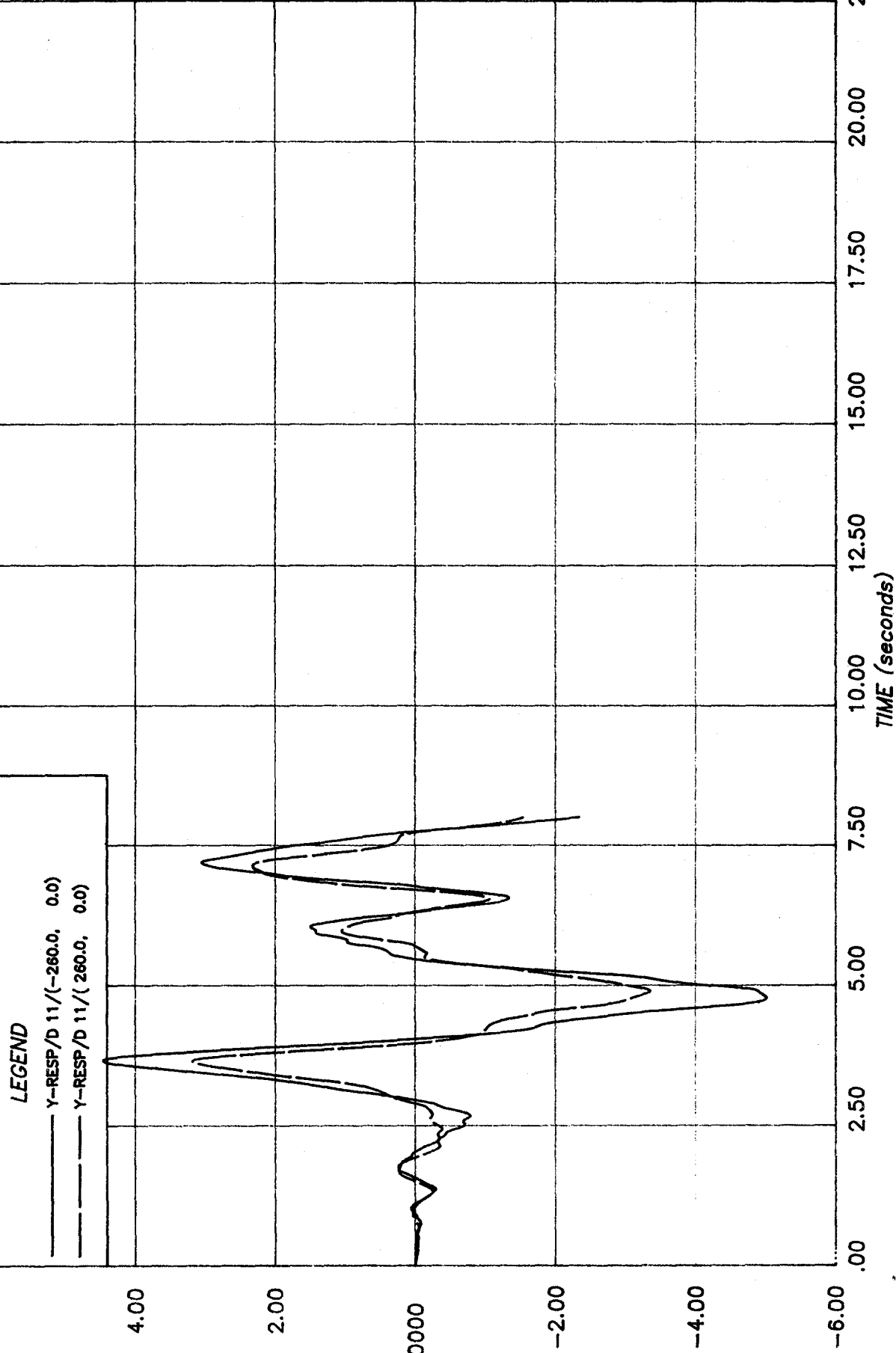


Figure 6.9(a) N-S Response, Wall Masses Included, Taft Scaled to $A_a = 0.2$

computech
 engineering services, inc.
 Berkeley, California

JOB NO.	DATE	TIME
J 502	01/10/82	13:02:45

PROJECT : ST. LOUIS PRUITT-IGOE CORRELATION STUDY
CLIENT : NATIONAL SCIENCE FOUNDATION
SUBJECT : SEISMIC RESPONSE : TAFT '52 E/Q, S69E COMPONENT, A_g = .2
 E-W RESP. OF FRAMES 2 AND 4 (w/ WALL MASSES), AT LEVEL 11

LEGEND
 — X-RESP/D 11/(0.0, 235.0)
 - - - X-RESP/D 11/(0.0, -235.0)

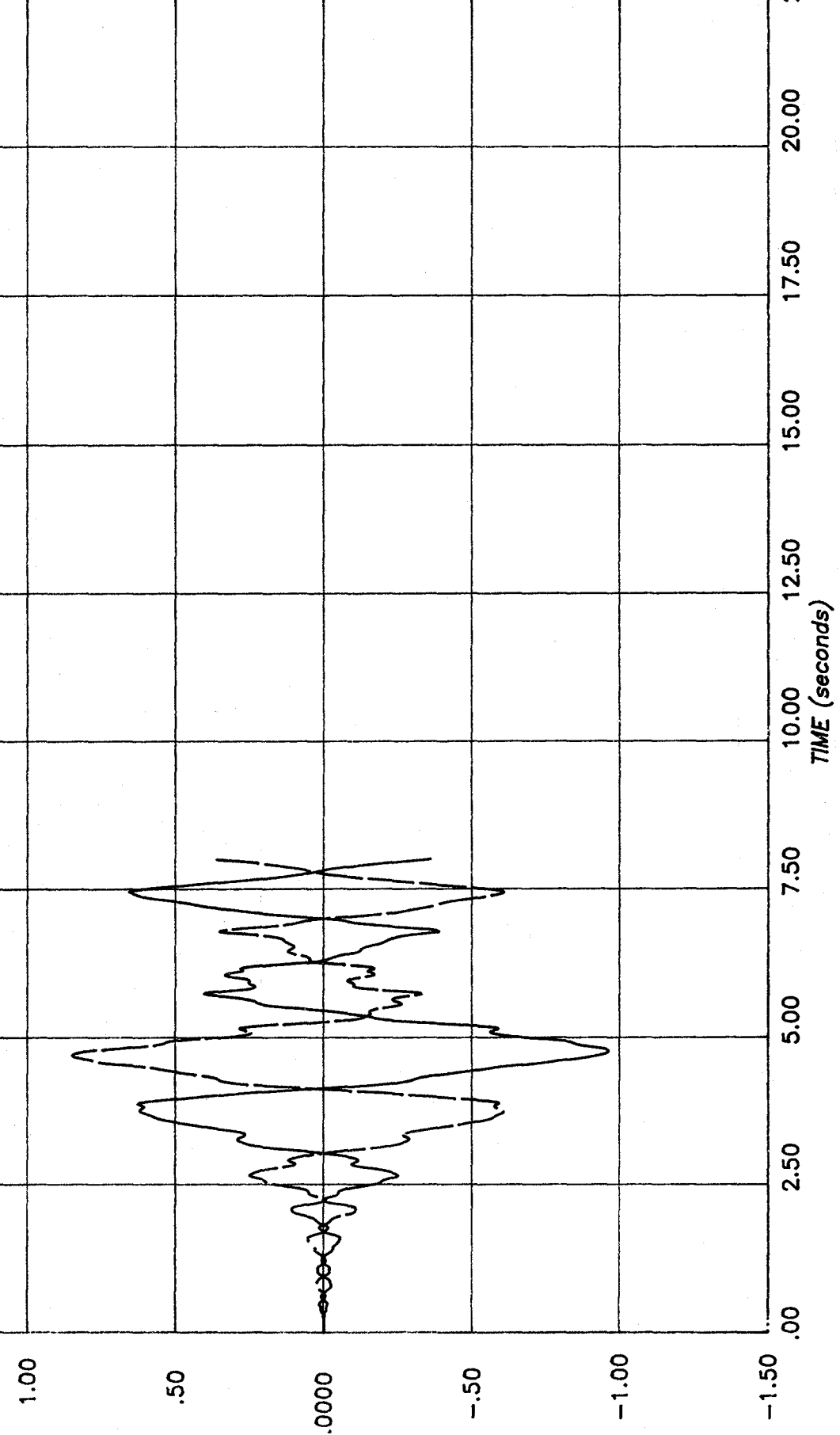


Figure 6.9(b) E-W Response, Wall Masses Included. Taft Scaled to A_a = 0.2

computech
 engineering services, inc.
 Berkeley, California

JOB NO.	DATE	TIME
J 502	01/10/82	12:33:49

PROJECT : ST. LOUIS PRUITT-IGOE CORRELATION STUDY
CLIENT : NATIONAL SCIENCE FOUNDATION
SUBJECT : SEISMIC RESPONSE : TAFT '52 E/Q, S69E COMPONENT, Aa = .1
 N-S RESP. OF FRAMES 1 AND 3 (w/ WALL MASSES), AT LEVEL 11

LEGEND

- Y-RESP/D 11/(-260.0, 0.0)
- - - Y-RESP/D 11/(260.0, 0.0)

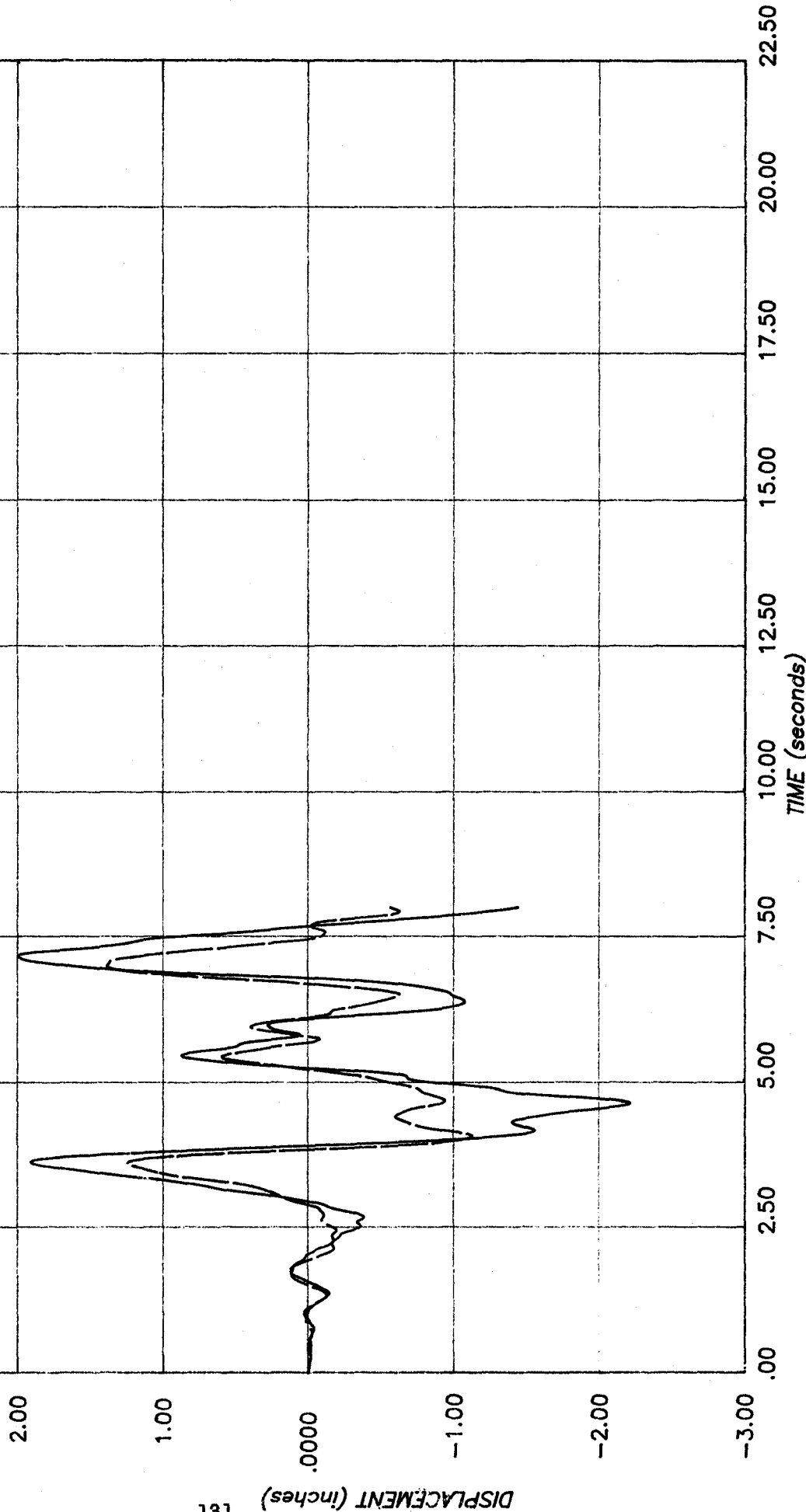


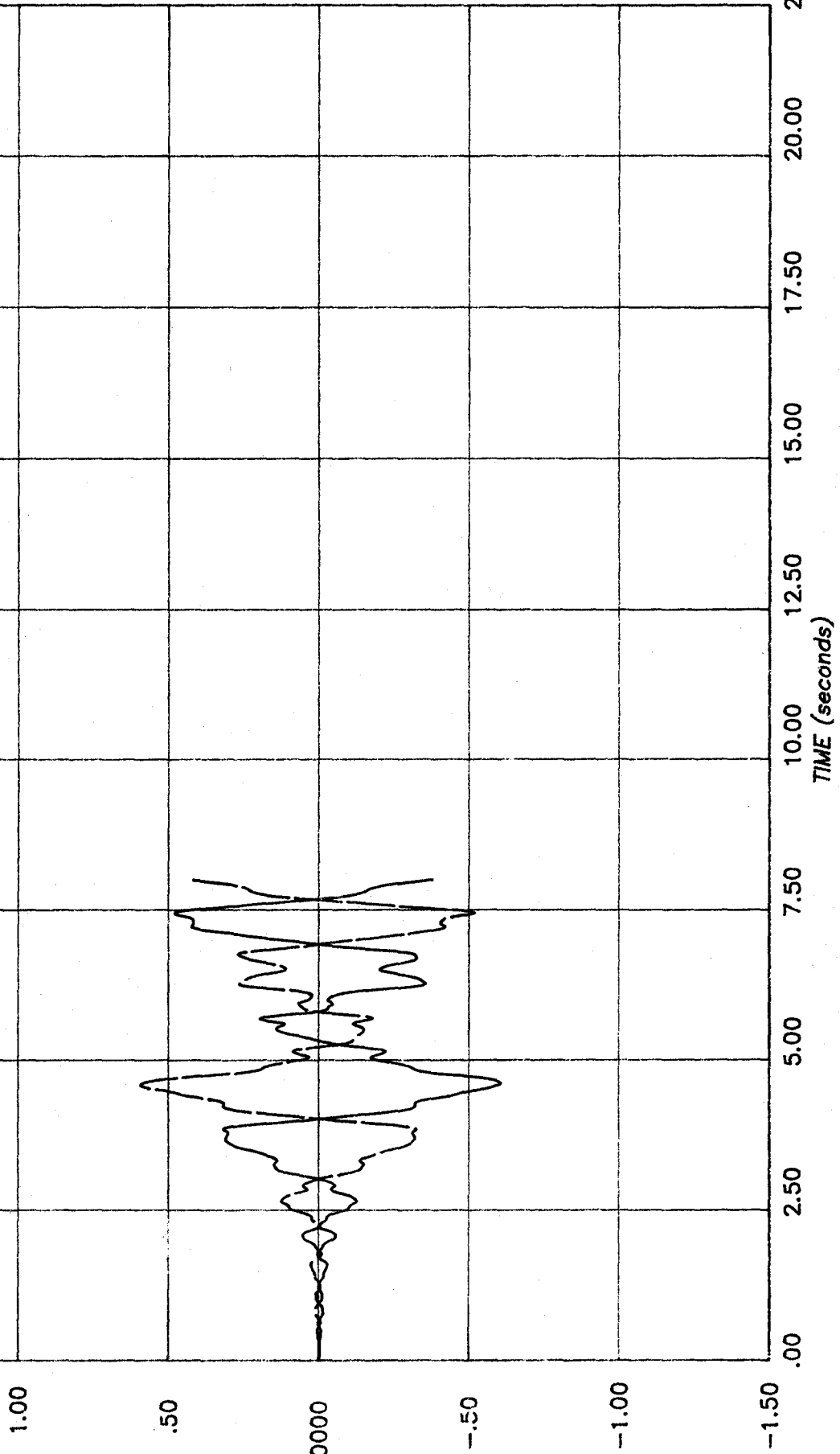
Figure 6.10(a) N-S Response, Wall Masses Included, Taft Scaled to Aa = 0.1

computech
 engineering services, inc.
 Berkeley, California

JOB NO.	DATE	TIME
J 502	01/10/82	12:33:49

PROJECT : ST. LOUIS PRUITT-IGOE CORRELATION STUDY
CLIENT : NATIONAL SCIENCE FOUNDATION
SUBJECT : SEISMIC RESPONSE : TAFT '52 E/Q, S69E COMPONENT, A_g = .1
 E-W RESP. OF FRAMES 2 AND 4 (W/ WALL MASSES), AT LEVEL 11

LEGEND
 ——— X-RESP/D 11/(0.0, 235.0)
 - - - X-RESP/D 11/(0.0, -235.0)



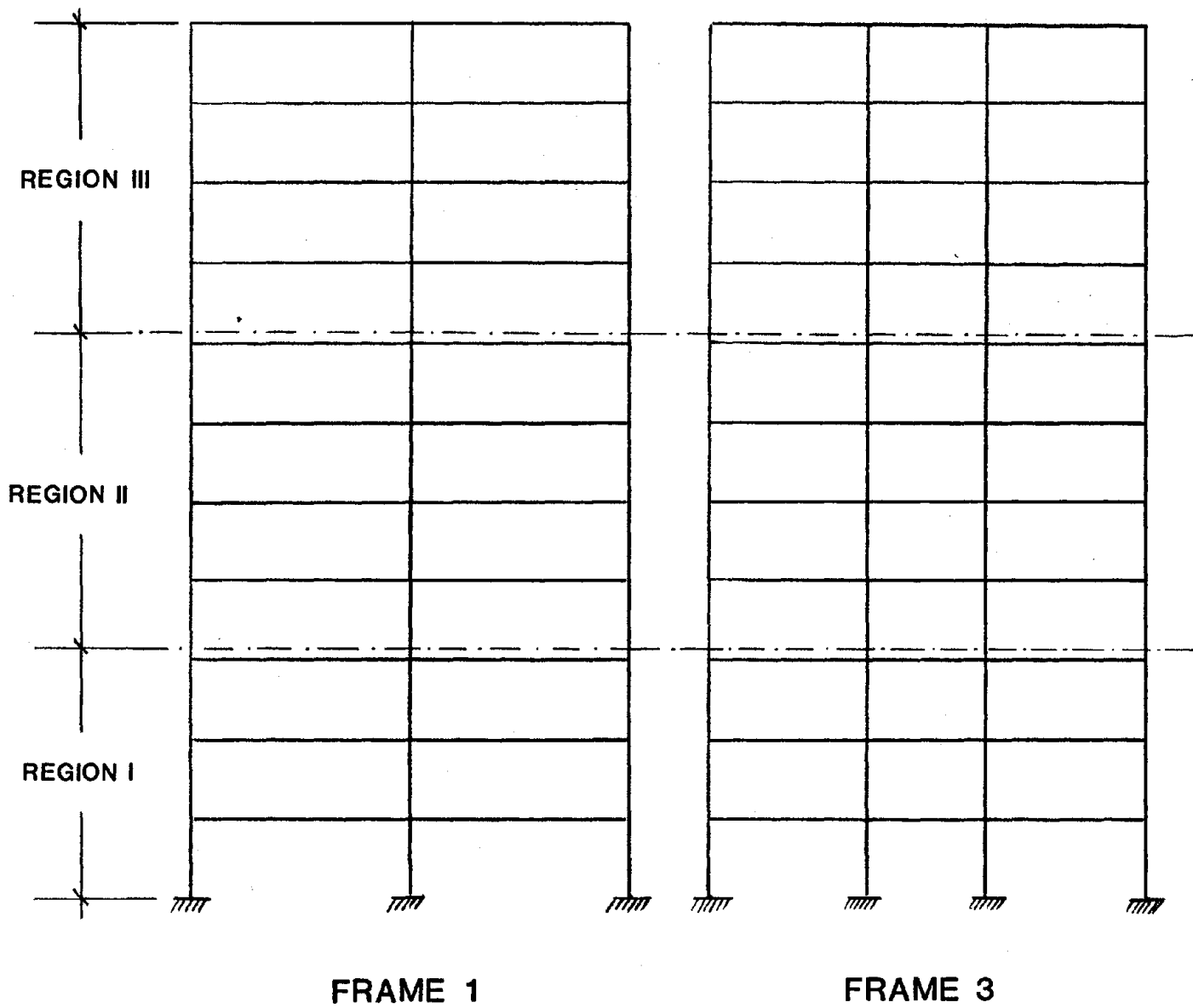


Figure 6.11 Definition of Frame Regions

7 CONCLUSIONS

This chapter presents the conclusions from the various chapters of this report. The correlation of the analytical models with the small and large amplitude test results is discussed in sections 7.1 and 7.2, respectively. Conclusions on the earthquake resistance of non-seismically designed reinforced concrete structures of this general type are presented in section 7.3. Finally recommendations for future research are presented in section 7.4.

7.1 SMALL AMPLITUDE CORRELATION

The SAP IV model of the structure gave good agreement with the measured results. Key parameters in the small amplitude correlation were the modelling of the stairways and the infill panels. A simple truss model for the stairs based on their gross concrete properties gave satisfactory results. The indeterminate nature of the interaction of the infill walls with the frame presented the biggest modelling problem. For unreinforced walls with no special construction features, such as in the St Louis building, a complex model does not seem warranted. Satisfactory modelling is obtained with inclined strut members, with properties based on the shear stiffness of the walls. A reduction in the modulus of elasticity to about 50% of the code value for masonry is necessary to allow for incomplete interaction of the infill walls and the reinforced concrete frame.

7.2 LARGE AMPLITUDE CORRELATION

In general, the correlation obtained with the large amplitude test results was very satisfactory. Good correlation was obtained with the mode shapes and periods measured at the start of the north-south tests, and also with the mode shapes and periods measured after the structure had been degraded. The degradation was modelled with the non-linear analysis program DRAIN-TABS. However, the version used was not an "off the shelf" version, as several new features had been developed specifically for this project. The modelling of continuous structural degradation under a sinusoidal load of slowly varying frequency presented the biggest challenge of the project. It is felt that this modelling was successful due in part to the new features developed for DRAIN-TABS. It is believed that reasonable correlation would have been difficult to achieve without the new features, and it is concluded that the modelling of the inelastic behavior of the end of the beams and the joints extended state-of-the-art analysis programs to the limit.

7.3 SEISMIC PERFORMANCE

The seismic performance of the test structure was evaluated by performing time history analyses of the "best fit" non-linear model of the structure. The model provided an adequate representation of the damage that was observed during the large amplitude tests, but it did not include the stiffness contribution of the infill panels. Thus the analytical results can be considered

as an upper bound on the expected response. The earthquake ground motions used were representative of regions of varying seismic risk. The ATC-3-06 [6] design ground motion spectra was used as the basis for scaling the El Centro, Taft and Pacoima measured ground motions so they would be typical of various regions. The three regions selected were Regions 7, 5 and 3 of the ATC-3-06 report, with effective peak accelerations of 0.4, 0.2 and 0.1g, respectively. Region 7 represents areas of the highest seismic risk and includes most of California. Region 5 represents moderate seismic risk areas and includes areas such as Washington State, Utah and parts of Missouri and Arkansas. Region 3 represents areas of lower seismic risk and includes the northeastern United States and South Carolina.

The results of the time history analyses indicate that for Region 7 the test structure would collapse or be in a collapse mode and would represent a significant safety problem. For Region 5 the structure would be unlikely to collapse but would possibly require demolition or a substantial amount of repair for the cracks that develop before the building could be reoccupied. For Region 3 the structure would retain its structural integrity and would be functional after an earthquake.

The capabilities developed herein to model the non-linear response of the non-seismically designed reinforced concrete test structure are adequate to evaluate the seismic safety of this form of construction. However, since the seismic evaluation of existing buildings is being required by an increasing number of municipalities, improvements in the ability to evaluate structures of this type would be obtained if the research recommended in the following section is performed.

7.4 RESEARCH RECOMMENDATIONS

Perhaps the major short-coming of this study was the lack of an analytical model specifically for reinforced concrete joints with little or no shear and confining reinforcement and inadequate anchorage of the bottom beam steel. A model was developed to represent the behavior of the inadequately anchored beam steel, but a detailed model for the joint degradation was not developed because there is no detailed test data available on such joints. The approach used to model the joint degradation phenomenon was to use discrete hinges with specialized moment-rotation relationships at the extremities of the top of the columns. This approach proved to be adequate, but a more versatile solution could very well be obtained if a model of the joint degradation was formulated and based on test data.

With such an element developed and available for use, the important task of evaluating the seismic safety of existing structures of this general type would be much enhanced.

Another major area of uncertainty in this study has been the stiffness and strength properties of the masonry infill panels. Experimental data on such infill panels is not currently available, and this lack of data definitely hinders the development of accurate mathematical models of structures containing

these walls. The use of these infill panels is very typical of this form of construction, and is quite a prevalent form of construction east of the Rockies. Experimental data on the characteristics of these panels subjected to cyclic loads would again enhance the ability to accurately assess the seismic safety of such structural systems.

It is therefore recommended that further research be conducted in the following areas:

1. A test program should be formulated, to specifically collect data on the behavior of inadequately reinforced concrete joints under cyclic loads. A dynamic test set-up would be preferable, although a pseudo-static one would be adequate.
2. On the basis of the test results obtained in 1, an analytical model which captures the essential behavior of such joints should be formulated and extensively tested. Correlation with the results of the test program presented herein should then be performed with the new analytical model.
3. An experimental program should be set up to obtain data on the strength and stiffness properties of masonry infill panels.

8 REFERENCES

1. Gardiner, R.E., and Hatcher, D.S., "Material and Dimensional Properties of an Eleven-Story Reinforced Concrete Building", Research Report No. 52, Department of Civil Engineering, Washington University, St. Louis, August 1978.
2. Applied Nucleonics Company, "Moderate Level Vibration Tests on an Eleven Story Reinforced Concrete Building", Report No. 1158-1, September 1976.
3. Galambos, T.V. and Mayes, R.L., "Dynamic Tests of a Reinforced Concrete Building", Research Report No. 51, Department of Civil Engineering, Washington University, St. Louis, June 1978.
4. Bathe, K.-J., Wilson, E.L., and Peterson, F.E., "SAP IV - A Structural Analysis Program for Static and Dynamic Response of Linear Systems", Report No. EERC 73-11, Earthquake Engineering Research Center, University of California, Berkeley, Ca., June 1973.
5. Guendelman-Israeli, R. and Powell, G.H., "DRAIN-TABS : A Computer Program for Inelastic Earthquake Response of Three-Dimensional Buildings", Report No. EERC 77-08, Earthquake Engineering Research Center, University of California, Berkeley, Ca., March 1977
6. Applied Technology Council, "Tentative Provisions for the Development of Seismic Regulations for Buildings", Report No. ATC 3-06, June 1978.
7. Housner, G.W., "Behavior of Structures During Earthquakes", ASCE Journal, Engineering Mechanics Division, EM4, pp 109-129, October 1959.
8. Amrhein, J.E., "Reinforced Masonry Engineering Handbook", Third Edition, Masonry Institute of America, 1978.
9. Clough, R.W. and Penzien, J., "Dynamics of Structures", McGraw-Hill, Inc., 1975.
10. Park, R. and Paulay, T., "Reinforced Concrete Structures", John Wiley and Sons, 1975.
11. Ferguson, P.M., "Reinforced Concrete Fundamentals", John Wiley and Sons, 1965.
12. Minor, J. and Jirsa, J.O., "Behavior of Bent Bar Anchorages", ACI Journal, April, 1975.
13. Mathey, R.G. and Watstein, D., "Investigation of Bond in Beam and Pull-Out Specimens with High Yield Strength Deformed Bars", ACI Journal, March, 1961.

14. Bertero, V.V., Private Communication, 1981.
15. Takeda, T., Sozen, M.A. and Nielson, N.N., "Reinforced Concrete Response to Simulated Earthquakes". ASCE Journal, Structural Division, ST12, pp 2557-2573, December 1970.



1. 2. 3.